International Journal of Medical & Clinical Imaging
IJMCI, 6(1): 350-425
www.scitcentral.com
ISSN: 2573-1084
Original Research Article: Open Access

Phase and Frequency Coordination Improvement Among Neuron Firing for Improved CNS Self-Organization and Neural Repair in Parkinson and Spinal Cord Injury

Giselher Schalow*

*Non-Government-Organized Research (NGOR), Switzerland.

Received November 05, 2020; Revised January 15, 2021; Accepted March 15, 2021

ABSTRACT

Phase and frequency coordination among neuron firing is an organization principle of human central nervous system (CNS) organization/functioning. Following injury, malformation or degeneration, this coordinated firing between neurons becomes impaired and has to be repaired through movement-based learning besides that other parts of the brain have to take function over from the damaged ones by plasticity. In patients with Parkinson's disease this phase and frequency coordination becomes strongly impaired, so that neurons synchronize their firing because of missing inhibition, which leads to tremor and impaired movement functions. With the movement-based learning treatment "Coordination dynamics therapy" (CDT), this coordinated firing of neurons can partly be repaired with the consequence that the tremor reduces and coordinated movements like walking improve.

With the single-nerve fiber action potential recording method, the coordinated firing of neurons is measured during an operation and with the surface electromyography (sEMG) the coordinated firing of single motor units is recorded non-invasively in suitable patients. When exercising on a special CDT device, Parkinsonian tremor reduces and movement functions improve. The nervous system learns from the device to improve its functioning, which can be measured with ongoing therapy by a single value, the coordination dynamics value.

The coordinated firing among neurons could nicely be measured because for high activation the three kinds of human motoneurons fire rhythmically with three Eigenfrequencies of approximately 1, 5 and 10Hz and the phase and frequency could nicely be measured between oscillatory firing motoneurons and muscle spindle and other afferents. In the occasional firing mode, the motoneurons fire according to the size principle in each motoneuron group. Their firing is probably also coordinated, but difficult to measure. The tremor in patients with Parkinson's disease is generated when α_2-motoneurons, innervating fast fatigue resistant muscle fibers, fire already oscillatory for no or little activation because of too little inhibition (1), and synchronize their firing because of too little lateral field inhibition (2). When the large α_1-motoneurons, innervating fast fatigue muscles fibers, synchronize the firing with those of α_2-motoneurons (3), the full tremor appears. Muscle-limb mechanics contribute to the shaking of body parts.

The improvement of phase and frequency coordination through CDT substantially contributes to the repair in cerebrum and cerebellum injury, spinal cord injury (SCI), cerebral palsy, stroke, myelomeningocele, aging and cancer. Even sportsmen benefit from an improved phase and frequency among neuron firing, because the coordination of arms, legs and trunk improve, to play for example better tennis or football. Since CDT improves the functioning of every CNS, and the CNS is involved in nearly all body functions, the regulations of body functions improve, especially the cardio-vascular performance, to live longer with a better quality of life through 10 to 15 h CDT per week.

Keywords: Human neurophysiology, Electrophysiology, Single-nerve fiber action potentials, Conduction velocities, Natural firing patterns, Oscillatory firing, Phase and frequency coordination, Surface EMG, Human repair neurophysiology, Coordination dynamics therapy, Parkinson, Spinal cord injury

INTRODUCTION

For a repair of the injured, malformed or degenerating human central nervous system (CNS), firstly the impaired phase and frequency coordination of human CNS organization has to be improved to achieve efficient physiologic CNS organization again. This can mainly be achieved when the patient is exercising very coordinated movements on special coordination dynamics therapy (CDT) devices. Secondly, to achieve physiologic CNS functioning again, integrative coordinated movements like crawling, walking and running have to be trained so that other parts of the brain can take functions over from the injured ones by plasticity, which is especially strong in young children. Thirdly, movements have to be trained which stimulate the epigenetics for repair. In this article it is concentrated on the phase and frequency coordination of CNS organization and its consequences of improvement for neural repair.

Corresponding author: Giselher Schalow, Untere Kirchmatte 6, CH6207 Nottwil, Switzerland, Tel: 0041419371641; E-mail: g_schalow@hotmail.com

Citation: Schalow G. (2021) Phase and Frequency Coordination Improvement Among Neuron Firing for Improved CNS Self-Organization and Neural Repair in Parkinson and Spinal Cord Injury. Int J Med Clin Imaging, 6(1): 350-425.

Especially in patients with Parkinson's disease, the phase and frequency coordination among neuron firing is impaired and has to be improved through CDT. Because of the substantial loss of inhibition, the motoneurons synchronize and give rise to tremor. But movement functions are also impaired in the patients. For tremor reduction and movement repair, details of CNS organization have to be understood for neural repair through movement-based learning. The Eigenfrequencies and stabilities of firing of the three kinds of motoneurons are used to understand tremor occurrence and its reduction through learning.

The reason to update a previous paper on phase and frequency coordination [1] is because more data are available, and CDT has fully reached the clinics. Human patients benefit from this new development. It will be shown that, based on theory, the human CNS can partly be repaired by movement-based learning. Lack of this human repair-neurophysiology knowledge may lead to wrong treatments including operations.

To demonstrate the importance and power of human neurophysiology and repair physiology for CNS repair, a partial repair of a spinal cord injury (SCI) is shown. **Figure 1** shows the 5.5-years-old Nefeli after suffering a SCI, with approximately 70% cord damage, following a cancer operation by medical malpractice.

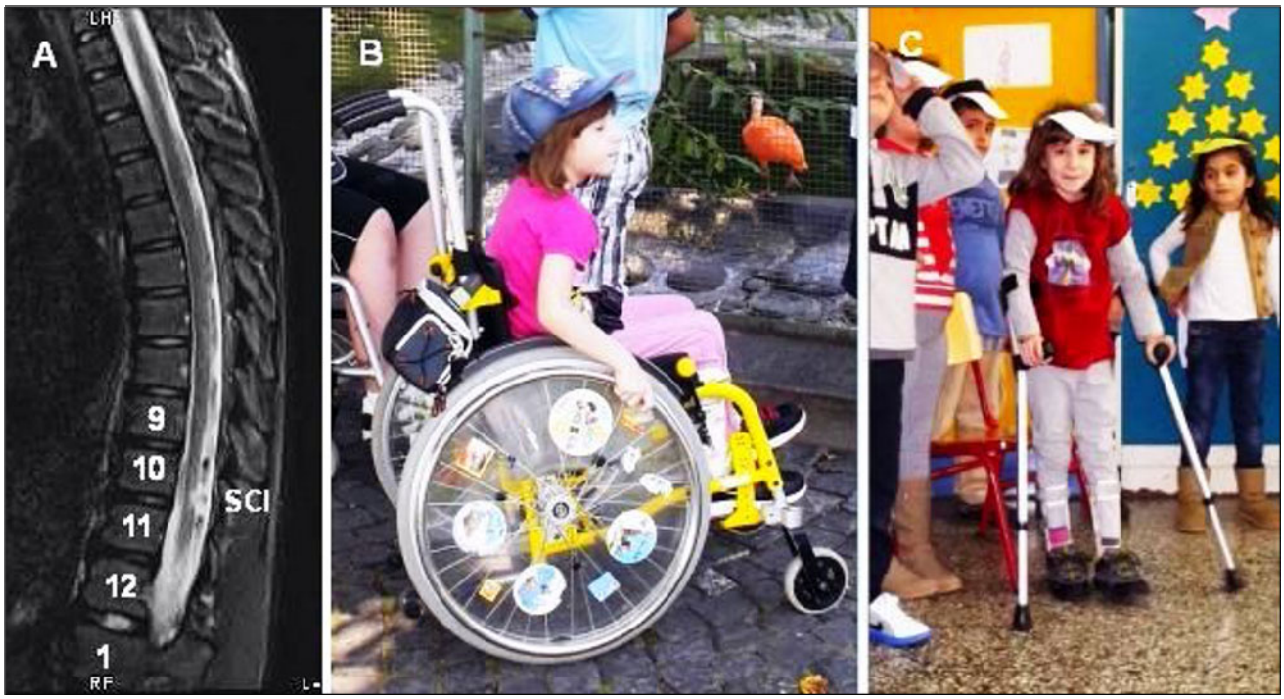

Figure 1. A. MRI of the spinal cord injury (SCI); injury approximately 70%. Because of scoliosis, the cord could not be brought fully into plane. B. The 5.5-year-old SCI patient Nefeli in the wheelchair. C. With orthosis and sticks she had had problems to manage at school.

At an age of 9, CDT was started for 4 years. The performed movements included exercising on a special CDT device **(Figure 2A)**, supported jumping on springboard **(Figure 2B)** and sky-walking (Figure 2C). Further, creeping, crawling, walking and other movements were trained.

Nefeli relearned walking (with deficits) so that she could walk at school to the whiteboard **(Figure 3B)** and write there **(Figure 3A)**. The achieved spinal cord repair, including a partial regeneration of the spinal cord [3], allowed her to manage quite well at school, which would have been difficult without CDT **(Figure 1C)**. The urinary bladder functions were mainly repaired through learning transfer [2] from exercising on the special CDT device and jumping on springboard. A bladder repair is most important for patients with SCI. Even a bit of normal cycling she learned **(Figure 3C)** first time in her life. The feet control was the main problem and not the balance. For details of SCI repair in general and this special SCI repair see [3]. In the Discussion it will be shown that the out-of-date 'Human Repair-Neurophysiology' of universities may become a danger to CNS injured patients.

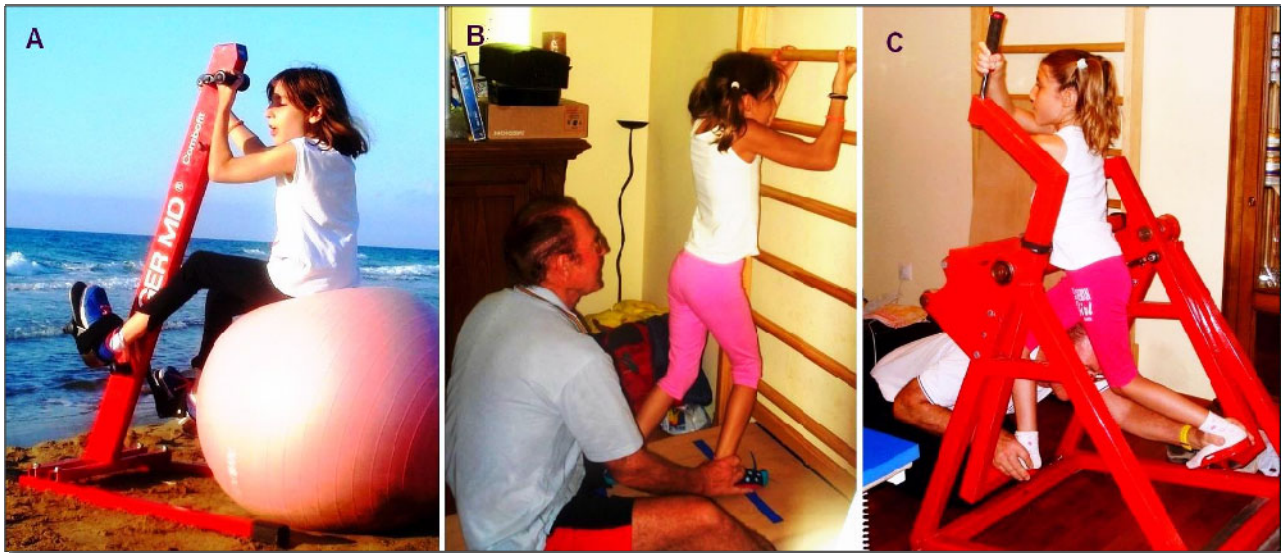

Figure 2. A. SCI patient Nefeli during exercising on a special CDT device on a ball at the beach, to train apart from phase and frequency coordination also balance. B. By the Author supported jumping on springboard in antiphase. C. Nefeli during sky-walking. To achieve a large stride length, the Author is supporting the feet to avoid the slipping of the feet from the pedals.

Figure 3. A, B. The SCI patient Nefeli learned to walk at school to the whiteboard and write there. C. 13-year-old Nefeli during cycling. She has problems to keep the feet on the pedals, but she could hold the balance.

The single-nerve fiber action potential recording method, the surface electromyography and the coordination dynamics recording method are used to analyze premotor spinal oscillators and the phase relations among them in brain-dead humans (HTs) and patients with Parkinson's disease. Based on the difference between physiologic phase and frequency coordination in HT's and pathologic coordination in patients, the repair method CDT is developed and used in connection with the plasticity of the human CNS to repair the human nervous system.

METHODS

For analyzing phase and frequency coordination and its improvement or repair, mainly four methods were used **(Figure 4)**: The single-nerve fiber action potential recording method (A) [4], the morphometry (B), the surface electromyography (sEMG) (C, D) and the coordination dynamics recording method (E) [5]. The single-nerve fiber action potential recording method and the morphometry were used to classify and identify human peripheral nerve fibers and measure and follow up

phase and frequency coordination among a set of single neurons. Surface EMG was used to record the coordinated firing of single motor units and the coordination dynamics recording method was used to measure CNS repair of patients during treatment progress by a single value.

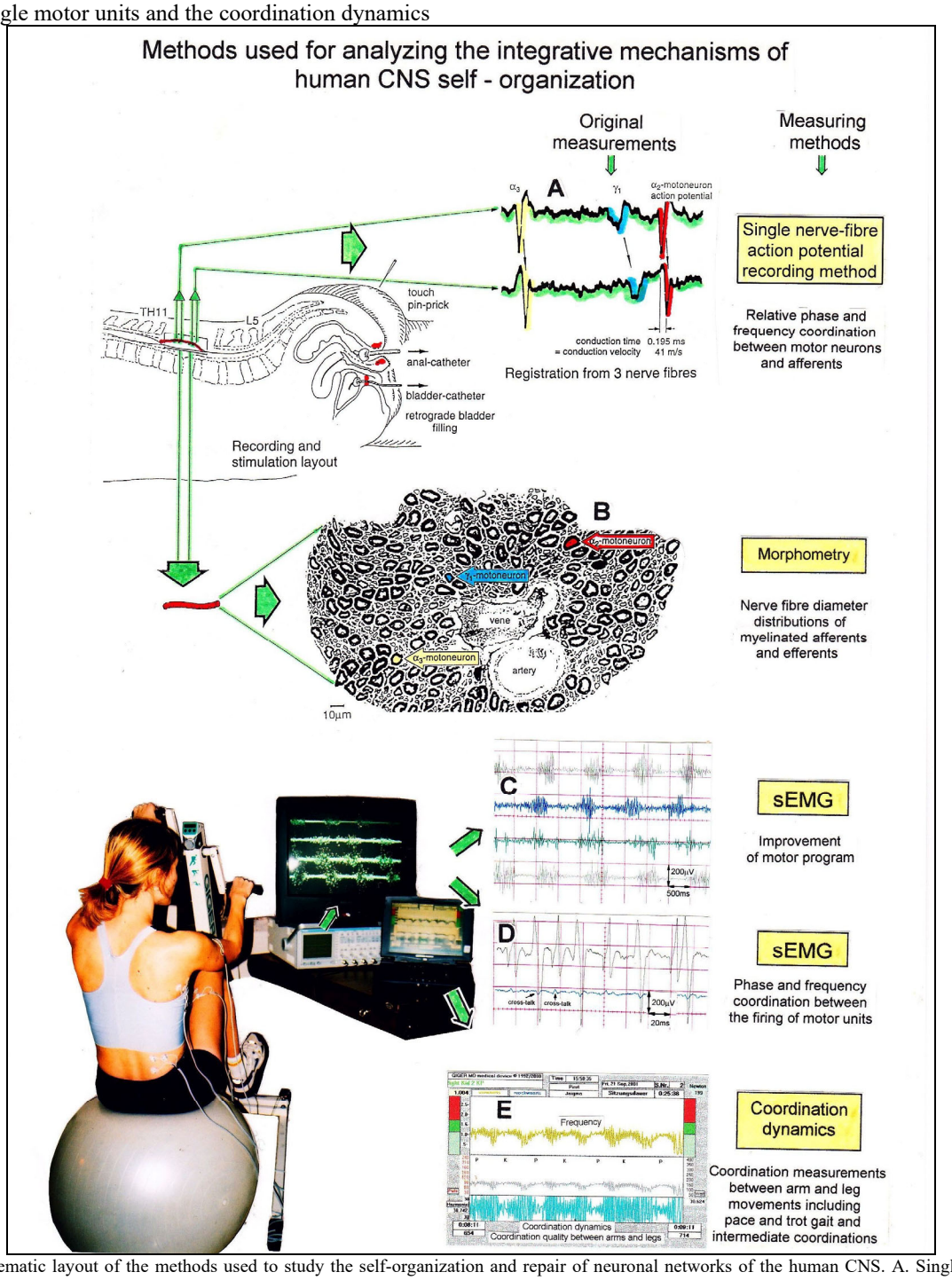

Figure 4. Schematic layout of the methods used to study the self-organization and repair of neuronal networks of the human CNS. A. Single-nerve fiber action potential (AP) recording method to measure with wire electrodes simultaneously from a set of single afferent (AP phase upward) and efferent (AP phase downward) nerve fibers to analyze the simultaneous impulse traffic running in and out of the spinal cord. B. Morphometry of nerve roots and nerves to identify groups of nerve fibers. C, D. By performing surface electromyography (sEMG) with up to 4 electrode pairs (2 indifferent electrodes, 1 earth electrode; pre-amplification x1000, 4-channel oscilloscope) the changes of motor programs were measured (C). When recording from appropriate patients, natural activation patterns of several single-motor units were obtained (D) and coordination between motor unit firing could be studied. E. Coordination between arms and leg movements was quantified by the single integrative parameter, arrhythmicity of turning (df/dt or df/dt/f; f = frequency) during exercising on a special coordination dynamics therapy device.

By recording with two pairs of platinum wire electrodes from sacral nerve roots containing between 200 and 500 myelinated nerve fibers (of which a few ones are only active), records were obtained in which single-nerve fiber action potentials (APs) could be identified from motoneuron axons (main AP phase downwards) and afferents (main AP phase upwards) **(Figure 5A-5C)**. By measuring the conduction times and with the known electrode pair distance (10 mm) conduction velocities could be calculated.

By comparing wave forms, conduction times/velocities and reoccurring action potential patterns, the summed impulse traffic of several active nerve fibers could be splitted into the impulse patterns of single nerve fibers **(Figures 5D and 5E)**.

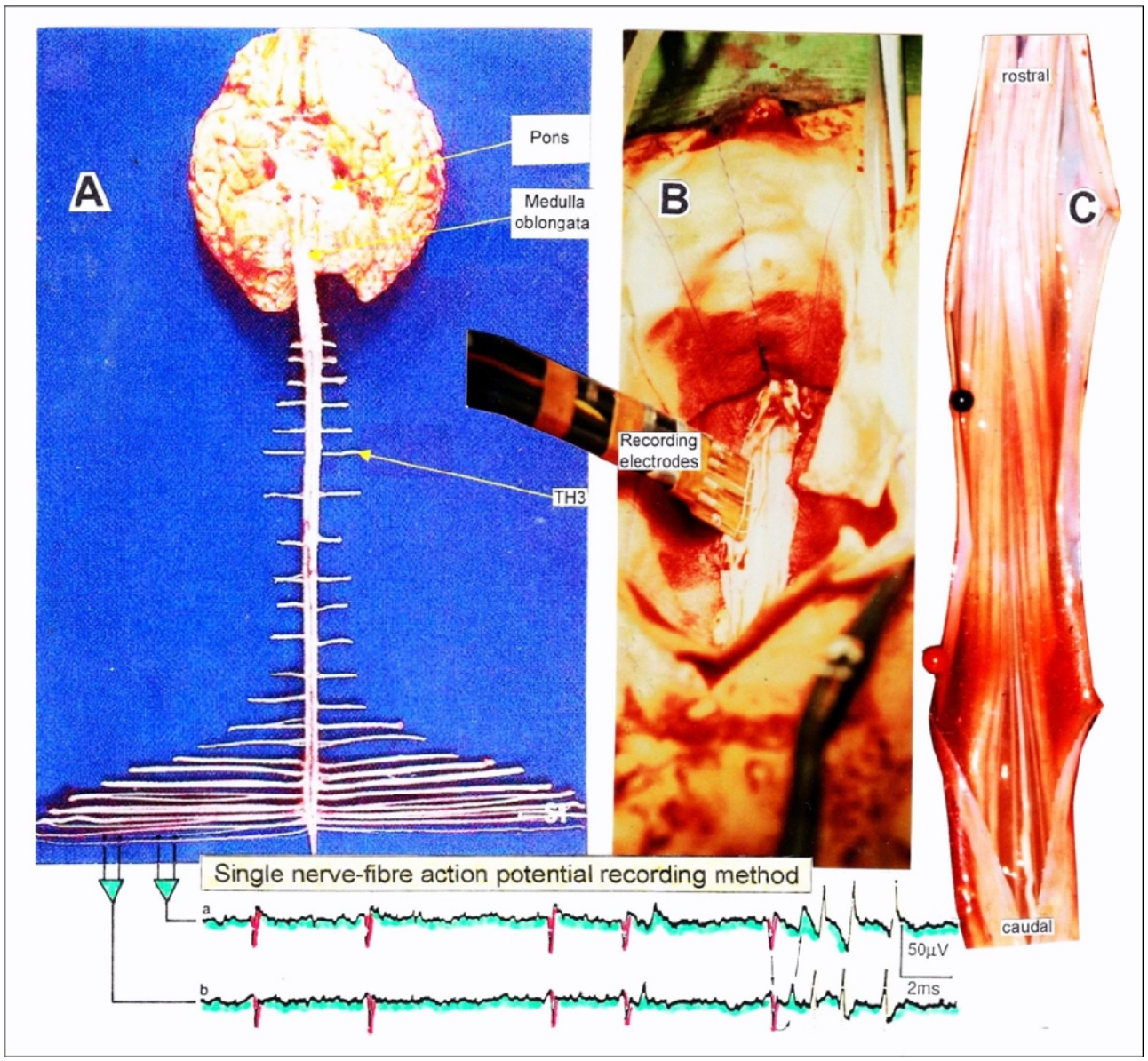

Figure 5A-C. Layout of the recording of single-nerve fiber action potentials to measure the self-organization of neuronal networks of the human CNS under physiologic and pathophysiologic conditions. By recording with two pairs of wire electrodes (B) from sacral nerve roots (cauda equina, C), containing between 200 and 500 myelinated nerve fibers, records were obtained in which single-nerve fiber action potentials (APs) were identified from motoneuron axons (main action potential (AP) phase downwards) and afferents (main AP phase upwards).

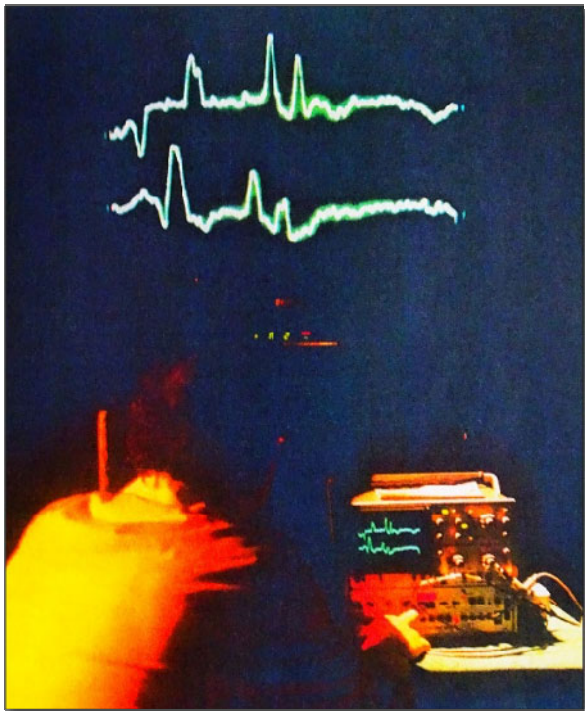

Figure 5D. Author during analyzing the summed impulse traffic.

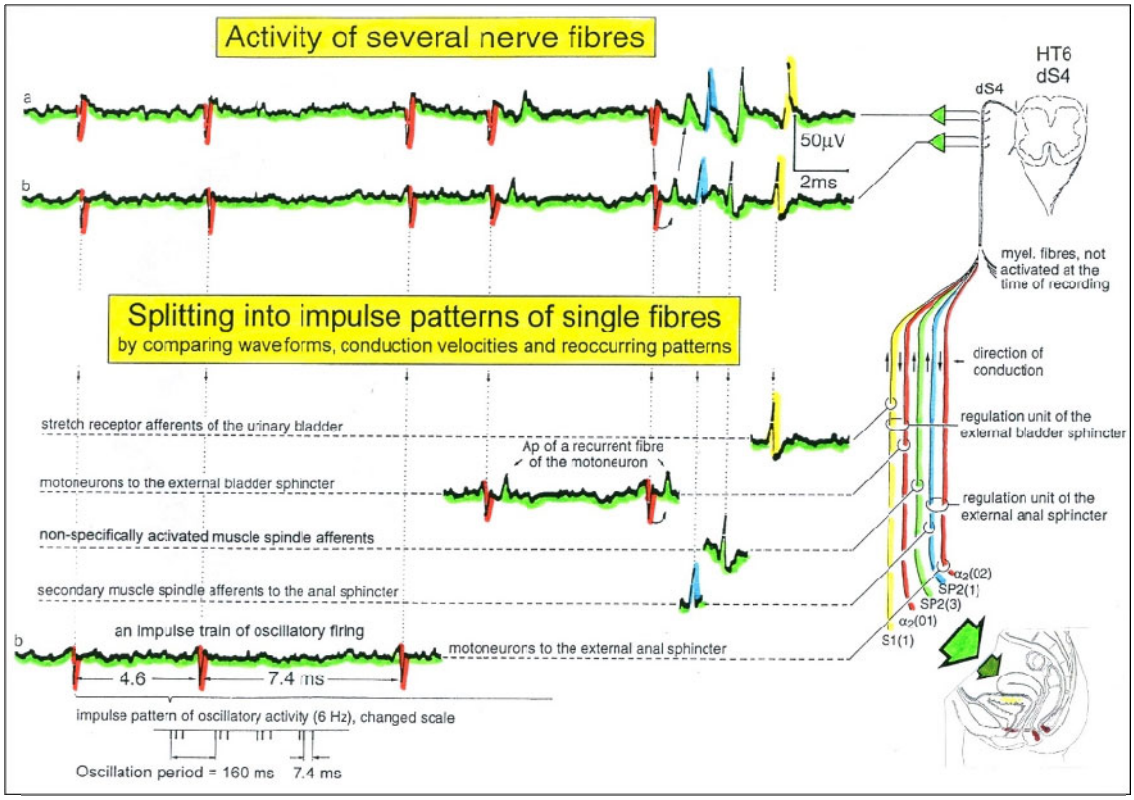

Figure 5E. Splitting of the summed impulse traffic of several active nerve fibers (Figure 5A) into the impulse patterns of single nerve fibers by comparing wave forms, conduction velocities and reoccurring impulse patterns (oscillatory firing motoneuron axons).

Conduction velocity distribution histograms were constructed in which the myelinated nerve fiber groups larger than 4 µm could be characterized by group conduction velocity value. Recording was followed by morphometry. Distributions of nerve fiber diameters were constructed, and nerve fiber groups were characterized by the peak values of asymmetrical distributions [6,7].

By correlating the peak values of the velocity distributions with those of the diameter distributions obtained for the same root, a classification scheme was constructed of the human peripheral nervous system **(Figures 6 and 7)** [7-9]. The group conduction velocities and group nerve fiber diameters had the following pair-values at 35.5°C:

Spindle afferents: SP1($65ms^{-1}$/13.1µm), SP2(51/12.1); touch afferents: T1(47/11.1), T2(39/10.1), T3(27/9.1), T4(19/8.1); urinary bladder afferents: S1($41ms^{-1}$/-), ST (35/-); α-motoneurons: α_{13} (-/14.4), α_{12} ($65ms^{-1}$/13.1µm), α_{11} (60?/12.1)[FF], α_2 (51/10.3)[FR], α_3 (41/8.2)[S]; γ-motoneurons: γ_β(27/7.1), γ_1(21/6.6), γ_{21}(16/5.8), γ_{22}(14/5.1); preganglionic parasympathetic motoneurons: ($10ms^{-1}$/3.7µm). Schematically the values are summarized in **Figure 7**.

With respect to electrical stimulation, it was found that the primary spindle afferents likely have the lowest threshold upon electrical nerve root stimulation, followed by α_1-motoneurons (FF), secondary muscle spindle afferents, α_2-motoneurons (FR), α_3-motoneurons (S), γ_β, γ_1 (dynamic), γ_{21} (static), γ_{22} (static), and parasympathetic motoneurons.

This classification and identification scheme represents a solid basis for classifying and identifying nerve fiber groups in the human peripheral nervous system (PNS) and analyzing central nervous system (CNS) functions at the single-neuron level, even though it is incomplete and holds so far only for nerve fiber diameters larger than approximately 3.5µm.

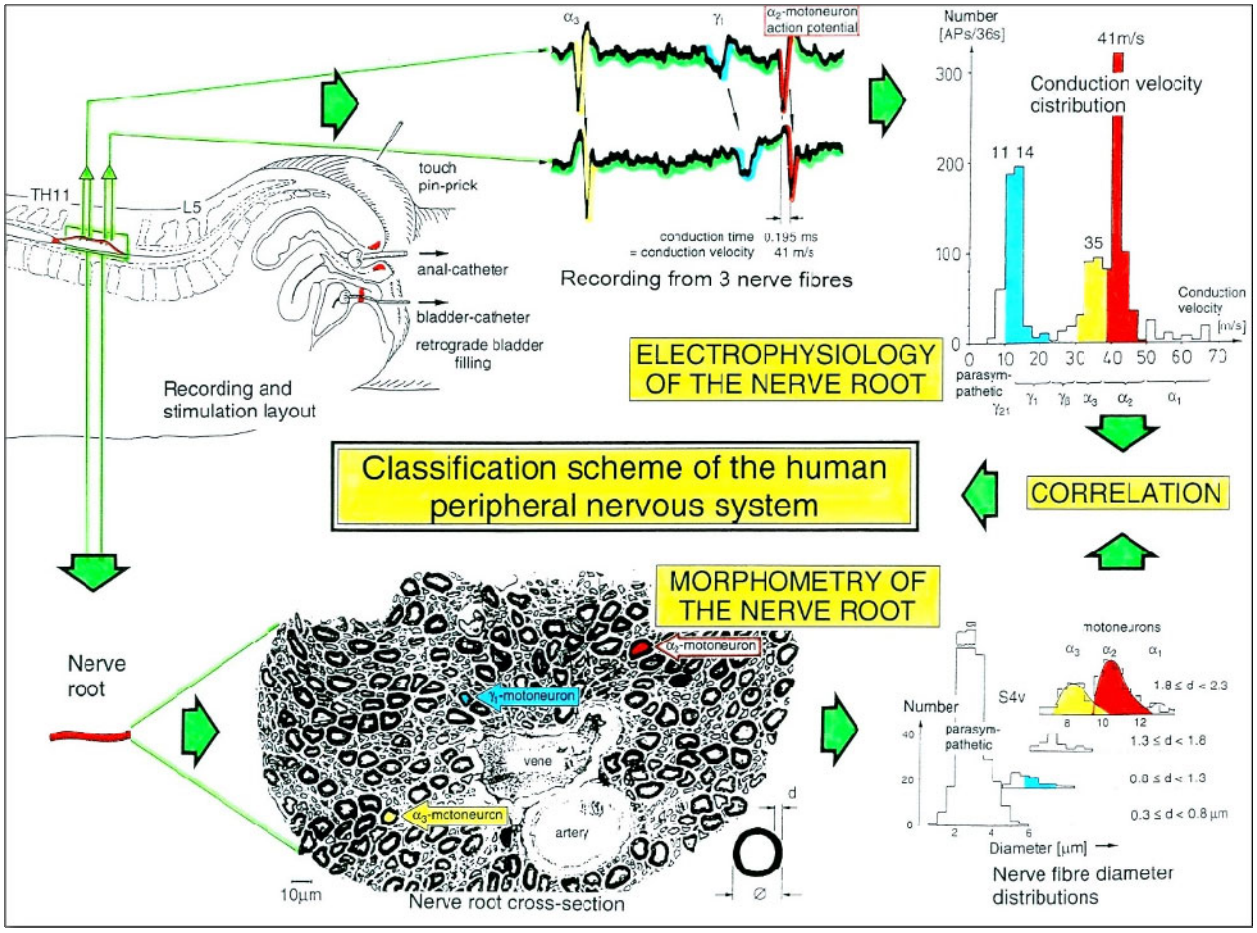

Figure 6. Development of a classification scheme for human peripheral nerve fibers. Conduction velocities (V) and nerve fiber diameters (∅) of afferent and efferent nerve fiber groups in normal humans and in patients with a traumatic SCI for 0.5 to 6 years.

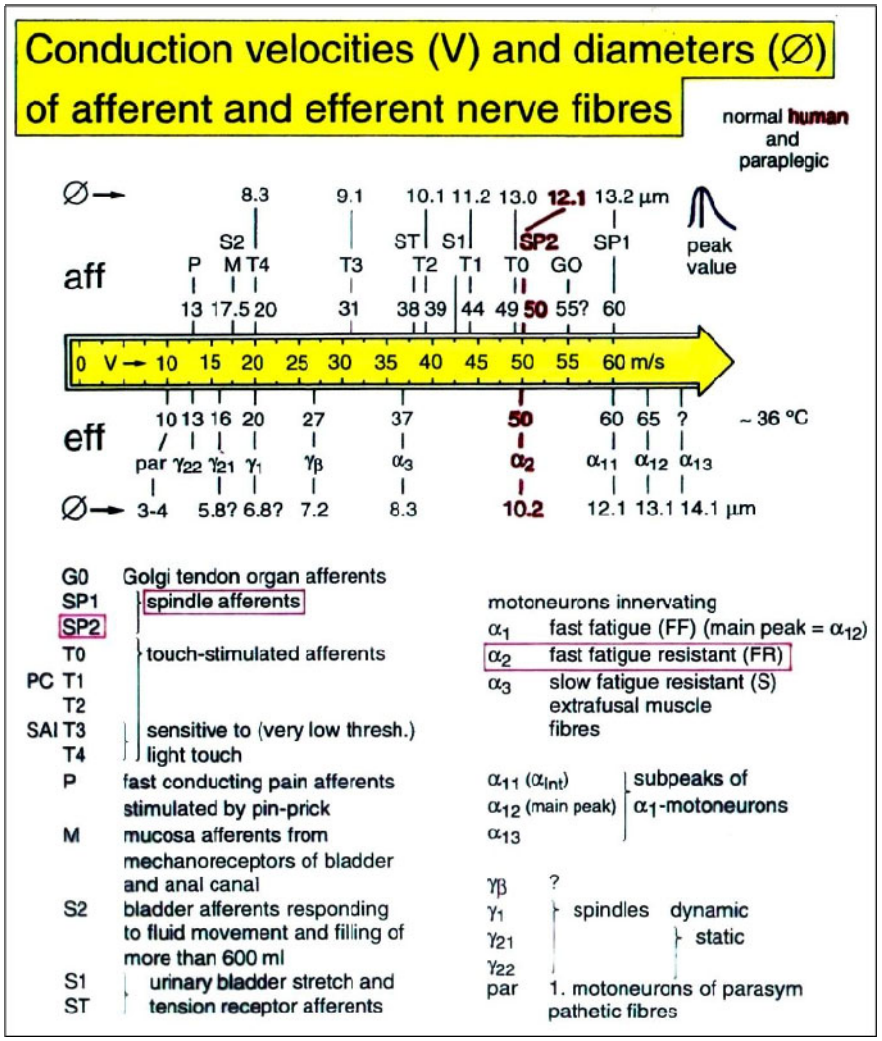

Figure 7. Classification scheme for human peripheral nerve fibers. Conduction velocities (V) and nerve fiber diameters (∅) of afferent and efferent nerve fiber groups in normal humans and in patients with a traumatic spinal cord lesion for 0.5 to 6 years. The splitting of the α_1-motoneurons into the 3 subgroups, α_{11}, α_{12}, α_{13}, has not yet been confirmed. This is the only existing classification scheme for human nerve fibers!

With this classification and identification scheme it became possible to record natural impulse patterns simultaneously from identified single afferent and efferent nerve fibers and analyze the self-organizing mechanism "phase and frequency coordination" of the human CNS under physiologic and pathologic conditions and find therapy to repair the human CNS.

The drawing back of the single-nerve fiber action potential recording method is that it is an invasive recording method. But with surface electromyography (sEMG) one can record non-invasively coordination among motoneurons via the motor units if one records from suitable patients, like incomplete spinal cord injury patients, when a certain muscle is only still innervated by a few motoneurons. With the sEMG the tremor of patients with Parkinson's disease will be analyzed.

The improvement of CNS functioning will be measured with the coordination dynamics values. With a single value the organization of the human CNS is characterized. Figure 8 shows a spinal cord injury patient during exercising on the special CDT device in the sitting position. The arrhythmicity of exercising, the coordination dynamics, of the patient is measured. Simultaneously sEMG is performed.

For treatment, especially for severely injured patients, the exercising on a special CDT in the lying position is suitable **(Figures 8 and 9)**.

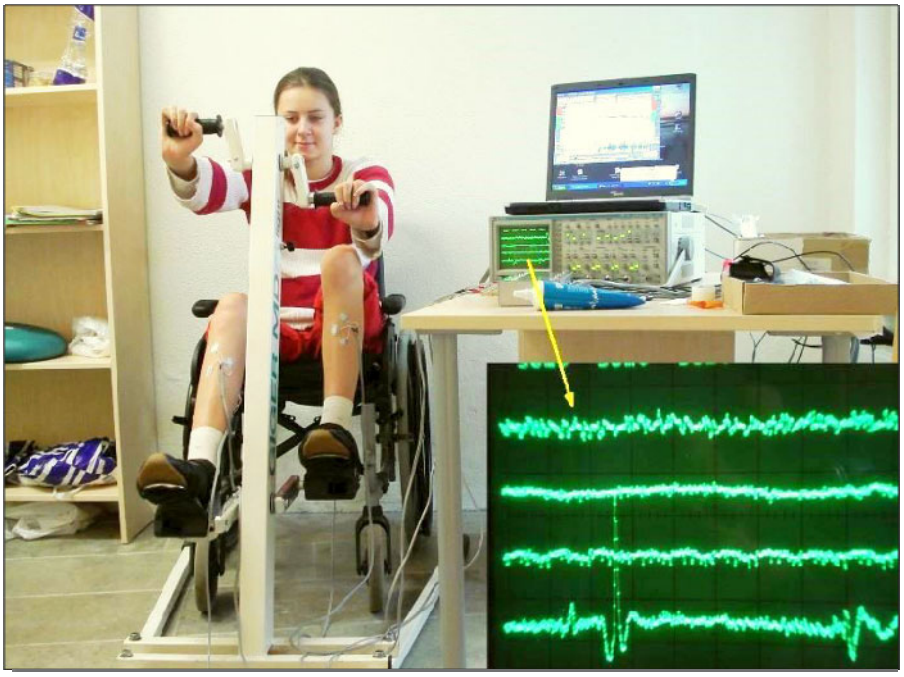

Figure 8. Layout for measuring coordination dynamics (arrhythmicity of exercising) between arm and leg movements, displayed on the laptop; for the intermediate coordination's between pace and trot gait, the fluctuation of the network states is larger. The recording of sEMG activity (displayed on the oscilloscope) from the tibialis anterior and other muscles is also shown. The inset shows single motor unit action potentials on the lowest trace. The recordings are taken from a patient (Kadri) with a motoric complete cervical SCI C5/6 (95% injury).

Figure 9. The 11-year-old Nefeli with an incomplete SCI during exercising coordinated arm, leg and trunk movements to improve the coordinated firing of neurons and sub-neural networks. This special CDT device for measuring and therapy (int.pat.) is produced by the firm: Giger Engineering, Martin Giger dipl.Ing.ETH/SIA, Herrenweg 1, 4500 Solothurn, Switzerland, www.g-medicals.ch.

RESULTS

OSCILLATORY FIRING OF HUMAN MOTONEURONS FOR HIGH ACTIVATION

Oscillatory Firing of α_1, α_2, and α_3-Motoneurons

The most important finding with the single-nerve fiber action potential recording method is that nerve cells in the human CNS are organizing themselves through phase and frequency coordination. In nerve fibers, this phase and frequency coordination can easily be measured, because the three motoneuron types fire for high activation oscillatory [10-13] and offer in this way a structure to which the timed firing of neurons can be related to. Since the α_2-motoneuron oscillations are most stable, firing phases of neurons will be related mostly to the α_2-motoneuron firings. It is started with the oscillatory firing of the three motoneuron types.

Figure 10 shows schematically the oscillatory firing patterns of the three kinds of motoneurons and the muscle fiber types they innervate. The differences between the three premotor oscillator types will be considered in more detail.

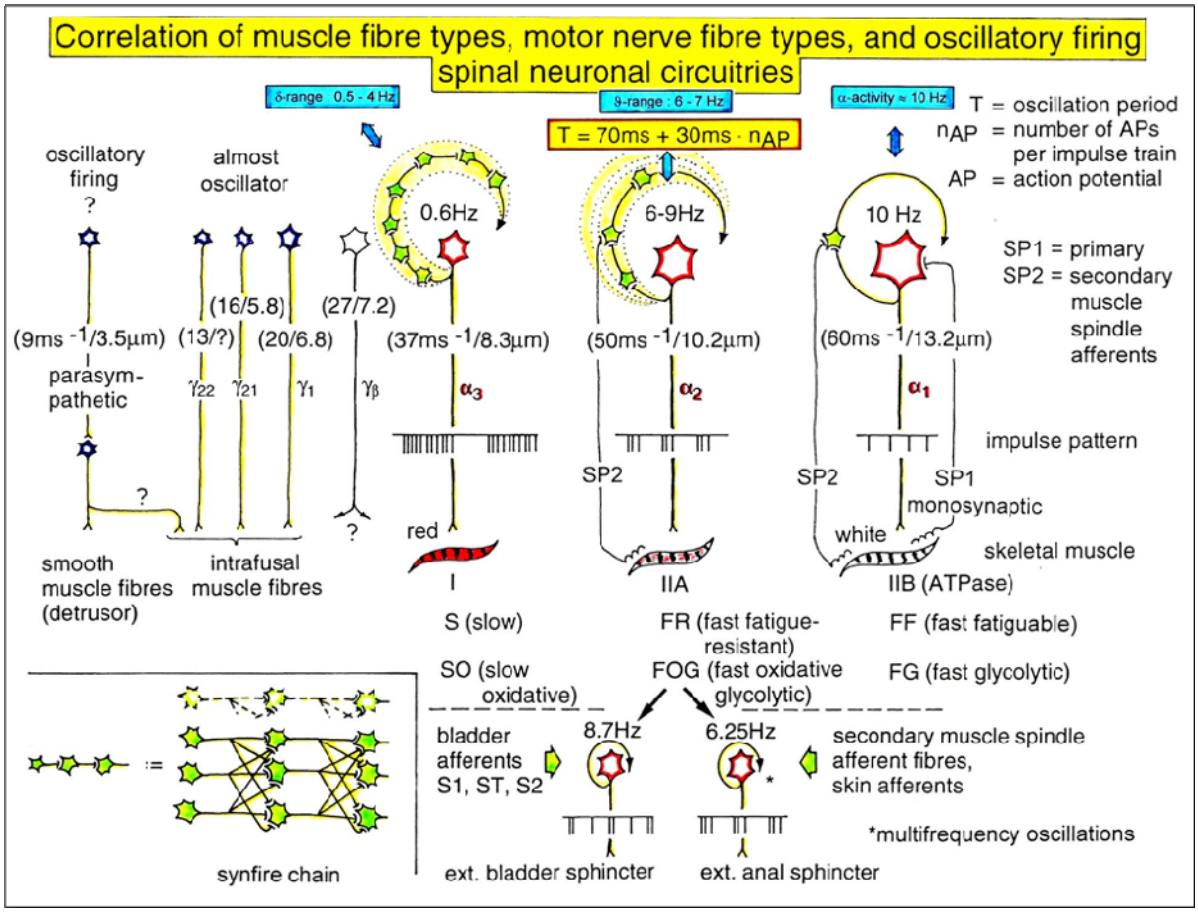

Figure 10. Correlation of muscle fiber types, motor nerve fiber types, and oscillatory firing spinal neuronal networks (oscillators), based on histochemical, morphological and physiological properties. This figure provides a simplified correlation between muscle fiber, motoneuron and sacral oscillator types. No additional subtypes have been included. The existence of α_1-motoneuron (FF) oscillators firing at 10 Hz has been predicted and they have been identified in paraplegics (unpublished observation). α = motoneuron, γ_1, γ_2 = dynamic and static fusimotors, parasympathetic = parasympathetic preganglionic motoneuron. S1, ST, S2 = stretch, tension and flow receptor afferents.

α_1-oscillators: The α_1-motoneurons fire oscillatory with one action potential at 10 Hz and higher and innervate fast fatigue (FF) muscle fibers. The stability of oscillatory firing is low, and they are driven by primary muscle spindle afferents. **Figure 11** shows an original recording of an α_1-motoneuron action potential (AP), activated by a primary spindle afferent AP. Duration of oscillation periods and phase durations between the oscillatory α_1-motoneuron and the primary spindle afferent fiber are given. They show an absolute correlation. α_1-motoneuron motor units can easily be recorded by sEMG.

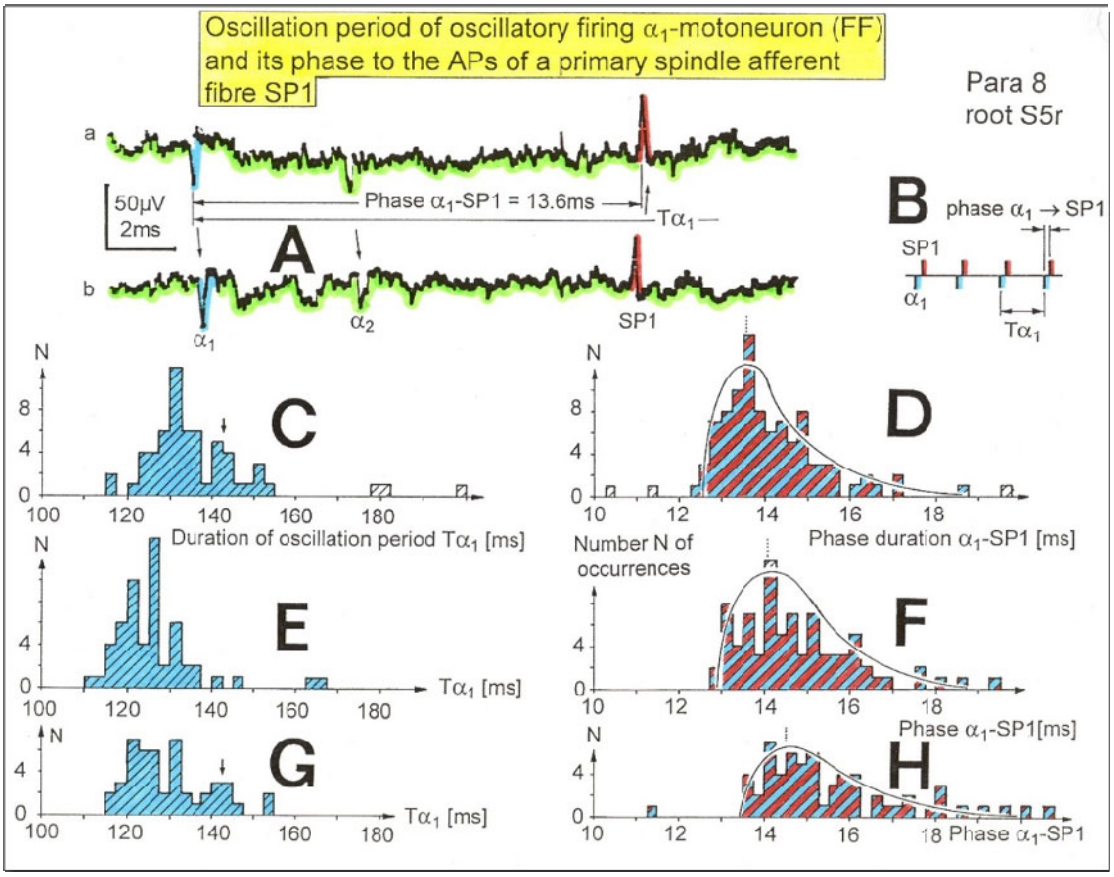

Figure 11. Distribution of the oscillation period of an oscillatory firing α_1 – motoneuron (FF) and the phase to its driving primary muscle spindle afferent fiber SP1. Recordings were taken with the single nerve-fiber action potential recording method. A. Original recording of the action potentials of the α_1 – motoneuron and SP1-fibre. B. Definition of oscillation period $T\alpha_1$ and phase $\alpha_1 \rightarrow$ SP1. C-H. Oscillation periods and the corresponding phases following different stimulation. In 'C' and 'G', the small arrows mark sub peaks in the oscillation period distributions. Para 8, right root S5.

α_2-oscillators: The α_2-motoneurons fire oscillatory with an action potential train of 2 to 4 APs at a frequency around 6 Hz and innervate fatigue resistant muscle fibers (FR). An original recording of oscillatory firing is shown in **Figure 12A**. It could be shown for a sphincteric urinary bladder α_2-motoneuron that with bladder filling the α_2-motoneurons fired occasional, transient oscillatory and continuous oscillatory **Figure 12D**). The characteristics of α_2-oscillators are in between those of the α_1 and the α_3-oscillators. They are self-organized by the adequate afferent input patterns from several kinds of receptors. During oscillatory firing the α_2-motoneurons showed relative phase correlation to the driving secondary muscle spindle afferents and bladder afferents **(Figures 12B and 13)**.

α_3-oscillators: An original recording from an oscillatory firing α_3-motoneuron is shown in **Figure 14.** The insert "C" shows a schematic layout of the firing. The duration of the interspike intervals of the impulse train increases regularly at the beginning of the impulse train and does alternate between long and short values at the end of the impulse train. This long-short alternation of interspike intervals may be due to a coupling phenomenon between oscillators. Alternating firing with short and long oscillation periods has also been observed for α_2-oscillators and may be connected with the existence of antagonistic inhibition of network structures similar to half-center oscillators.

Regular Oscillatory Firing of α_2-Motoneurons in Brain-Dead Human

Figure 15 shows an impulse train triplet of an oscillatory firing α_2-motoneuron (O2) of the brain-dead individual HT6 [14] to secure bowel continence. The firing pattern is schematically drawn in **Figure 15B**. Distributions of the oscillation period and of the first and the second interspike intervals are plotted in **Figure 15C-15E**.

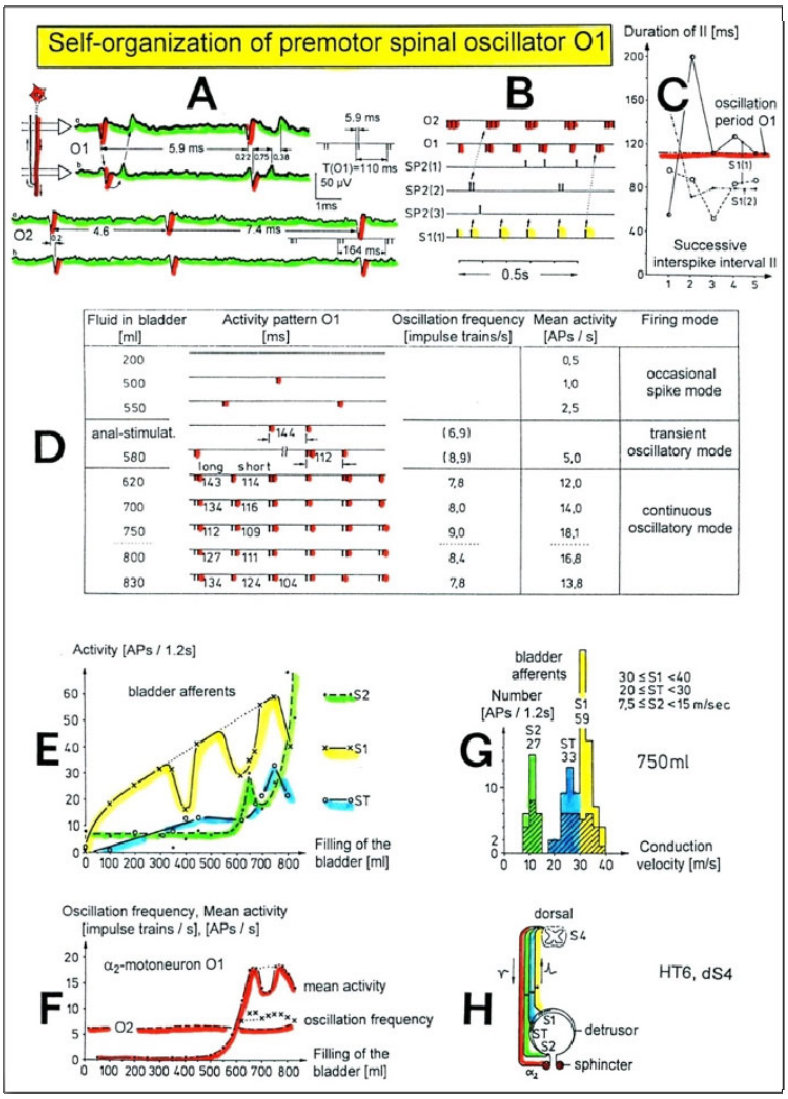

Figure 12. Self-organization of premotor spinal α_2-oscillator O_1, which innervates the external urinary bladder sphincter (skeletal muscle). Brain-dead human HT6; recording from a dorsal S4 nerve root. A. Recordings from α_2-motoneurons O_1 and O_2, firing in the oscillatory mode with impulse trains of 2 (upper recording) and 3 (lower recording) action potentials (APs). The durations of the oscillation periods were 110 (O_1) and 164ms (O_2). The interspike intervals of the impulse trains were 5.9ms (O_1) and 4.6 and 7.4ms (O_2). Motoneuron O_1 conducted at 36 m/s; its recurrent fiber conducted at 21 m/s. The measurement layout is shown schematically. The inserts show the oscillatory firing modes; they have not been drawn to scale. B. Impulse patterns of oscillatory firing α_2-motoneuron O_2 innervating the external anal sphincter, in relation to the muscle spindle afferent activity SP2(1 to 3), activated by the stretch of the anal sphincter by the anal catheter, and impulse patterns of oscillatory firing α_2-motoneuron O_1 innervating the external urethral sphincter, in relation to the stretch receptor afferent activity (S1(1)) of the urinary bladder, activated by 750 ml bladder filling. Phase relations between APs of SP2(2) and O2 and between APs of S1(1) and O_1 are indicated by the small arrows. C. Three series of successive interspike intervals of the 2-stretch receptor afferent fibers S1(1) and S1(2) activated by retrograde bladder filling. The oscillation period of oscillatory firing motoneuron O_1, activated only by bladder filling is shown. D. The firing in the occasional spike mode, the transient and the constant oscillatory firing mode of α_2-motoneuron O_1 in response to filling of the bladder. In the 'activity pattern' column changing durations of oscillation periods are given. The oscillation frequencies in the brackets give the frequencies at the moment of oscillation for the transient oscillatory mode. Downward deflections are schematized APs. Interspike intervals of the close APs ≈ 6.0ms (A). E. Activity levels of stretch (S1) and tension (ST) and flow receptor afferents (S2) (E) and of sphincter α_2-motoneuron O_1 (F) in response to retrograde filling of the bladder. The activity values of the S1, ST and S2 afferents are taken from histograms like the one in G. Filling of the bladder was stopped once between 600- and 650-ml. F. The small dotted lines represent mean activity (APs/s) and oscillation frequency (impulse trains/s) of α_2-motoneuron O_1 if bladder filling were not stopped in between. Note that the mean activity increases continuously with the filling of the bladder from 550 to 650 ml, even though motoneuron O_1 started to fire in the oscillatory mode from 620 ml on (D). Note further that the oscillatory firing motoneuron O_2 (frequency of firing with impulse trains is shown) is nearly not affected by the filling of the bladder and by the start of the oscillatory firing of motoneuron O_1. G. Conduction velocity frequency distribution histogram of stretch, tension and flow receptor afferent activity at 750 ml. The activities of afferents S1, ST and S2 are quantified by counting the afferent conduction velocities under the peaks (open plus hatched part), with the conduction velocity limits given in the insert. The counts (27, 33, 59) are given below the peak labeled S1, ST and S2 and plotted into E for the afferent activity at 750 ml. H. Schematic drawing of the anatomical arrangement of the afferents and the motoneuron O_1.

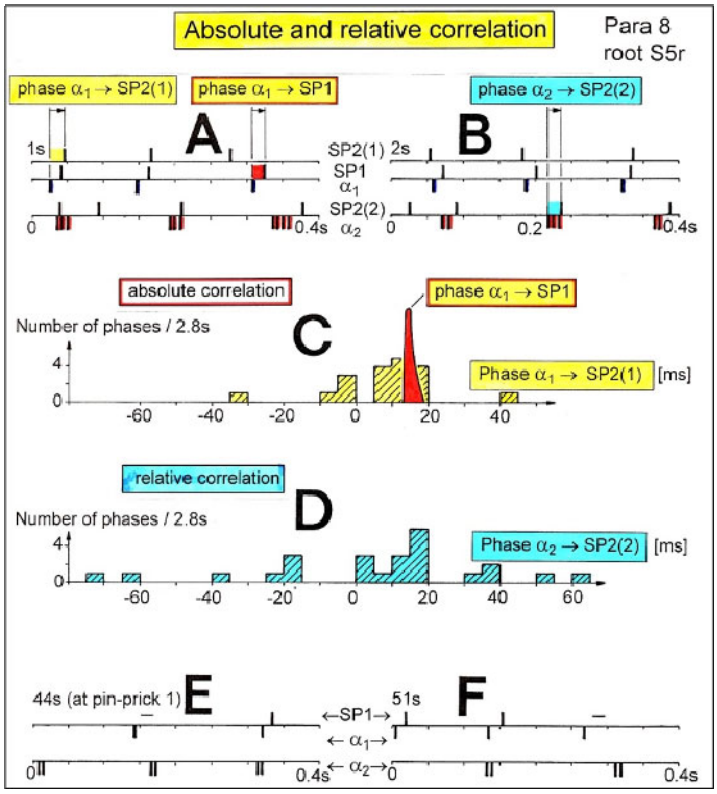

Figure 13. Absolute and relative correlation quantified by phase relations between the α_1 (FF) and α_2-motoneurons (FR) and their driving primary (SP1) and secondary (SP2) muscle spindle afferent fibers. A, B. Definition of the different phases. C. Distribution of the phases between α_1-motoneuron and the secondary muscle spindle afferent fiber SP2(1). Note that the phase distribution $\alpha_1 \rightarrow$ SP2(1) is approx. 40 times wider than that of the $\alpha_1 \rightarrow$ SP1 distribution (phase $\alpha_1 \rightarrow$ SP1 taken from Fig.65). D. Distribution of the phases between α_2-motoneuron and the secondary muscle spindle afferent fiber SP2(2). Note that the phase distribution $\alpha_2 \rightarrow$ SP2(2) is similar to that of $\alpha_1 \rightarrow$ SP2(1) (approx. 4 times wider). E, F. Note that every SP1-action potential is accompanied by a time-locked α_1-motoneuron action potential (AP). Para 8, root S5r.

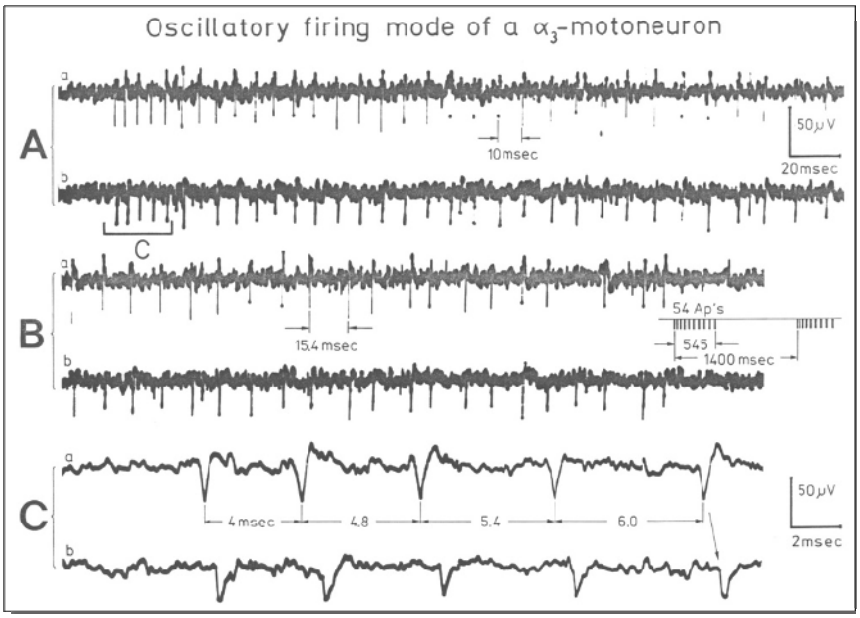

Figure 14. An impulse train (54 APs) of oscillatory firing α_3-motoneuron O_3 of brain-dead HT5. "B" is the continuation of "A." The duration of the oscillation period was approximately 1400 ms (insert "B"). The start of the impulse train is shown time-expanded in C.

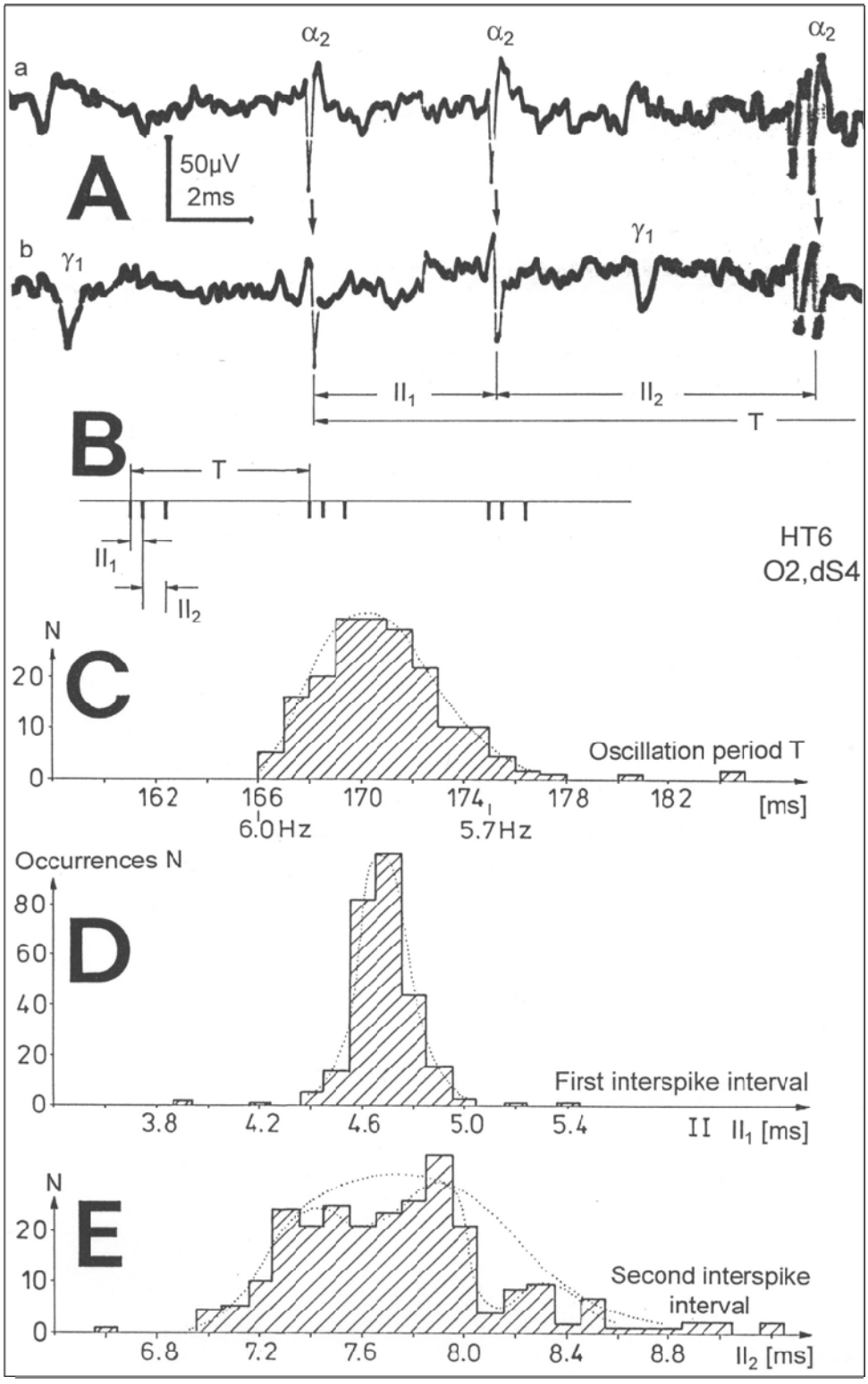

Figure 15. Distribution of oscillation period (T) (C), first (II_1) (D) and second interspike intervals (II_2) (E) of a α_2-motoneuron, firing repeatedly with three AP impulse trains. A. Original recording of the three AP impulse train; II_1, II_2 and T are indicated. γ_1 marks APs from a γ-motoneuron. B. Schematic drawing of the impulse pattern of the α_2-motoneuron. Note that, the distribution of II_2 (E) may consist of three subpeaks. Brain-dead human HT6.

The distributions of the oscillation period and of the first interspike interval are smooth and show no obvious subpeaks. The distribution of the second II shows subpeaks suggesting interactions with other oscillatory firing circuitries. The narrow distribution of the oscillation period, and the interspike intervals of the impulse train show that the oscillatory firing network fired very regularly. Other spinal oscillators in brain-dead individuals fired just not as regularly as the one shown in **Figure 15**. It is concluded that in brain-dead and normal individuals, the neuronal networks, driving the motoneurons, fire regularly with some variation. The impulse patters show little variation, are stable and can easily identified **(Figure 16)**. It will be shown below that this regularity is lost following spinal cord injury.

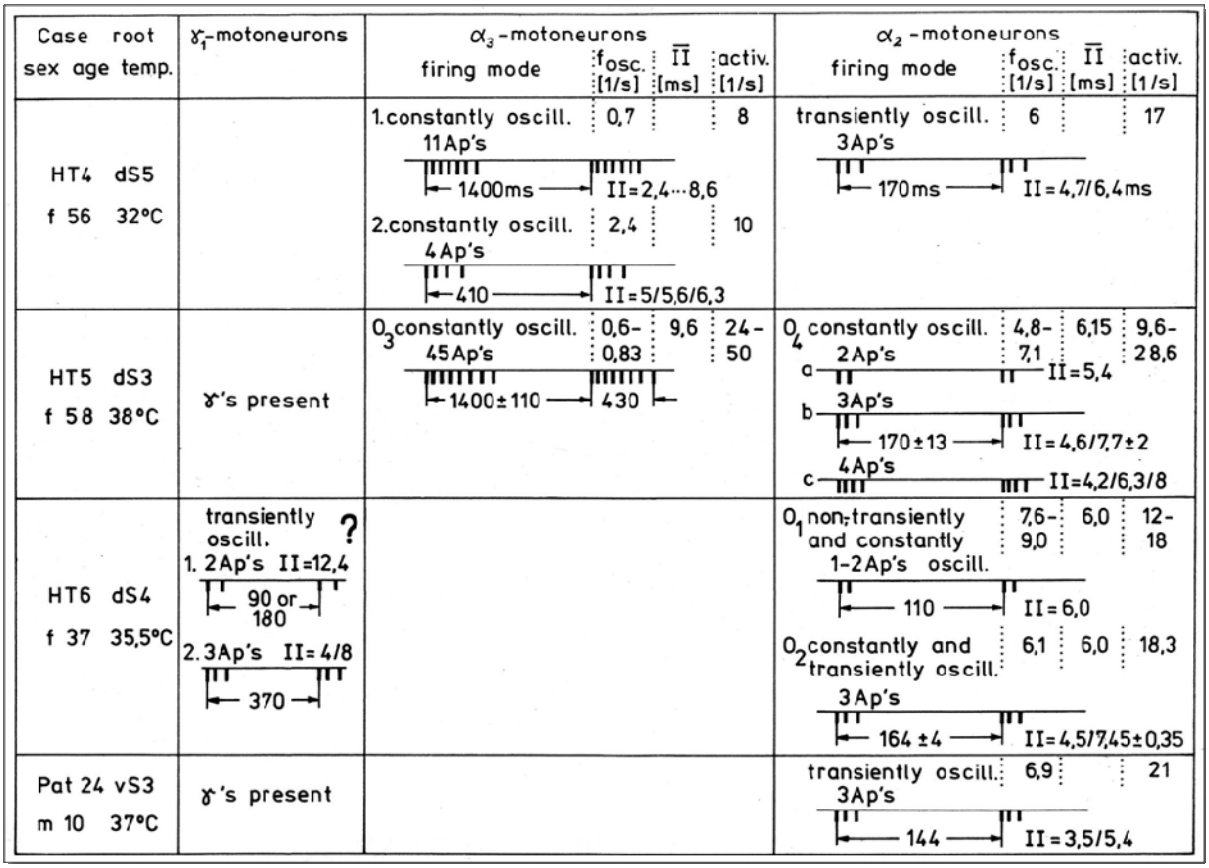

Figure 16. Oscillatory firing modes of α_2, α_3 and γ-motoneurons measured from three HTs and one patient (Pat), m = male, f = female, age in years, temp = central temperature, d = dorsal, v = ventral, S = sacral, fosc = oscillation frequency, mean II = mean inter spike interval, activ. = activity (APs/s), s = sec, ms = ms. Downward deflections in the schematically drawn activity modes indicate the APs of the repetitive activity. Time from impulse train to impulse train indicates the duration of the cycle period in ms. II = interspike interval in ms, ± = absolute error (standard deviation, number of measurements between 50 and 100). O1, O2, O3, O4 = designation of motoneurons, which will be referred to in all Figures, non- = occasional spike mode, transiently oscill. = transient oscillatory firing mode, constantly oscill. = constant oscillatory firing mode.

Irregular Oscillatory Firing of α_2-Motoneurons Following Spinal Cord Injury

Following spinal cord injury, mean values of oscillation period and interspike intervals for oscillatory firing motoneurons show much more variation **(Figure 17)** than do normal values (HTs, **Figure 16**) [10,14].

The most regular oscillatory firing α_2-motoneuron in a paraplegic patient fired nearly as regularly as the α_2-motoneuron of the brain-dead individual HT6 **(Figure 15)**. On the other hand, some oscillatory firing α_2-motoneurons of paraplegics fired extremely irregularly so that it was difficult or even impossible to identify the kind of the motoneuron from the impulse patterns **(Figure 17)**. The distributions of the oscillation period and interspike intervals of the impulse train from an α_2-motoneuron in paraplegic 8 showed more scatter than those obtained for HT6 **(Figure 15)**. For further, see Chapter III of [7].

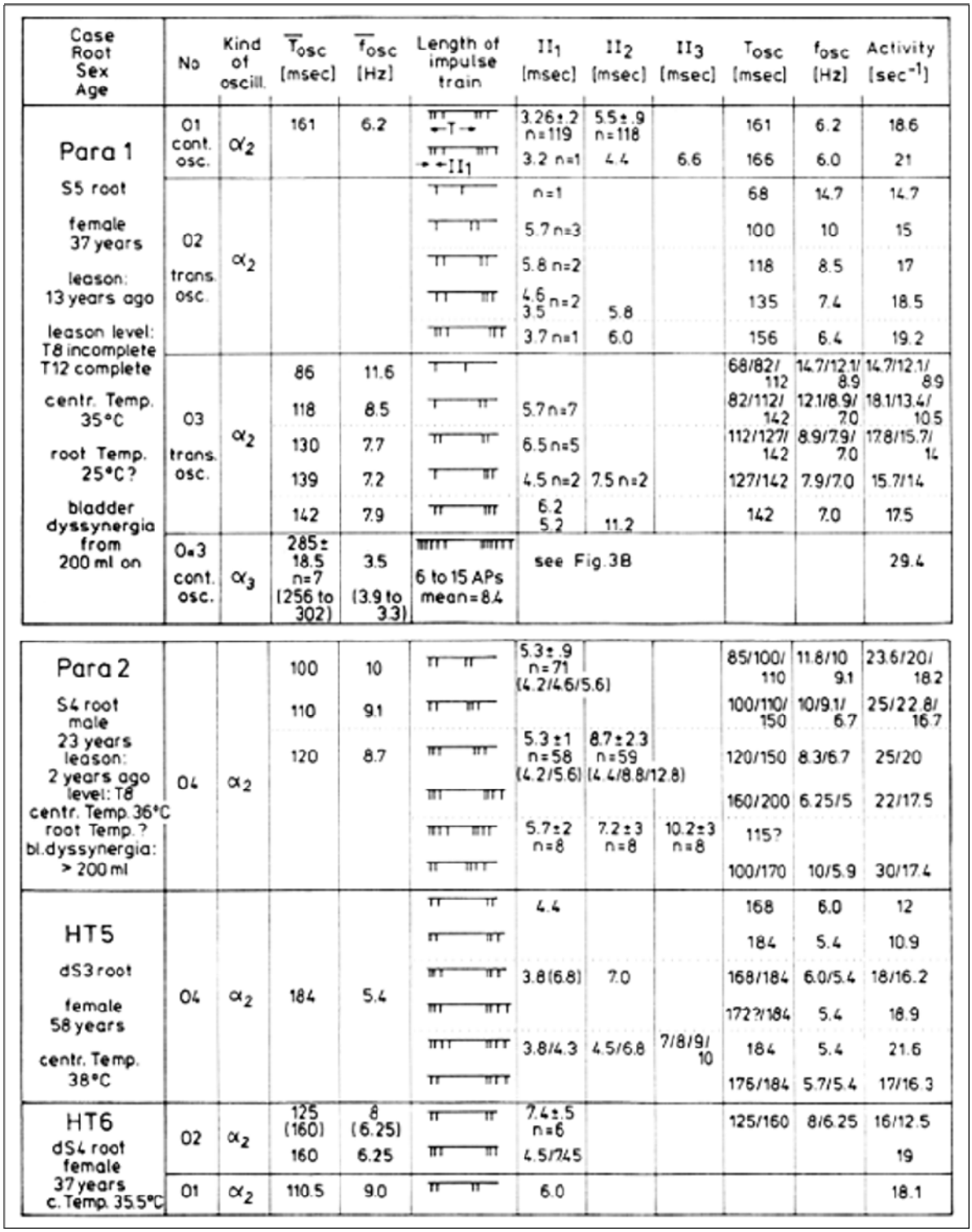

Case Root Sex Age	No	Kind of oscill.	$\overline{T}_{osc}$ [msec]	$\overline{f}_{osc}$ [Hz]	Length of impulse train	II_1 [msec]	II_2 [msec]	II_3 [msec]	T_{osc} [msec]	f_{osc} [Hz]	Activity [sec^{-1}]
Para 1	01 cont. osc.	α_2	161	6.2	←T→	3.26±.2 n=119	5.5±.9 n=118		161	6.2	18.6
					←II_1→	3.2 n=1	4.4	6.6	166	6.0	21
S5 root female 37 years lesion: 13 years ago lesion level: T8 incomplete T12 complete centr. Temp. 35°C root Temp. 25°C? bladder dyssynergia from 200 ml on	02 trans. osc.	α_2				n=1			68	14.7	14.7
						5.7 n=3			100	10	15
						5.8 n=2			118	8.5	17
						4.6 3.5 n=2	5.8		135	7.4	18.5
						3.7 n=1	6.0		156	6.4	19.2
	03 trans. osc.	α_2	86	11.6					68/82/112	14.7/12.1/8.9	14.7/12.1/8.9
			118	8.5		5.7 n=7			82/112/142	12.1/8.9/7.0	18.1/13.4/10.5
			130	7.7		6.5 n=5			112/127/142	8.9/7.9/7.0	17.8/15.7/14
			139	7.2		4.5 n=2	7.5 n=2		127/142	7.9/7.0	15.7/14
			142	7.9		6.2 5.2	11.2		142	7.0	17.5
	0a3 cont. osc.	α_3	285± 18.5 n=7 (256 to 302)	3.5 (3.9 to 3.3)	6 to 15 APs mean=8.4	see Fig. 3B					29.4
Para 2 S4 root male 23 years lesion: 2 years ago level: T8 centr. Temp. 36°C root Temp.? bl.dyssynergia: > 200 ml	04	α_2	100	10		5.3±.9 n=71 (4.2/4.6/5.6)			85/100/110	11.8/10 9.1	23.6/20/18.2
			110	9.1					100/110/150	10/9.1/6.7	25/22.8/16.7
			120	8.7		5.3±1 n=58 (4.2/5.6)	8.7±2.3 n=59 (4.4/8.8/12.8)		120/150	8.3/6.7	25/20
									160/200	6.25/5	22/17.5
						5.7±2 n=8	7.2±3 n=8	10.2±3 n=8	115?		
									100/170	10/5.9	30/17.4
HT5 dS3 root female 58 years centr. Temp. 38°C	04	α_2	184	5.4		4.4			168	6.0	12
									184	5.4	10.9
						3.8(6.8)	7.0		168/184	6.0/5.4	18/16.2
									172?/184	5.4	18.9
						3.8/4.3	4.5/6.8	7/8/9/10	184	5.4	21.6
									176/184	5.7/5.4	17/16.3
HT6 dS4 root female 37 years c. Temp. 35.5°C	02	α_2	125 (160)	8 (6.25)		7.4±.5 n=6			125/160	8/6.25	16/12.5
			160	6.25		4.5/7.45					19
	01	α_2	110.5	9.0		6.0					18.1

Figure 17. Oscillatory firing modes of α_2 and α_3-motoneurons from two paraplegics (Para 1,2) and two HTs (brain-dead humans). Centr. Temp. = central temperature; cont. osc. = continuously oscillating; trans. osc. = transiently oscillating. Mean T_{osc} = mean oscillation period; f_{osc} = mean oscillation frequency; II_1, II_2, II_3 = first, second and third interspike interval of the impulse train; activity measured in action potentials (APs) per second. Downward bars in the schematically drawn activity modes indicate APs of the repetitive activity. ± = error (standard deviation); n = number of observations. O1, O2, O3, O4, Oα3 = designations of oscillatory firing motoneurons, which will be referred to in all Figures. The central temperature of 38°C in HT5 was due to an infection.

A change from two to three AP impulse train firing in an α_2-motoneuron can be mimicked if one records intracellularly with glass electrodes from frog twitch or denervated slow muscle fibers. When the depolarizing pulse amplitude is increased to mimic depolarization through excitatory postsynaptic potentials, the action potential train changes from two to three action potentials **(Figure 18)**. An impulse train consisting of two, three or four action potentials could therefore be generated by a depolarization of the human motoneuron. The repeated firing with impulse trains, during the oscillatory firing could be achieved through an excitatory loop of interneurons. For theories of hypothetical network oscillators see chapter III of [7].

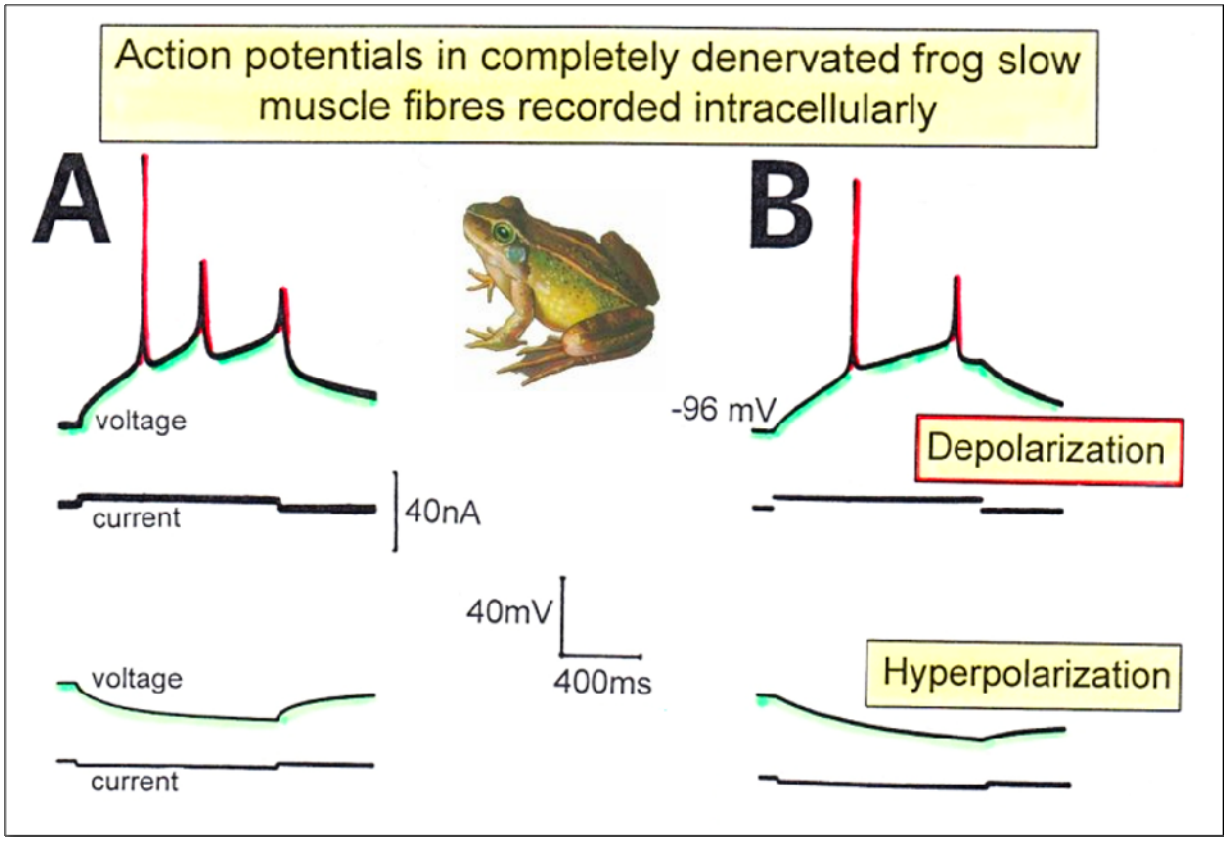

Figure 18. APs generated in denervated slow muscle fibres of frog piriformis muscles upon depolarization by transient current pulses of 100 ms duration. The slow time course of the voltage upon hyperpolarizing the fibre shows that the microelectrodes were impaled into slow muscle fibres. With increasing depolarizing current pulses (and fully developed AP mechanism), first one AP is mostly generated, then two APs (B) and then three APs (A). Note with respect to the relative length of the interspike intervals that the two AP impulse train in B and the three AP impulse train in A bear's similarity to the impulse trains recorded from oscillatory firing human α_2-motoneuron axons.

The deterioration of the intrinsic apparatus of the spinal cord, following spinal cord injury, can be most easily seen when plotting frequency distributions of premotor spinal oscillators from a brain-dead human, a paraplegic and a predicted healthy human **(Figure 19)**. The premotor network oscillator lost nearly the specific eigenfrequency **(Figure 19)** and could be activated by all kinds of input with the consequence of the generation of pathologic patterns called spasticity. The extensor spasticity can be very strong especially in thoracic spinal cord injury **(Figure 20)**. By a movement-based learning therapy, called coordination dynamics therapy, the neural networks of the intrinsic apparatus of spinal cord can partly be repaired, so that SCI patients can relearn walking **(Figures 1-3)** and get the urinary bladder and other functions repaired [3].

In Parkinson disease patients the pathology is different. The intrinsic apparatus of the spinal cord is not traumatically damaged. Because of missing inhibition, motoneurons synchronize and generate tremor. Pathology and the network repair are analyzed below.

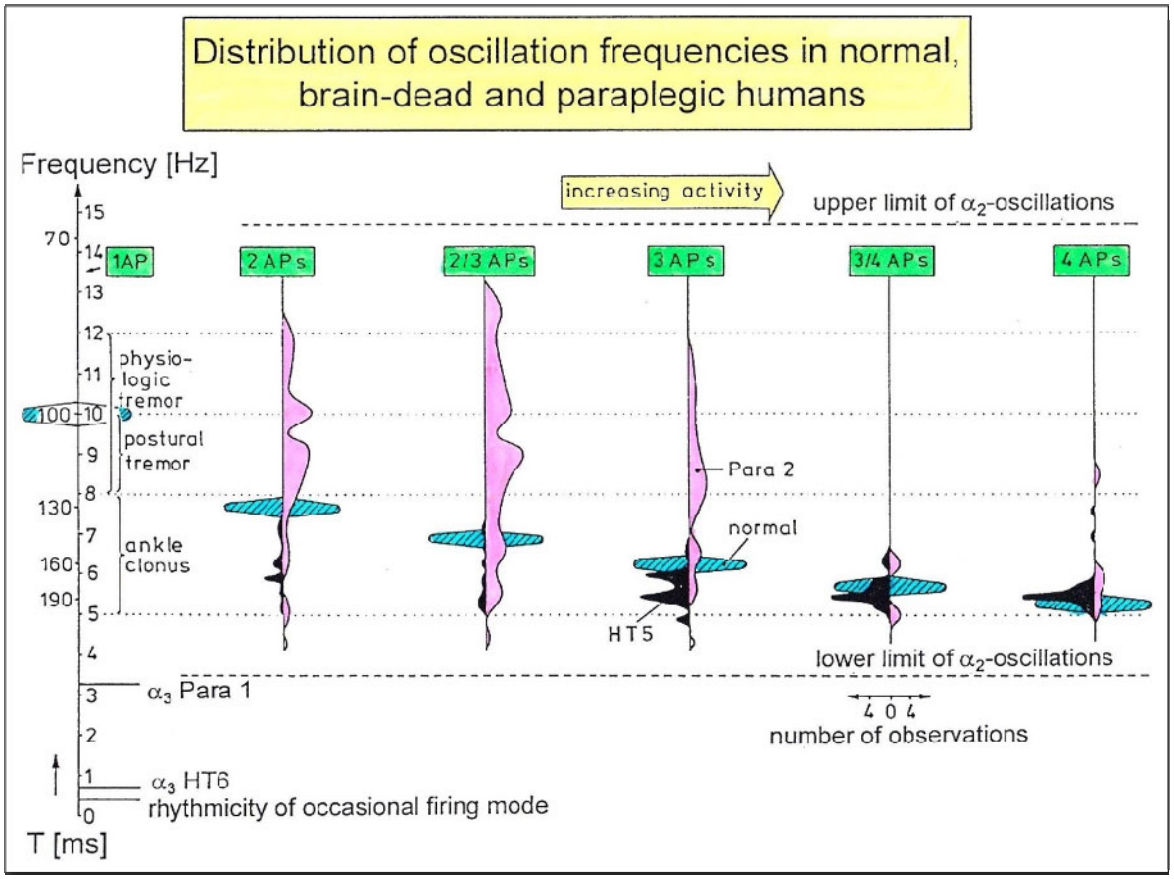

Figure 19. Distributions of oscillation frequencies of continuously oscillatory firing α_2-motoneurons with increasing number of APs per impulse train (increased activity) in paraplegic 2 (open), in the brain-dead HT5 (filled), and in probably normal humans (cross-hatched). Frequencies and rhythmic activity changes in the occasional and oscillatory firing mode are indicated. Ranges of physiologic tremor, postural tremor and ankle clonus are also drawn. Note that frequencies for the brain-dead HT5 are too low, and the oscillation frequencies of the spinal cord isolated for a long time (Para 2) are too high and to spread as compared to the theoretically predicted frequency ranges of healthy humans (cross-hatched). T = oscillation frequency.

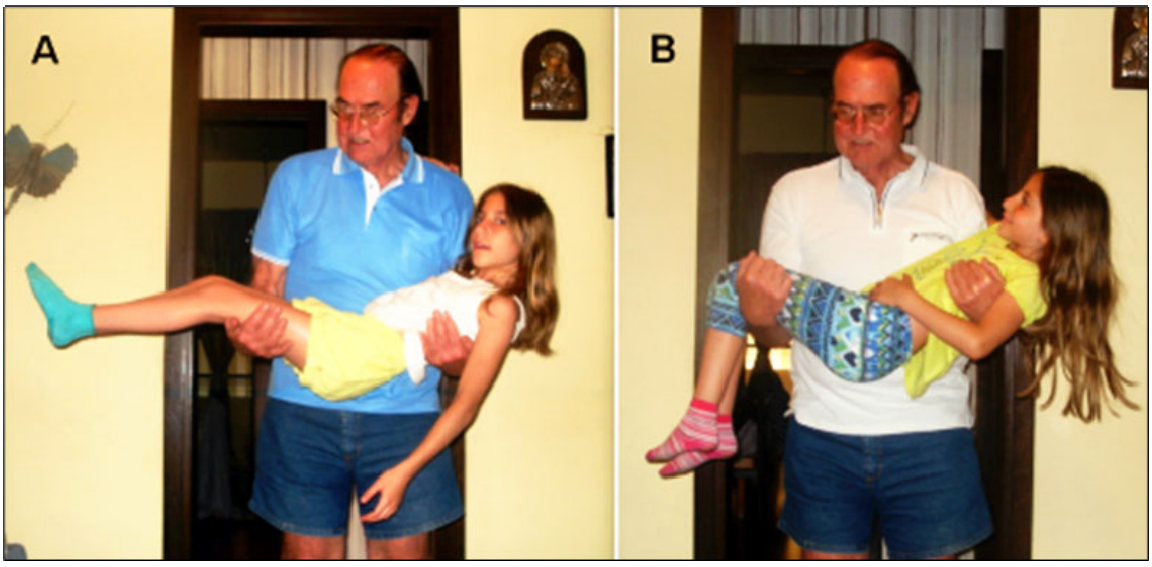

Figure 20. Practical judgment of extensor spasticity. When the Author holds the patient Nefeli (SCI Th10), one can judge her extensor spasticity by the extension of her legs (A). Her present spasticity is medium strong. A physiologic leg position can be seen in B. The healthy seven-year-old sister has no spasticity and the legs are flexed.

Static-dynamic behavior and oscillator stability of premotor spinal oscillators

With respect to dynamics, α_1-oscillators are the opposite of α_3-oscillators. The α_1-oscillators respond very dynamically but have only little oscillator strength. In **Figures 11 and 13** it can be seen that the firing of the α_1-motoneuron is absolutely correlated to the firing of the primary spindle afferent fiber SP1(phase $\alpha_1 \rightarrow$ SP1). Each AP of the SP1-fibre is correlated to an AP of the α_1-motoneuron. The SP1-fibre (primary spindle fiber) and the α_1-motoneuron fire rhythmically in absolute correlation. This is known from the stretch reflex. But the firing of α_1-motoneurons has also some correlation to secondary muscle spindle afferent activity: When the SP1-fibre stopped firing, the oscillatory firing α_1-motoneuron continued firing for one more oscillation period; in other words, it fired one further AP **(Figure 13F)**. The α_1-motoneuron could also start to fire before the SP1-fibre **(Figure 13E)**, which means that the α_1-motoneuron was getting also drive from other afferents, probably secondary muscle spindle afferents as the α_1-motoneuron fired also in relative correlation with a secondary spindle afferent fiber (**Figure 13C**, phase distribution $\alpha_1 \rightarrow$ SP2(1)). A simultaneously recorded oscillatory firing α_2-motoneuron fired oscillatory in relative coordination with a secondary muscle spindle afferent fiber (SP2) **(Figure 13D)**.

The static behavior of α_3-motoneurons can nicely be seen when they fire oscillatory. In **Figure 21**, the oscillatory firing α_3-motoneuron shows only little or no specific response to natural stimulation like bladder or anal catheter pulling. The dynamic of the response is weaker in comparison to that of the oscillatory firing α_2-motoneuron. In **Figure 22** an α_2-oscillator responded still less dynamically than an α_1-oscillator.

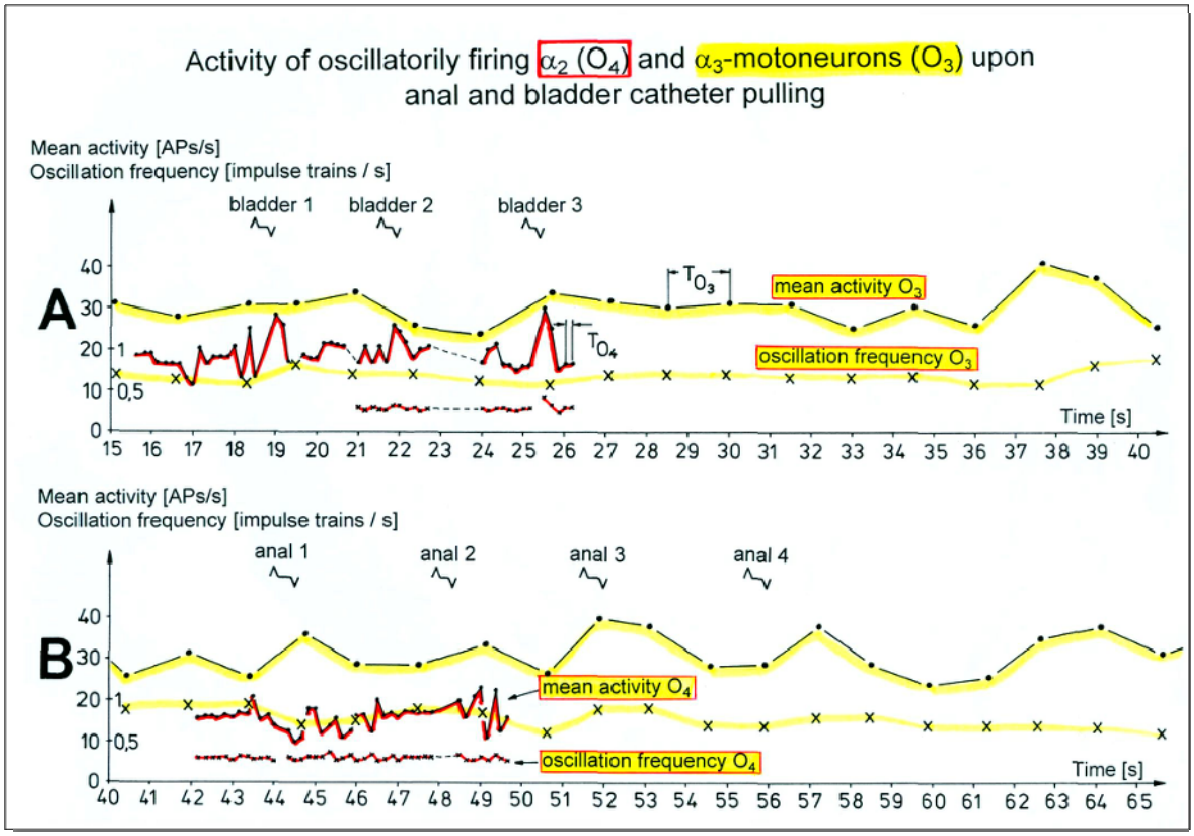

Figure 21. Mean activity (APs/s) and oscillation frequency (impulse trains/s) in response to urinary bladder (A) and anal catheter pulling (B) from oscillatory firing α_2-motoneuron O_4 (red) and α_3-motoneuron O_3, recorded simultaneously. Dots = mean activity, crosses = oscillation frequency, large dots and crosses refer to α_3-motoneuron O_3, the small ones to α_2-motoneuron O_4. Values from α_2-motoneuron O_4 only calculated for certain periods; the dashed lines indicate that the oscillation was not interrupted. The scale 0 to 1 relates to the oscillation frequency of α_3-motoneuron O_3; scale 0 to 40 relates to the mean activity of α_3-motoneuron O_3, and the mean activity and oscillation frequency of α_2-motoneuron O_4. $T(O_3)$ and $T(O_4)$ mark oscillation periods. Dots and crosses mark the mean activity and oscillation frequency at the end of the oscillation cycle period. Lines connect discrete values of mean activity to make trends more obvious. The time and duration of the pulling of bladder and anal catheters are marked; repeated stimulation is marked with numbers. Time, in seconds, continuous. HT5, dS3 root.

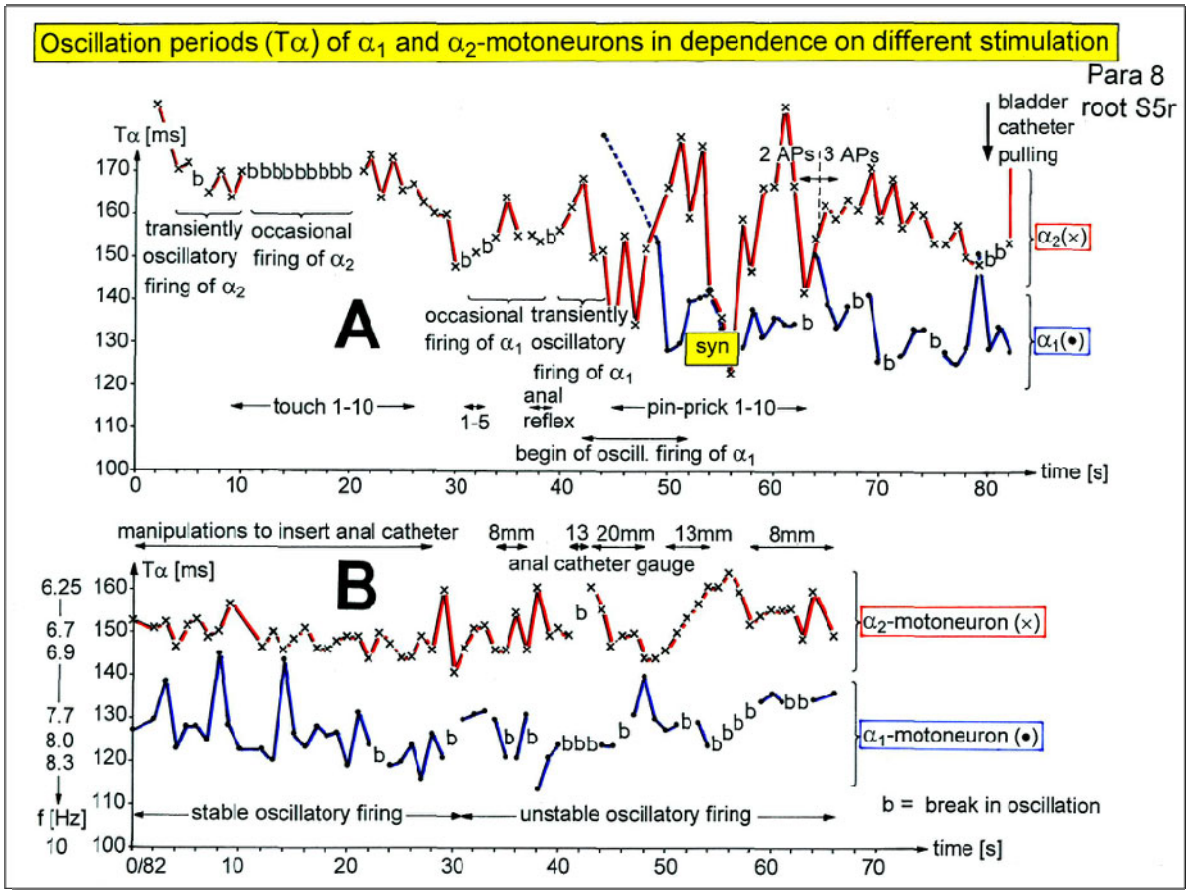

Figure 22. Oscillation periods (Tα) of an α_1 (FF) and an α_2-motoneuron (FR) in dependence on different stimulations; "B" is a continuation of "A." Touch 1 - 10 = Touching with a needle at points 1, 2,3,4,5 (upper row) and 6,7,8,9,10 (lower row). 1-5 = Touching from point 1 to point 5 (perpendicular to the direction of anal stimulation). 8, 13, 20, 13, 8mm = changing the diameter of the anal catheter from 8 to 13 to 20 to 13 and back to 8 mm (three gauges of anal catheter were used). syn = partial synchronization of the oscillatory firing patterns of the α_1 and the α_2-motoneurons. Two APs / three APs = impulse train of the α_2-motoneuron mainly consisted of two or three APs respectively. Note that α_1 and α_2-motoneurons first fired transiently oscillatory before firing continuously oscillatory. Note further that the oscillatory firing was most regular upon manipulation at the anus (0-30s in "B," anal reflex stimulation to secure continence).

The dynamics, therefore, increase from α_3 via α_2 to α_1-oscillator, in accordance with the dynamics of responses of the α-motoneuron firing in the occasional firing mode and in accordance with the muscle fiber types the three types of α-motoneurons innervate. The slow (S), medium fast (FR) (fast fatigue-resistant) and fast contracting muscle fibers (FF) (fast fatigable) have their own corresponding premotor networks in the spinal cord, namely the α_3, α_2 and α_1-networks **(Figure 10)** respectively.

The oscillator strength of the network firing is high for the α_2-oscillator. In **Figure 22B** the oscillation of the α_2-oscillator breaks (b) only once, the oscillation of the α_1-oscillator breaks 15 times. The α_3-oscillator oscillates continuously **(Figure 21A)**, but its function is unspecific. Generally, of course, the oscillation of all three oscillators depends on the input strength.

The α_2-motoneurons fire rather stable oscillatory for high activation and respond dynamically to specific input. If they are not inhibited, they will give rise to tremor in patients with Parkinson's disease (see below).

The firing patterns of α_1, α_2 and α_3-motoneurons can easily recorded with the single-nerve fiber action potential recording method but not with sEMG **(Figure 23)**. From spinal cord injury patients, on the other hand, single-motor unit APs can be easily recorded from α1 motor units but not from α_2 and α_3 motor units **(Figure 23)**, because their AP amplitude seems to be very small. Clinical EMG recordings therefore show mainly the activity of α1 motor units. Since only few α_1 motoneuron axons are contained in the lower sacral roots (not needed

for continence functions), α_1 motor activity has to be obtained from suitable sEMG recordings. The generation of patterns of α_1-motoneuron firings with increasing load has to be recorded with sEMG.

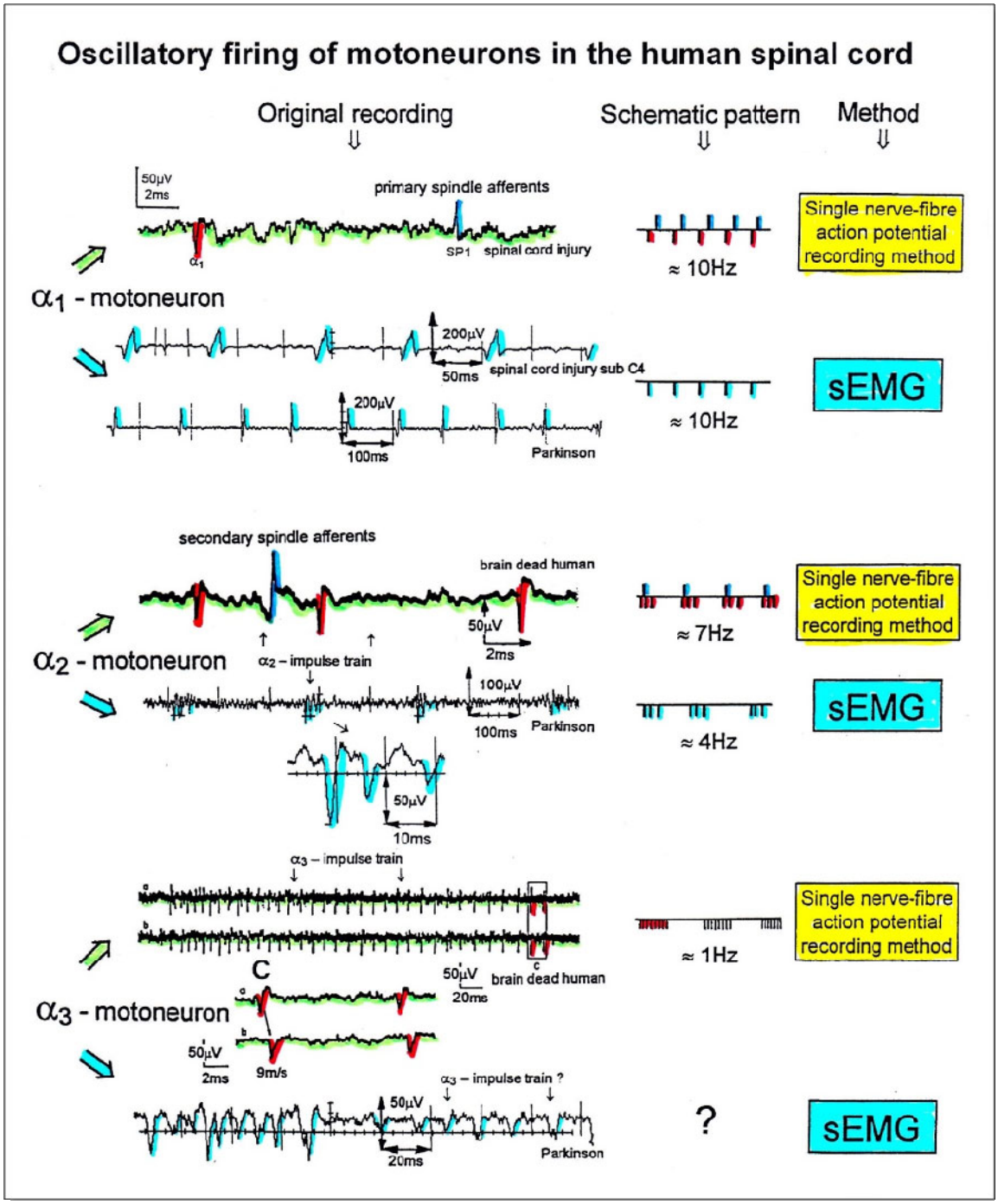

Figure 23. Oscillatory firing patterns of α_1, α_2, and α_3-motoneurons recorded from motoneuron axons with the single-nerve fiber action potential recording method and by surface electromyography (sEMG) from FF, FR, and S-type motor units. The left panel shows original recordings, the middle panel the schematic patterns; the recording methods are indicated on the right side. The recordings were taken from patients with spinal cord injury and Parkinson's disease and from brain-dead humans.

Coordinated Firing of Premotor Spinal Oscillators

The rhythmic firing of network oscillators is mainly coordinated **(Figure 24)**. Similarly, also the neuron firings of the whole neuronal network of the CNS are mainly coordinated. This coordination is achieved by the organization tendencies of the network, the descending impulse patterns from the brain and the spatiotemporal afferent impulse patterns from the periphery.

If the premotor spinal oscillators would not coordinate their firing and synchronize their firing for longer periods, tremor would occur. Such pathologic synchronization can be observed in patients with Parkinson's disease and will be shown below via sEMG **(Figure 51)**. If the neural networks are damaged by trauma, degeneration or malformation, the coordination between neuron firings becomes impaired and has to be repaired by movement-based learning.

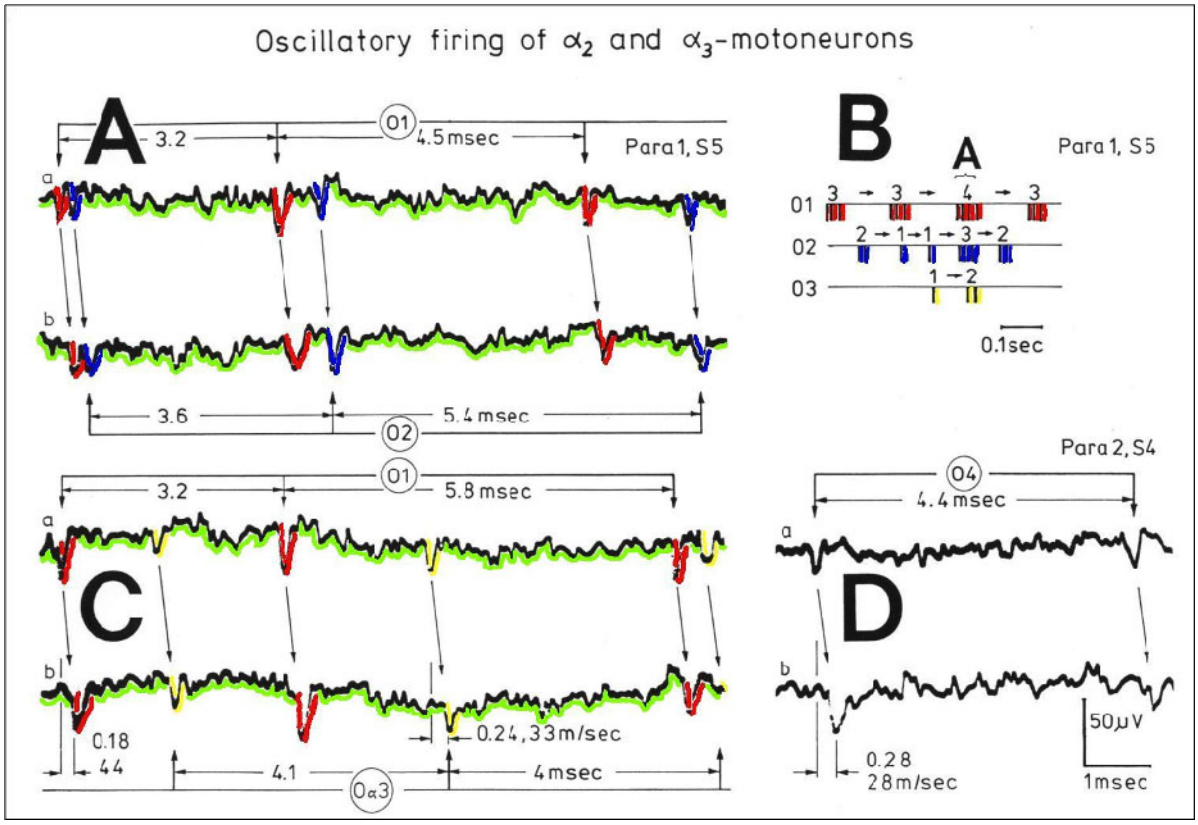

Figure 24. Recordings of impulse trains of oscillatory firing motoneurons in paraplegic 1 and 2. A. Impulse train of the continuously oscillatory firing α_2-motoneuron O1 (three of the four APs are shown) together with the impulse train of the transiently oscillatory firing α_2-motoneuron O2. Interspike intervals are indicated. B. Impulse patterns of the three oscillatory firing α_2-motoneurons O1, O2 and O3: O1 continuously oscillatory firing, O2 and O3 transiently oscillatory firing. "A" marks the sweep piece shown in A. Paraplegic 1. C. Impulse train of the α_2-motoneuron O1 together with a part of the impulse train of the oscillatory firing α_3-motoneuron Oα3. Interspike intervals, conduction times and conduction velocities are indicated. Paraplegic 1, S5 root recording. D. Impulse train (consisting of two APs) with the corresponding interspike interval, conduction time and conduction velocity of the continuously oscillatory firing α_2-motoneuron O4. Paraplegic 2, S4 root recording.

PHASE AND FREQUENCY COORDINATION AMONG OSCILLATORY FIRING MOTONEURONS AND ITS IMPAIRMENT FOLLOWING INJURY, MALFORMATION AND DEGENERATION

Phase and Frequency Coordination Between α_2-Motoneurons and their Adequate Afferent Drive in Brain-Dead Human

The coordination among neuron firings will be analyzed now in detail. It includes most likely all neurons of the CNS. It is an organization principle of CNS organization. With the single-nerve fiber action potential recording method the coordination is measured among the firings conducted in afferent and efferent nerve fibers. It was found that the coordination is given by the phases and frequencies among the action potentials (APs).

The relative phase and frequency coordination between the APs of the oscillatory firing α_2-motoneuron O2 and the secondary muscle spindle afferent fiber SP2(1) can directly be seen in the original recordings of **Figure 25** (brain-dead human).

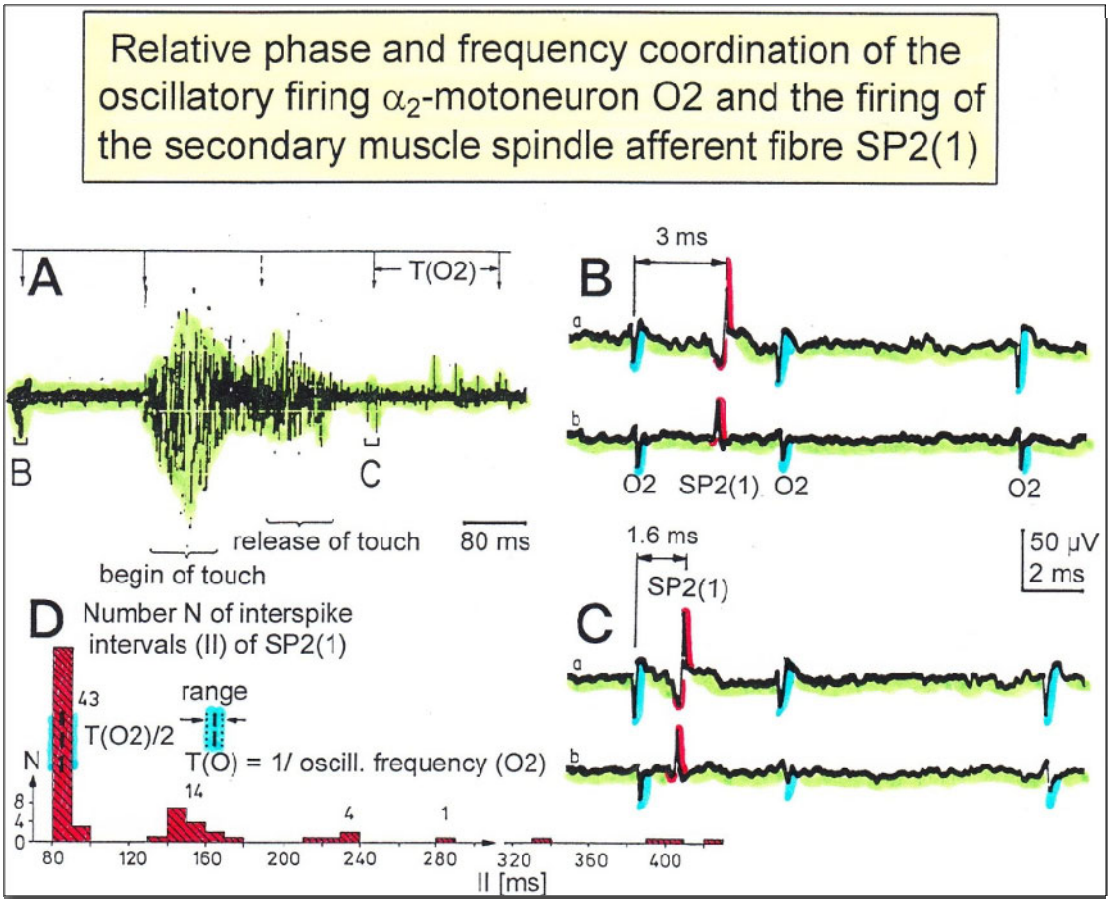

Figure 25. Time relation between the occurrence of the action potentials (APs) of oscillatory firing α_2-motoneuron O2 and the firing of the secondary muscle spindle afferent fiber SP2(1). HT6. S4 dorsal root recording. A. Overall view of the used sweep piece; only trace "a" shown. Four oscillation cycle periods of motoneuron O2 are indicated (T(O2)). The APs of the impulse trains can be recognized only partly, because of the slow time base and poor digitalization. One impulse train (dashed arrow) is lost in the touch stimulated activity, which consists of a touch (large overall activity) and a release part (lower overall amplitude). B, C. Sweep pieces from A, time stretched. In B, motoneuron impulse train APs is marked O2, spindle afferent APs are marked SP2(1). Note that the APs of the spindle afferent fiber are not time-locked to the first AP of the impulse train of the rhythmically firing motoneuron (relative phase coordination). Digitalization four times better than in A, but still rather poor, as can be seen from the low amplitudes of the motoneuron APs on trace "b" in C. D. Occurrence of interspike intervals of the secondary muscle spindle afferent fiber SP2(1). The numbers give the amount of IIs in each distribution peak. The oscillation period of motoneuron O2 (and the range of variation) and the half period are indicated by short dashed lines. Note that the IIs of fiber SP2(1) are very similar to the oscillation period (or the half of it) of α_2-motoneuron O_2 (relative frequency coordination).

The firing of the oscillator and the sweep pieces that are shown time-expanded are indicated at the summary trace **(Figure 25A)**. **Figures 25B and 25C** shows the action potential (AP) impulse train of oscillator O2 in connection with one of its driving spindle afferent AP. Because of the duration of the phase relation of around zero milliseconds between the firing of the driving SP2(1)-fiber and the impulse train of the oscillatory firing motoneuron O2, the SP2(1)-fiber AP (every second AP of the SP2(1)-fiber) appeared at a similar time as the impulse train. Because the AP of the spindle afferent fiber had a characteristic waveform, it was easy to extract its impulse pattern from the summed impulse traffic of this S4 dorsal (!) root. During touch-induced skin afferent activity **(Figure 25A)**, the activities of the motoneuron and the spindle afferent fiber were covered by the skin afferent activity. After the

cessation of the skin afferent activity, the afferent and efferent APs were found again at their expected time positions of the regular firings. The phase coordination between the firings of the oscillatory firing motoneuron O2 and the secondary muscle spindle afferent fiber SP2(1) at the time when records B and C were taken, was 1.6 ms (3 ms - 1.4 ms, **Figures 17B and 17C**). In Figure 25D, the relative frequency coordination between the firings of the SP2(1)-fiber and the impulse train of the oscillator is indicated. For the time period evaluated, the correlation between the firing of the motoneuron and the spindle afferent fiber was in the range of between 3 and 5ms.

Relative Frequency Coordination

In **Figure 26**, considerations concerning the relative frequency coordination are extended to the activity of further afferent fibers and γ-motoneurons of the same root. **Figure 26G** shows sweep pieces of the original recordings; A through F show the interspike interval distributions of spindle afferents and γ-motoneurons. It can be seen from the overlapping of the oscillator frequency distribution ranges (and the half of it) and from the interspike interval distributions of the afferents that from the viewpoint of frequency coordination, fiber SP2(1) contributed strongly to the drive of oscillator O2, whereas there was a weaker contribution from other afferents (less overlapping between the distributions of the afferents and the range of the basic frequency or the first harmonic of the oscillator). Also, γ-motoneurons showed only little frequency correlation at that time period.

Figure 27 shows the interspike interval distributions of more afferents (including the afferents for bladder filling; stretch receptor afferents S1(1), S1(2)) of another root, together with the oscillation period range (and the half of it) of a second α_2-oscillator (O1). By comparing the oscillation periods (and their halves) and their ranges with the interspike interval distributions of the afferents, it can be suggested which afferents made a (frequency coordination) contribution to the drive of what oscillator at that time interval. For example, the S1(1) urinary bladder stretch afferent fiber activity contributed to the drive of oscillator O1 (activating the external bladder sphincter) because its interspike interval distribution overlaps strongly with the range of the oscillation periods of O1. But the S1(1) distribution does not overlap with the range of the oscillation periods of oscillator O2 or with their halves or quarters. The S1(1) afferent fiber will therefore not have made a substantial contribution to the drive of oscillator O2. On the other hand, the secondary muscle spindle afferent fiber SP2(12) activated oscillator O2 innervating the external anal sphincter, since its interspike interval distribution overlaps with the range of O2 oscillation periods. But the secondary muscle spindle afferent fiber SP2(12) did not activate oscillator O1, as its interspike interval distribution does not overlap with its oscillation period range or the half of it **(Figure 27)**.

By comparing interspike interval distributions of afferent fibers with oscillation period distributions, it can be estimated what afferents made a (frequency coordination) contribution to the drive of the spinal oscillators. These considerations need no knowledge of the connectivity of the neuronal networks. In the frequency coordination between the firings of afferents and oscillators and among oscillators, entrainment or coordination may occur sub- or super-harmonically. The energy transfer, and therefore the coupling strength, will be smaller if the APs coincide in their firing less often.

As indicated by my measurements, the coupling and the relative coordination during the self-organization of the neuronal networks of the human spinal cord are of an enormous complexity; this self-organization is induced by sets of mutual impulse patterns from stimulated receptors, which are ordered, in time and space, so as to reflect, in the spinal cord and higher centers, the interplay of the body with the external world.

Impaired Organization of Premotor Spinal Oscillator Following Spinal Cord Injury as an Indicator for Pathologic Network Organization

Following a spinal cord injury, the oscillatory firing networks lose specific properties. The Eigenfrequencies of the premotor spinal oscillators change from a narrow to a broad frequency band **(Figure 19)**.

Self-organized α_2-oscillators fire physiologically at an Eigenfrequency (varying within a small frequency band as probably indicated with the hatched distributions in **Figure 19**) with impulse trains consisting of two to three action potentials. Following brain death, this Eigenfrequency band enlarges (black area in **Figure 19**). Following a spinal cord injury, the Eigenfrequency band enlarges strongly and includes in this case the frequencies between 4 and 14Hz for firing with two or three action potentials per impulse train **(Figure 19)**. The premotor spinal oscillators have lost their specific properties and could now be excited at frequencies at which they physiologically would not be excited. This is one reason for spasticity.

Stable phase coordination in the brain-dead individual

To make the phase relation changes better recognizable with time, a representation of phase relations is used, which comes from the measuring of the speed (frequency) of rotation.

The speed of rotation of a turning cylinder with a spot on its surface can be measured with a stroboscope.

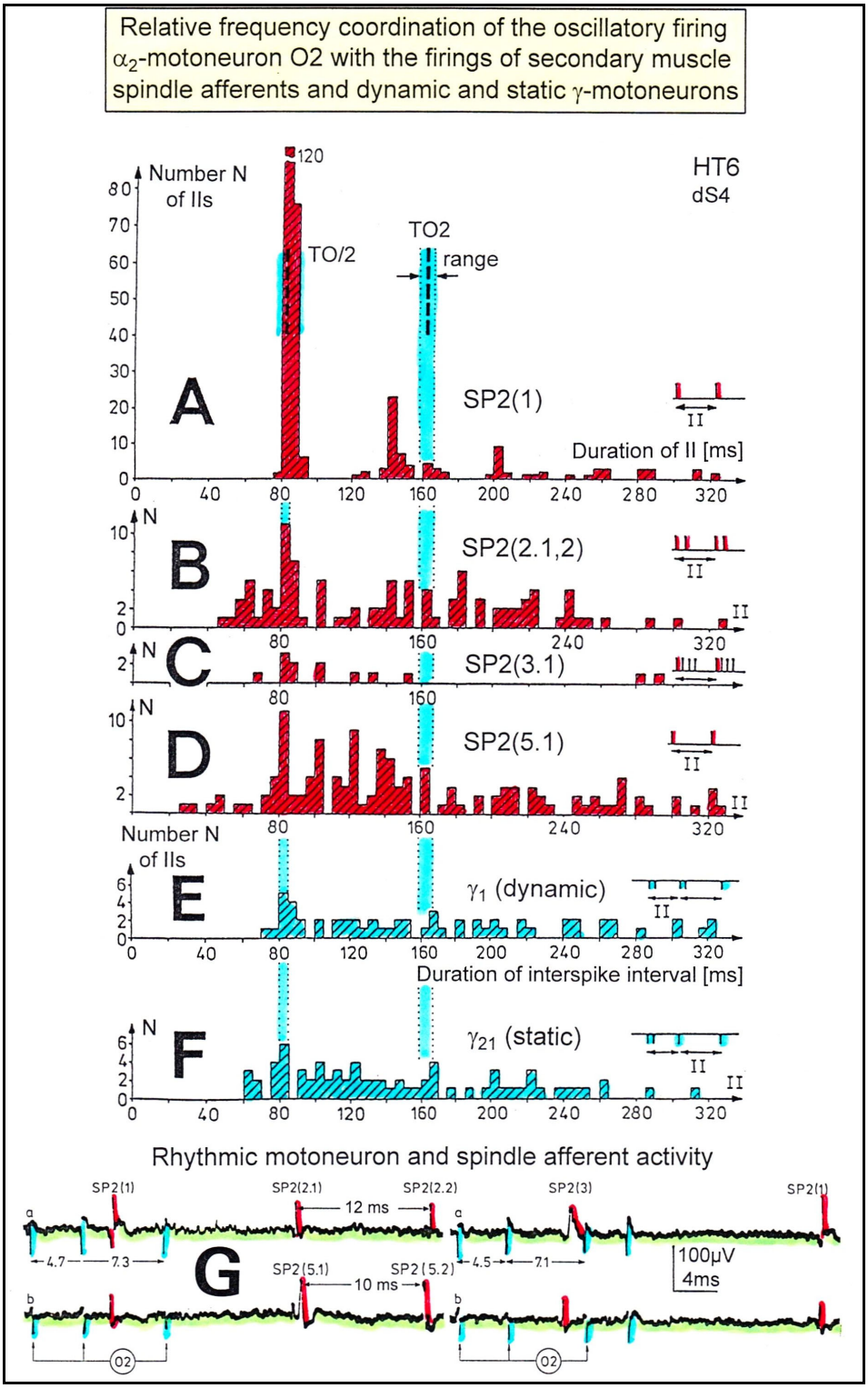

Figure 26. Interspike interval distributions of single endings of four secondary muscle spindle afferents (SP2) and two γ-motoneurons, recorded simultaneously. In A, the oscillation period TO2 (impulse train length = 3 APs) with its range of simultaneously recorded oscillatory firing α_2-motoneuron O2 (see G) is drawn for comparison; also, the halves of the oscillation period TO2/2 are indicated. Note that the interspike interval distributions of spindle afferents and γ-motoneurons have shortest interspike interval, nearly identical to the half of the oscillation period (relative frequency coordination). The schematic impulse pattern in A to F shows the procedure for measuring the interspike intervals. Original records of the firing patterns of α_2-motoneuron O2 and the secondary muscle spindle afferents SP2(1), SP2(2), SP2(3) and SP2(5) are shown in G. Brain-dead human HT6, dS4 root.

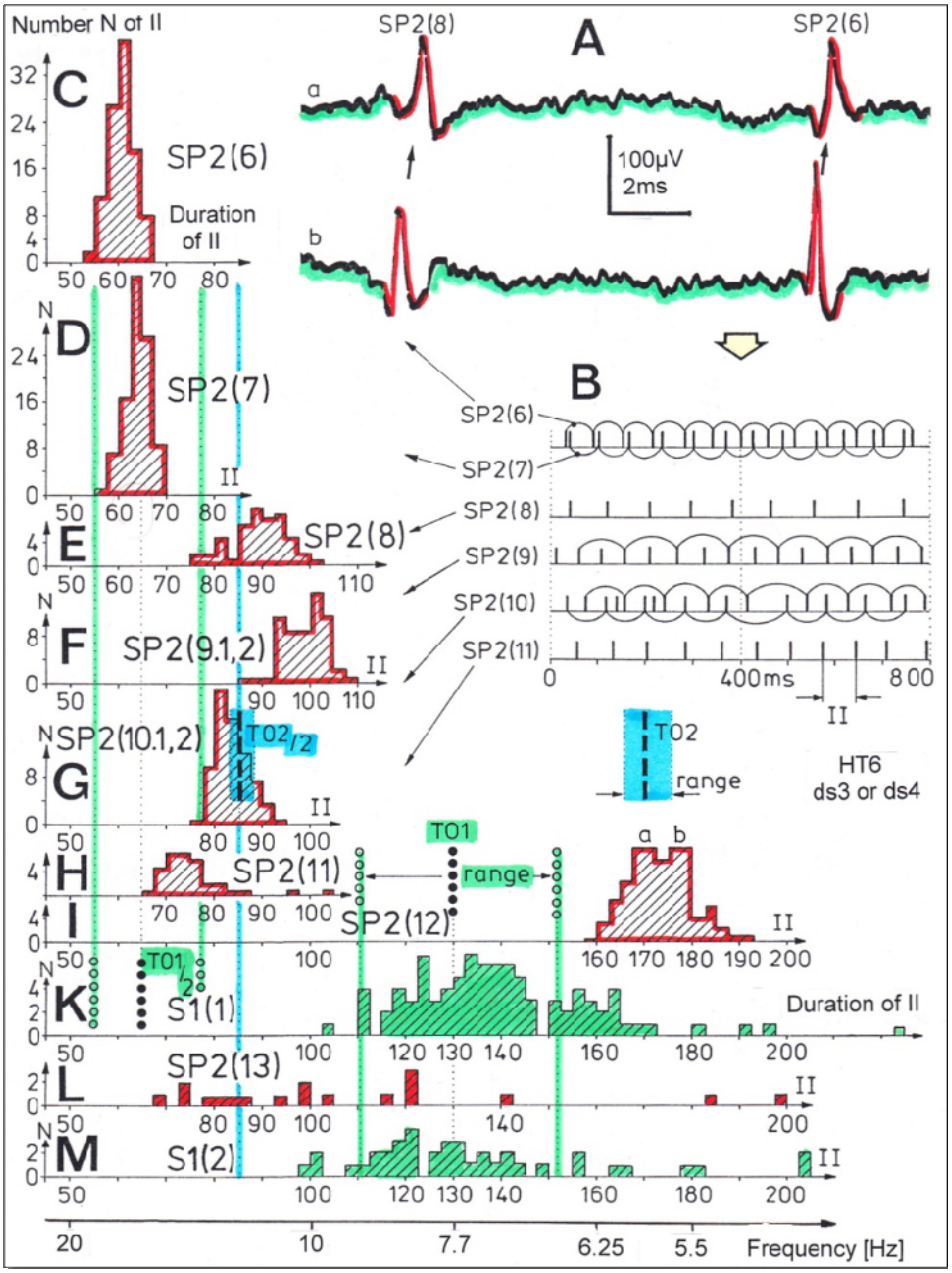

Figure 27. Measurements from brain-dead human HT6 from different spinal cord segments after retrograde bladder filling (700 to 800 ml), with the exception of "I," which was obtained before filling. A. Sweep piece of a recording from a dorsal S3 or S2 root filament. It can be seen that the secondary muscle spindle afferent SP2(6) AP can be distinguished by the waveform on the two traces from the secondary spindle afferent fiber SP2(8) AP (different amplitude of the three phases of the triphasic APs). B. Simultaneously recorded impulse patterns of the six parent secondary spindle afferents SP2(6) through SP2(11) obtained from dS3 or dS2 root recordings. The impulse patterns of SP2(6) and SP2(7) fibers are not separated to show the similarity of the patterns. The impulse patterns of the parent spindle afferents SP2(9) and SP2(10) are split into patterns of the single endings (single ending activity partly connected by circle lines) with the assumption that single endings of parent secondary muscle spindle afferents should have interspike intervals of duration longer than 50 ms. C to H. Interspike interval distributions of six simultaneously recorded single secondary spindle afferent endings. F, G. Interspike interval distributions of parent fibers, which are the sums of the distributions from the two activated endings. I. Interspike interval distributions of a secondary spindle afferent fiber (SP2(12)) of a coccygeal root. K, L, M. Interspike interval distributions of single-fiber afferent activity from a lower sacral dorsal root. In L, most likely the activity from a secondary spindle afferent fiber is shown. In K and M, most likely the interspike intervals from afferents (S1(1) and S1(2)), innervating stretch receptors of the urinary bladder wall, are shown. In G, H and K, the durations of the oscillation periods (mean and range) of the oscillatory firing α_2-motoneurons are indicated by thick dashed and dotted lines; the motoneurons innervate the external anal sphincter (TO2) and the external bladder sphincter (TO1). The sites of innervation of the oscillatory firing motoneurons are identified (and distinguished from each other) by anal reflex stimulation, bladder filling and catheter pulling. Note that the TO1 and TO2 ranges and their halves overlap with the interspike interval distributions of the secondary spindle and stretch receptor afferents (relative frequency coordination).

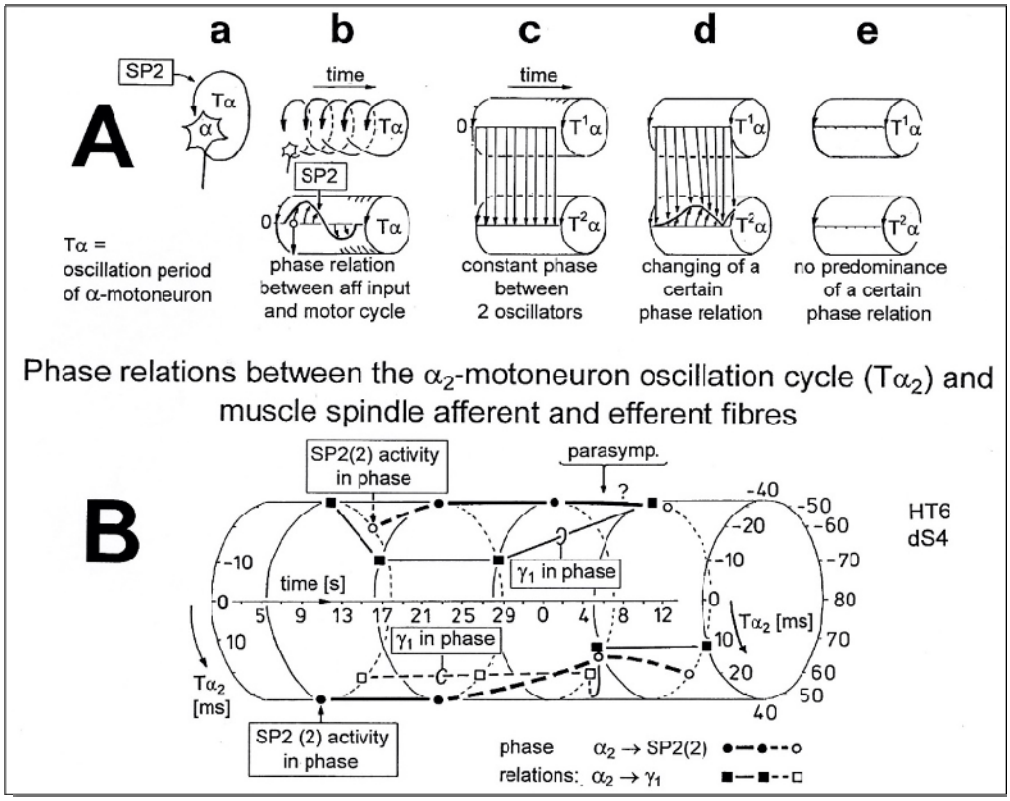

Figure 28. (A) Derivation of the simultaneous description of interspike intervals and phase relations. (a,b) The oscillation period of an oscillatory firing α-motoneuron is schematically characterized by the length of the loop (perimeter). Successive oscillation periods with ongoing time yield a cylinder. Flashing with a stroboscope on such a cylinder with the same frequency as that of the rotation of the cylinder would make a black spot on the turning cylinder not move up or down. If the frequency of the cylinder or the stroboscope changed slowly, the black spot would move up or down. If the black spot moves from left to right with ongoing time, a curve is obtained. By replacing the flashing of the stroboscope by the occurrence of the APs of the spindle afferent fibre (or another oscillatory firing motoneuron) with respect to the APs of the oscillatory firing motoneuron, phase relation changes are made visible in the lower part of "b" for a constant oscillation period (cylinder with no diameter changes). (c) A constant phase between two oscillatory firing motoneurons results to a constant line on the cylinder with ongoing time. (d) A changing phase gives a curve on the cylinder circumference. (e) If there is a loss of predominance of a certain phase between two motoneurons (the black spot gets diffused with ongoing time and is then lost), there is no line or curve. (B) Interspike interval and phase data from the brain-dead human HT6 (root dS4) are plotted in the representation of A. Filled dots and squares represent average phases (phase relations); thick and thin lines connect the dots to show trends. Note that the phase relations change only little; the frequency of the sphincteric α_2-motoneuron ($1/T\alpha_2$) changes only little - the cylinder does not change its diameter.

If the stroboscope flashes light with the same frequency as the cylinder is turning, the spot on the circumference seems to stand still. There is a constant phase between the two frequencies (frequencies are same or multiples of each other). If the phase relation changes, the spot will move.

If no phase relation exists between the turning of the cylinder and the flashing of the light, no spot will be seen. In similarity to stroboscopic measurement of frequencies of turning cylinders, the phase relation between two oscillatory firing spinal oscillators is pictured in **Figure 28A**. A time axis is introduced on the horizontal line to make phase relation changes visible in dependence on time.

In **Figure 28Aa**, the loop excitation is pictured for this oscillator model. In **Figure 28Ab**, the phase relation between the SP2 fiber activity incidence and the oscillatory firing is pictured on the circumference of the oscillation period cylinder of the oscillator. **Figure 28Ac,d,e** shows different phase relations, namely a constant phase relation (c), a changing phase relation (d), and no phase relation (e). In **Figure 28B**, phase relation changes are plotted between an α_2-motoneuron and the activity of a secondary muscle spindle afferent fiber and between an α_2 and a γ_1-motoneuron. The data were taken from **Figures 4 and 5** of [15] of a brain-dead individual (probably normal with respect to the number of phases per oscillation cycle and with respect to phase changes). It can be seen that there were two phase relations per α_2-oscillation cycle and that the phase relation changed only little with time. The phase coordination between the firings of the α_2 and a γ_1-motoneuron and the secondary muscle spindle afferent fiber was stable.

Unstable phase coordination in a patient with a spinal cord injury

In **Figures 29A and 28B**, different phase relation changes are with respect to the α_3-oscillation cycle (A) and the α_2-

oscillation cycle (B). It can be seen that the different phase relations changed strongly in value over time (upon different stimulation) and that also the number of phase relations per oscillation cycle changed. The phase stability of the cooperative and competitive interplay among neurons became impaired. Whether the change of the number of phase relations from two to three following the activation of the parasympathetic nervous system in the sacral micturition center is physiologic or not is not clear. See also **Figures 32i, j**.

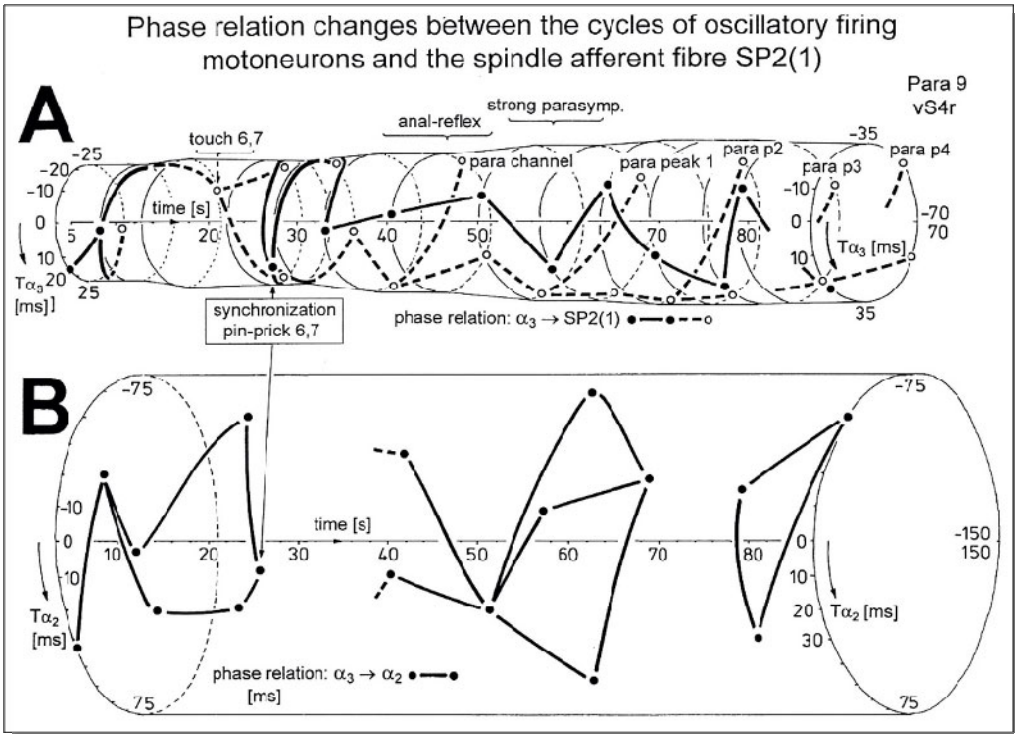

Figure 29. (A) Phase relations between the secondary muscle spindle afferent fiber SP2(1) and the oscillatory firing α_3-motoneuron, taken from **Figures 10-12** (and additional data), are plotted on the oscillation period cylinder $T\alpha_3$ (mean oscillation periods are taken from **Figures 11A,12A**) according to **Figure 21A**. The cylinder is changing its diameter (perimeter) because the oscillation period changes. Phase changes in ms are scaled on the cylinder circumference. The ongoing time (to the right) is scaled on the axis of the cylinder (time intervals are taken from **Figure 10A**). Existing phase relations are represented by dots (filled and open (back-side)); lines (filled and dashed (back-side)) only connect the phase relations to show trends. para peak 1, para p2, para p3, para p4 = activity peaks of the SP2(1) fibre due to parasympathetic activation (see **Figure 10A** right). (B) Phase relations between the α_3 and α_2-motoneurons plotted onto the oscillation period cylinder of the α_2-motoneuron. Dots represent phase relations, taken from **Figures 11B,12B**. Note that the phase relations of the paraplegic 9 are much more variable than those of the brain-dead human HT6 **(Figure 21B)**; also, the number of phase relations changes.

Difference of phase stability between a brain-dead human and a paraplegic

The most obvious difference of the phase relation changes between the above-mentioned brain-dead human and the paraplegic was that in the paraplegic. The phase relations varied very much, whereas they changed only little in the brain-dead human. The strong phase relation changes in the paraplegic can be interpreted as instability in the organization of neuronal networks. The correlation of neuronal subnetworks was instable in relation to those of the brain-dead human. Assuming that the neuronal network organization and functioning was rather physiologic in the brain-dead with respect to the firing patterns of the premotor spinal oscillators, the functioning of the networks became instable following spinal cord injury.

The more frequent occurrences of changes of phase relations between the different nerve fibers in combination with the changing number of phase relations per oscillation may mean that subnetworks reacted and interacted more quickly and easily with others according to the afferent input. Especially because the oscillatory firing networks lost specific properties, their resonance frequencies changed from a narrow to a broad oscillator frequency band, which means that the oscillators were not excited at a certain frequency anymore but by a broad frequency band. They could now be excited at frequencies at which they physiologically would not be excited. Over-activation and mass effects could be the result. On the other hand, certain networks could escape from driving afferent influence by changing their phase-by-phase escape to avoid interaction. Functionally far away networks are not reached anymore, which also would

result in a loss of specific properties. Therefore, because of the loss of specific properties, some interactions could have occurred more easily and other ones not at all.

W.R. Hess tried, in 1944, to compare biological order and human society [16]. In a society, the upper behavior of spinal oscillators could be called "putting its flag to the wind." There could be similarities between the organizations of the human nervous system and the organizations between very many individual nervous systems.

Natural firing patterns of proprioceptive afferents and α and γ-motoneurons, measured simultaneously, and the phase and frequency relations between them

Figure 30 shows such schematic natural simultaneous impulse patterns of a static and a dynamic γ-motoneuron, two secondary muscle spindle afferents and an oscillatory firing α_2-motoneuron O2 in a dorsal S4 nerve root (there are afferents and efferents in dorsal or ventral lower sacral roots) during continence pattern changes. The small arrows and the dotted lines indicate existing relative phase coordination's between the static and the dynamic γ-motoneurons and motoneuron O2, and between γ-motoneurons and secondary muscle spindle afferents. The dashed-circle line indicates a phase relation between the APs of the static γ-motoneuron (γ_1) and the cross-correlation between SP2(2)-fiber (single ending one of the mother fiber) and SP2(5)-muscle spindle afferent fiber

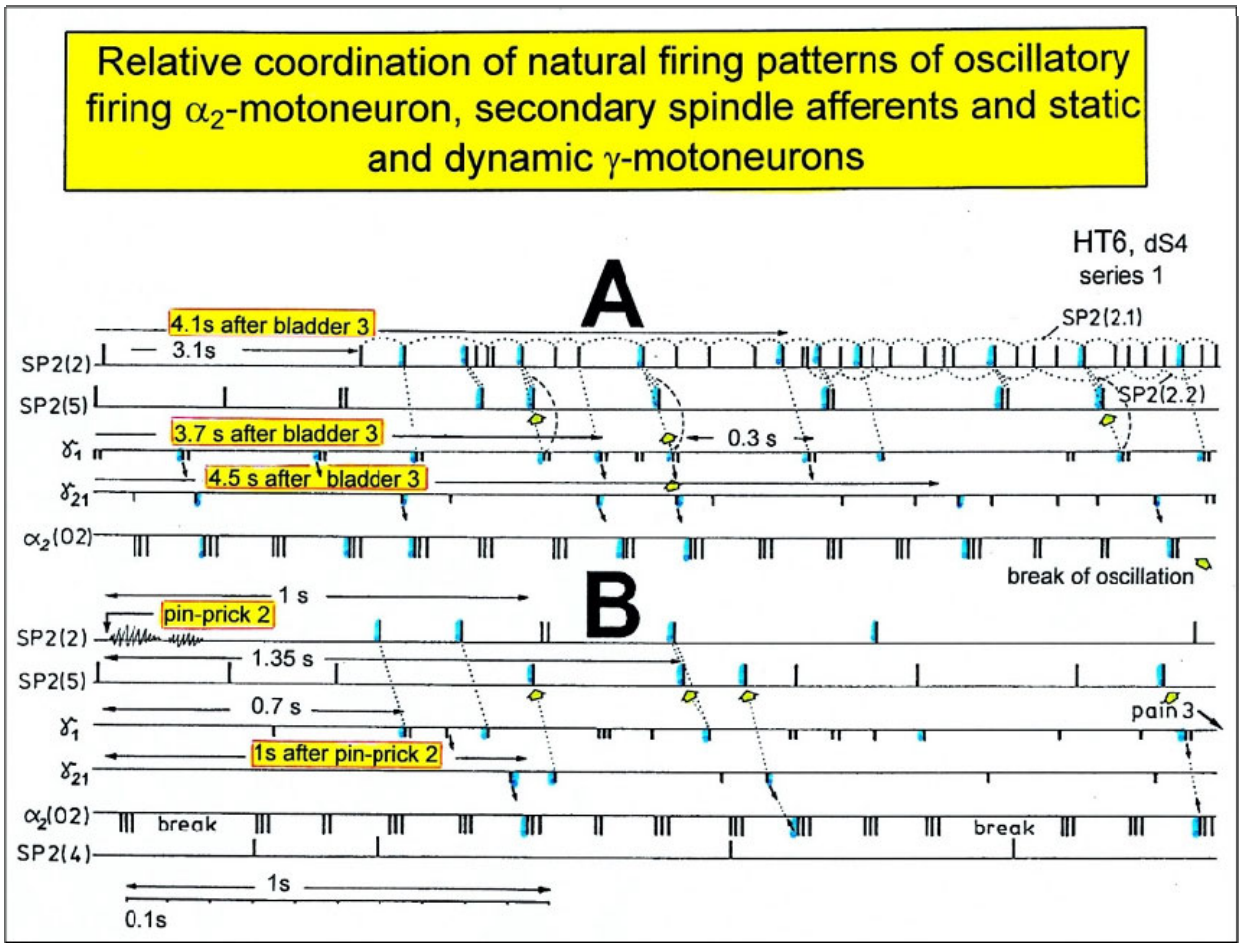

Figure 30. Impulse patterns of simultaneously recorded γ-motoneurons (γ_1 and γ_{21}), secondary spindle afferent fibers (SP2(2), SP2(4), SP2(5)) and oscillatory firing α_2-motoneuron O2 following bladder catheter pulling (bladder 3) (A) and pinprick 2 (B). B was recorded before A. In A, the impulse patterns of the two encoding sites SP2(2.1) and SP2(2.2) of the single parent fiber SP2(2) are indicated by the dotted curves. Times to the activity increases of γ-motoneurons and secondary spindle afferents following stimulation are indicated. Similar time intervals of the occurrence of γ-motoneuron APs and SP2(5) fiber APs (phase coordination) are indicated by the open arrows, and the similar time intervals of γ-motoneuron APs and α-motoneuron APs are indicated by small arrows. Similar time intervals of the APs of fibers SP2(2) and SP2(5) are indicated by the double dotted lines, those of γ_1-APs and the SP2(2) fiber APs by a dotted line, and those of γ_1-APs and the SP2(2)-SP2(5) correlation by a curved dashed line. HT6; dS4.

Including the phase relations between the firings of secondary muscle spindle afferents and the oscillatory firing motoneuron O2, we obtain interlaced loops of coordination's between the firings of γ-motoneurons and secondary muscle spindle afferents, and between secondary spindle afferents and α-motoneurons and

between α-motoneurons and γ-motoneurons (co-activity of α and γ-motoneurons) **(Figure 31)**. It becomes obvious from the correlations between the natural impulse patterns (including those of single encoding sites of spindle afferents) that the γ-loop is not a single loop, but a network of loops, because of the divergent projections of γ-motoneurons onto muscle spindles and the probably divergent and convergent projections of secondary muscle spindle afferents into the neuronal network of the spinal cord, consisting of α and γ-motoneurons and interneurons.

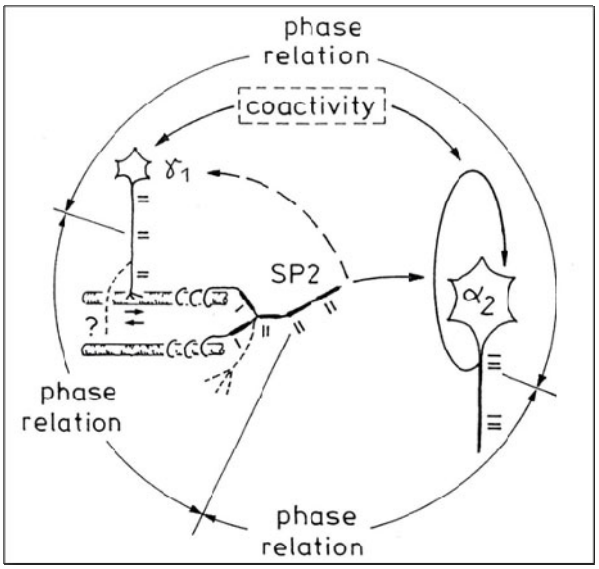

Figure 31. Schematized existing phase relation between α_2 and γ_1-motoneurons and a secondary muscle spindle afferent fiber (SP2). Parallel existing phase relations between other parent afferents and the α_2-motoneuron and between parent secondary spindle afferents are not shown. Phase relation means the increased occurrence of phases in ms in a certain phase range between the action potentials (APs) of the two compared nerve fibers. The complex afferent and efferent muscle spindle innervation were not attempted to be shown. Small arrows at intrafusal muscle fiber indicate local contraction, which is in nuclear chain fibers readily transmitted to the place of afferent innervation. A possible reason of the doublet firing of the SP2 fiber is pictured to occur from single APs (schematized by bars) of two myelinated endings, not necessarily from pacemaker switching. More endings of the parent SP2 fiber and γ_1-motoneurons are indicated by dashed line branches. "Coactivity" indicates a correlation between γ and α-motoneuron spinal cord circuitries for higher activations.

More general, phase and frequency coordination can be seen among the natural firing patterns in the afferent and efferent fibers; this means that upstream in the CNS, there should also be phase and frequency coordination among neuron firing. Two phase relations have been observed to occur mostly between the APs of the secondary muscle spindle afferents and the oscillatory firing motoneuron per one oscillation period (Figure 32) (for somatic activation) in accordance with the "in phase" and "anti-phase" jumping on springboard and crawling. With this coordinated natural impulse traffic to and from the periphery, the change of integrative pattern states can also partly be understood from bladder to movement states.

Phase relation changes between the action potentials of the α and γ-motoneurons and secondary muscle spindle afferents in paraplegic 9 upon somatic and parasympathetic activation of the sacral micturition center

As shown in **Figures 11 and 12** of [7], the number (and the values) of phase relations changed between the firings of the different nerve fibers upon different stimulations. In the brain-dead human HT6, two phase relations were found between the α_2-motoneuron and the secondary muscle spindle afferent fiber SP2(2) and the α_2 and the γ_1-motoneuron (**Figure 5** of [15]). Also, in the paraplegic, two phase relations often existed between the firings of the different nerve fibers. Probably a third phase relation occurred when the activated parasympathetic division channeled an additional input to the oscillatory firing somatic neuronal network.

It may therefore be worthwhile to further analyze the number of occurring phase relations per oscillation cycle upon different somatic and parasympathetic stimulations.

Since two phase relation occurred per oscillation cycle between the α_3 and γ_1-motoneurons and the SP2(1) fiber in paraplegic 9, and also their IIs were rather similar, it is concluded that the neuronal networks of the α_3 and γ_1-motoneurons formed together with the spindle afferent fiber SP2(1) a part of a functional unit. The neural ensemble is built by efficiencies of synapses and projections between the convergence of several γ-motoneurons on one muscle spindle and by the divergence of muscle spindle projections onto several rhythmically firing populations of neurons driving α and γ-motoneurons. Such a functional unit is partly pictured in **Figure 31** and schematized drawn by three circles in **Figure 32**. The α_2-motoneuron and the SP2(2) fiber belonged to another functional unit (another ensemble) (longer IIs and the existence of only one phase relation). The two functional units (ensembles) are characterized in **Figure 32** by two sets of three circles each. The two functional units interacted with each other, as there existed a phase relation between the α_2 and α_3-motoneurons **(Figure 32)**.

Before stimulation (but with the anal and bladder catheters positioned), there were two phase relations in unit 1 **(Figure 32a)**.

When touching sites, the skin outside the anal reflex area **(Figures 4A and 6)**, only slight changes occurred in the two units with respect to the number of phase relations **(Figure 32b)**. But when touching the skin of the anal reflex area, a partial synchronization occurred **(Figure 32c)**, and functional unit 1 reduced the number of phase relations to one. When pinpricking the skin outside the reflex area, two phase relations occurred again in unit 1 **(Figure 32d)**.

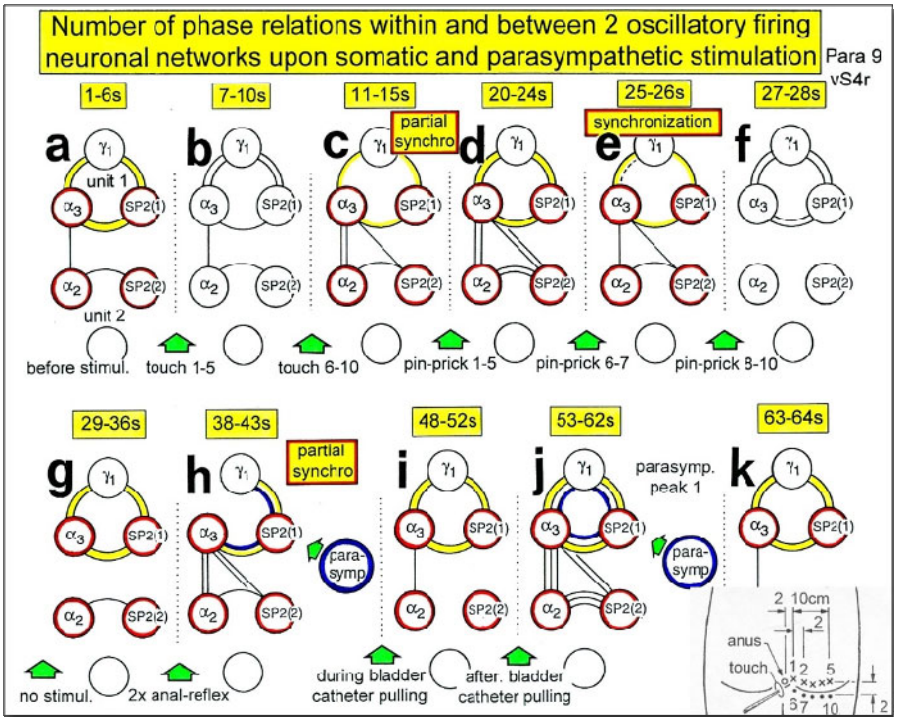

Figure 32. Number of phase relations within and between the two functional units α_3/γ_1/SP2(1) and α_2/-/SP2(2). Time intervals are those of Figure 2A. Note that in "a," the functional unit 1 is with two phase relations per oscillation period in a stage similar to those seen in the brain-dead individual; with synchronization, only one phase relation occurred (e) and the parasympathetic division channeled an extra phase relation to interact with the somatic division (j). The insert shows the sites of stimulation.

Upon pinpricking sites inside the anal reflex area, the number of phase relations between all the components of the two units dropped to one **(Figure 32e)**, and synchronization occurred between the firing patterns. Since in the brain-dead human two-phase relations per oscillation cycle were observed in the functional units, it is possible that synchronization and the existence of only one phase relation for two to three seconds reflected a slight pathologic organization of the networks. Even though upon touching sites 6 to 10 **(Figure 32c)** or upon pinpricking sites 6 to 7 **(Figure 32e)** only one phase relation existed in unit 1, and synchronization occurred with both stimulations, it was shown (**Figures 8 and 9** of chapter V of [7]) that the touch afferent input organized a different functional state of unit 1 than pinpricking. The response time until the shortening of the oscillation period was longer than the oscillation period (≈ 100 ms) for pinprick and shorter for touch. The repetitive touch stimulation (most effective inside the anal reflex area) reinforced the sustained stretch reflex of the anal sphincter (continence pattern), and repetitive pinprick stimulation replaced the continence pattern by the protection reaction of the anal sphincter. The number of phase relations alone therefore only provides limited information on the functional state of the organization of the neuronal networks of the human spinal cord. Measurements of a number of parameters are necessary to yield a rather complete description of the functional state of neuronal networks.

Following pinprick 8 and 10 and with no stimulation, two phase relations existed again in functional unit 1 **(Figure 32f, g)**, in some similarity to pre-stimulation status **(Figure 32a)**. Following two anal reflex stimulations, partial synchronization occurred in the components of the two units (**Figure 5** of [17]) and mainly two-phase relations existed **(Figure 32h)**. But the organizational state was still not very similar to the pre- **(Figure 32a)** or post-stimulation state in unit 1 **(Figure 32g)**, since the parasympathetic division was slightly activated following anal reflex stimulation, as was measured by the impulse pattern (increase of doublet activity) of the secondary muscle spindle afferent fiber SP2(1) (**Figures 5 and 7** of [18] (part 2)). Therefore, probably one phase relation was due to the somatic activation in similarity to **Figure 32c, e**, and the other phase relation was due to the activation by the parasympathetic division. During bladder catheter pulling **(Figure 32i)** and with no stimulation **(Figure 32k)**, the number of phase relations and possibly the functional organization was again similar to the pre-stimulation state **(Figure 32a)**. Following strong (painful) bladder catheter pulling with a strong activation of the parasympathetic division (time interval 53-62s **(Figure**

32j)), measured by the increased doublet firing (see **Figure 5** of [18] (part 2)) of the SP2(1) fiber, the functional organization of the sacral micturition center of the disconnected spinal cord changed completely. Functional unit 1 was now correlated by three phase relations per α_3-oscillation cycle. The functional unit 2 also showed three phase relations per an α_2-oscillation cycle and interacted with functional unit 1 by three phase relations as well (between the α_3 and α_2-motoneurons; **Figure 32j** [53-62s]). Between the first and second parasympathetic peak at the time interval 63-64s (Figure 32k), the organization form of the two functional units was similar to that before the first parasympathetic activation [49-52s] **(Figures 32)**, only the values of the phase relations changed (**Figure 12Bd** of chapter 5 of [7]). With the second strong activation of the parasympathetic division (parasymp. peak 2, time interval 65-72s), the functional unit 1 was bound together again by three phase relations10A), in similarity to the first strong activation of the parasympathetic division [15], measured by the burst firing of the secondary muscle spindle afferent fiber SP2(1) (**Figure 8** of [18]) and the increased doublet firing of the SP2(1) fiber (**Figure 5** of [18]). The functional unit 2 was disorganized, but phase relations still occurred between the α_3 and the α_2-motoneurons and the SP2(2) fiber [15]. The α_2-neuronal network and the γ-motoneuron networks, driving the SP2(2) spindle afferent fiber, were integrated differently. After the second strong parasympathetic activation, in the time interval 73-76s (**Figure 10A** of chapter V of [7]), the functional organization of the two functional units in the spinal cord was similar to that before the activation of the parasympathetic division. Functional unit 2 was slightly disorganized as the SP2(2) fiber strongly reduced its firing [15]. For further details see chapter V of [7].

This intricate analysis shows how complex neural network organization changes are. But such analyses are a first real step to understand human neural network organization and its consequences for disorders.

Building up of external loops to the periphery by premotor spinal oscillators

With the building up of simultaneous phase relations between α, γ and SP2 fibers, an external loop of premotor spinal oscillators is built up to the periphery, which makes it possible to directly influence the firing of spinal oscillators by a rhythm training.

Upon jumping on springboard **(Figure 2B)** (and other rhythmic movements like sky-walking (Figure 2C) or running), premotor spinal oscillators organize themselves to fire transiently oscillatory according to the motor pattern and build up an external loop to the periphery **(Figure 33)**. If the frequency of the rhythmic movement has an integer relationship to the Eigenfrequencies of the premotor networks and more rostral networks, these premotor networks get entrained for more specific self-organization.

Entrainment of premotor spinal oscillator networks by rhythmic movement-induced afferent input and inputs from supraspinal centers

If one approximates for high activation spinal neuronal networks into premotor spinal oscillators (driving the motoneuron) and propriospinal oscillators, then premotor spinal oscillators can be handled in a first approximation as single linear oscillators. The premotor spinal oscillators and the spinal pattern generating networks are self-organized and driven by peripheral afferent and supraspinal inputs. When training dynamic, rhythmic, stereotyped movements, the premotor spinal oscillators, approximated as linear oscillators, are driven by movement-induced afferent input from the periphery (mainly the legs) and surrounding pattern generating networks and possibly supraspinal inputs. These spinal oscillators and most likely their neuronal network can be entrained at least by use of the external loop for a better self-organization.

If one assumes that loop circuits do not only exist between the premotor spinal oscillators and the periphery, but are a general structure in the CNS, then motor learning involves the formation of loop circuits (or better loop network circuits) between the cortex and the periphery involving the sensory cortex and the thalamus. When a linear oscillatory system is driven by an external periodic input its response contains both frequency components. This is also, in general, true with nonlinear oscillators. However, in this case, if the external frequency is close to the Eigenfrequency of the oscillator itself, then it is possible to have a response at the external frequency only. This phenomenon is known as entrainment or synchronization. It is of paramount importance with respect to biological oscillators because it allows them to “latch on” to the environment. Thus, a rhythm with a free-running period of 24.7 h may be synchronized to 24 h when exposed to the natural sequence of day and night.

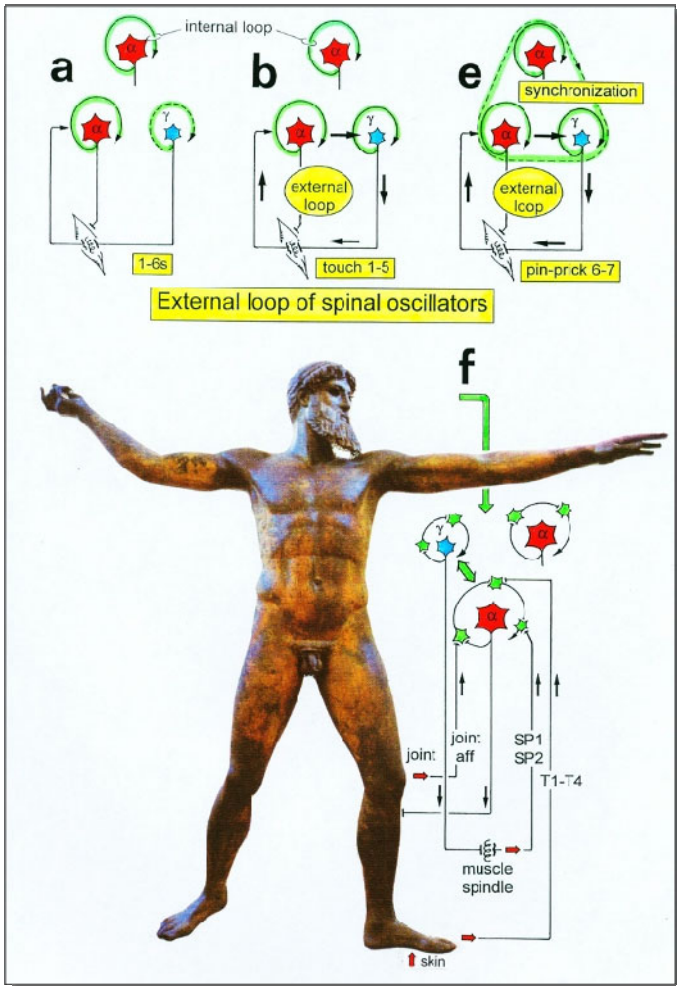

Figure 33. Spreading of oscillatory firing from α-motoneuron neuronal network to include muscle spindles (periphery) and synchronization of different α and γ-motoneuron neuronal networks caused by touch and pinprick stimulation. (a) α-motoneuron neuronal networks fired oscillatory (solid line loop), γ-motoneuron neuronal network did not or did only partly (dashed line loop), upon no additional stimulation. (b) Oscillatory firing α and γ-motoneuron neuronal networks built up a phase relation with muscle spindle afferents and efferents (external loop to the periphery, indicated by thick arrows) upon touch. (e) Oscillatory firing α (internal circuitry loop) and γ-motoneuron neuronal networks (external loop) synchronized (broad peak phase relation) upon pinpricks. The dashed line loop represents synchronization. (f) Oscillatory firing α (internal circuitry loop) and γ-motoneuron neuronal networks (external loop). The open arrows indicate that it may be possible to synchronize spinal oscillators by rhythmic afferent input, generated by rhythmic movements (such as jumping on a springboard or running), and to re-preformat the neuronal circuitry by synapse remodeling to fire more physiologically oscillatory to reduce spasticity and improve locomotion. Extensive pathologic movement like tremor may entrain neuronal circuitry to increase tremor movement. The Greek good is a bronze statue of Zeus found close to the cape of Artemision 460 BC.

Need for improving the stability of phase and frequency coordination to allow specific patterns formation and learning transfer

A young mother, with stress incontinence after giving birth to the first child, could well improve her continence status upon jumping on springboard in addition to other training, because her CNS is not injured; just the periphery has to be repaired by means of changing the CNS.

In severe cervical spinal cord injury, the jumping on springboard **(Figure 2B)** is not sufficient for bladder repair (the biggest problem in spinal cord injury). First, of course, the patient has to regain movement functions back (especially the trunk stability) to be able to perform the jumping on springboard. Further, the self-organization of CNS networks by phase and frequency coordination has to be improved to make learning transfer from movements to bladder functions possible, since in every CNS injury, the phase and frequency coordination is impaired. Large instabilities in phase and frequency coordination will not allow specific pattern formation as a basis for learning transfer. However, the stability of phase and frequency coordination can be improved when the patient is exercising on special coordination dynamics therapy devices, especially the one shown in **Figure 9**.

The importance of stable phase and frequency coordination to allow specific pattern formation and in consequence learning transfer to other patterns can be understood at the collective variable level (System Theory of Pattern formation [19,7]) and at the neuron level. The behavioural information F_{inf} of the coordination pattern dynamics, characterized by equations of motion of collective variables, $dX/dt = F_{intr}(X) + \sum c_{inf}F_{inf}(X,t)$, affect the whole coordination pattern dynamics, including stability, rather than only certain coordination patterns. If the behavioural information includes the exercising of extremely coordinated, integrative movements, like exercising on the special CDT device for turning, then the quality of the CNS self-organization can be enhanced by improving the exactness of self-organization, namely the precision of phase and frequency coordination between neuron and neural assembly firing. By improving the precision of organization of the intrinsic dynamics $F_{intr}(X)$, that is, the specific variability of the injured networks, certain patterns do then already reappear (Chapter V of [7]).

Neurons often serve more than one network pattern at the same time by time sharing of neuron firing and, in this way, give rise to learning transfer among the activated patterns. If subnetworks are improved in the organization of one pattern, the organization of the other pattern will also improve. Neurons involved in the organization of breathing and activating intercostal muscles, for example, are also involved in the organization of trunk stability. By reducing spasticity of the trunk (in patients with Parkinson's disease), the breathing will also improve. Similarly, sphincteric motoneurons are involved in continence and pelvic floor weight bearing. If during pregnancy the (non-trained) pelvic floor is not trained, sometimes incontinence occurs and after birth stress incontinence.

Entrainment of oscillators through jumping on springboard

Upon jumping rhythmically on springboard **(Figure 2B)**, in addition to the stimulation of mechanoreceptors for movement control, also mechanoreceptors for bladder and rectum control are synchronously activated with the movement. Continence functions are synchronously activated with the jumping (coherent activation of bladder and movement patterns). Since, additionally, for high activation premotor spinal oscillators build up an external loop to the periphery, neural assemblies are directly entrained to improve their "Eigenfrequencies" and to coordinate their firing with other oscillators **(Figure 33)**. The springboard has an Eigenfrequency ($f \approx 1$Hz; $\omega=2\pi f$), which makes a training in the entrainment region possible. A jumping frequency of 1 Hz is especially efficient for the entrainment of α_3-oscillators because they have an "Eigenfrequency" also around 1 Hz.

REPAIR OF PHASE AND FREQUENCY COORDINATION

Re-learning of phase and frequency coordination through training of very coordinated movements on the special CDT device

A completely different contribution to learning and learning transfer is induced if the patient is exercising on the special coordination dynamics therapy device for turning **(Figure 9)**. This training of very coordinated arm, leg, and trunk movements, imposed by the device, is especially improving the impaired phase and frequency coordination of neuron firing. Following spinal cord injury, the phase and frequency coordination becomes impaired, as turns out when comparing the coordinated firing of neurons in a brain-dead human (rather physiologic) with that of a patient with a spinal cord injury **(Figures 28 and 29)**. The network organization becomes deteriorated and escapes entrainment, learning, and learning transfer. Following injury, the variability of the coordinated firing of neurons becomes too large to enable efficient and specific learning and learning transfer. But when patients exercise very coordinated arm, leg, and trunk movements on the special coordination dynamics therapy device for turning (on which a precise coordination between arm and leg movements is imposed by the device, to which the training individual has to adapt to) **(Figures 9 and 33A)**, the CNS of patients can relearn specific self-organization, which means can relearn more exact phase and frequency coordination among neuron firings from the device. Since the CNS network is an open system, many different very coordinated integrative movements should be trained, not to allow the pathologic organization to escape from the repair.

Figure 33A. The spinal cord injury patient Nefeli during exercising on a special CDT device in the sitting position. Because of adduction spasticity of the legs, soft material is put around the device.

An impaired phase and frequency coordination between the firings of single neurons and neuron assemblies **(Figures 19 and 29)** can be expected to have consequences in the coordination between arm and leg movements because motoneurons innervate muscle fibers. Rhythmic coordinated firing of single motor units has been measured electromyographically with surface electrodes **(Figure 34)**. Indeed, the coordination between arm and leg movements is partly or fully lost following CNS (brain and spinal cord) injury and is often not taking place in the malfunctioning CNS.

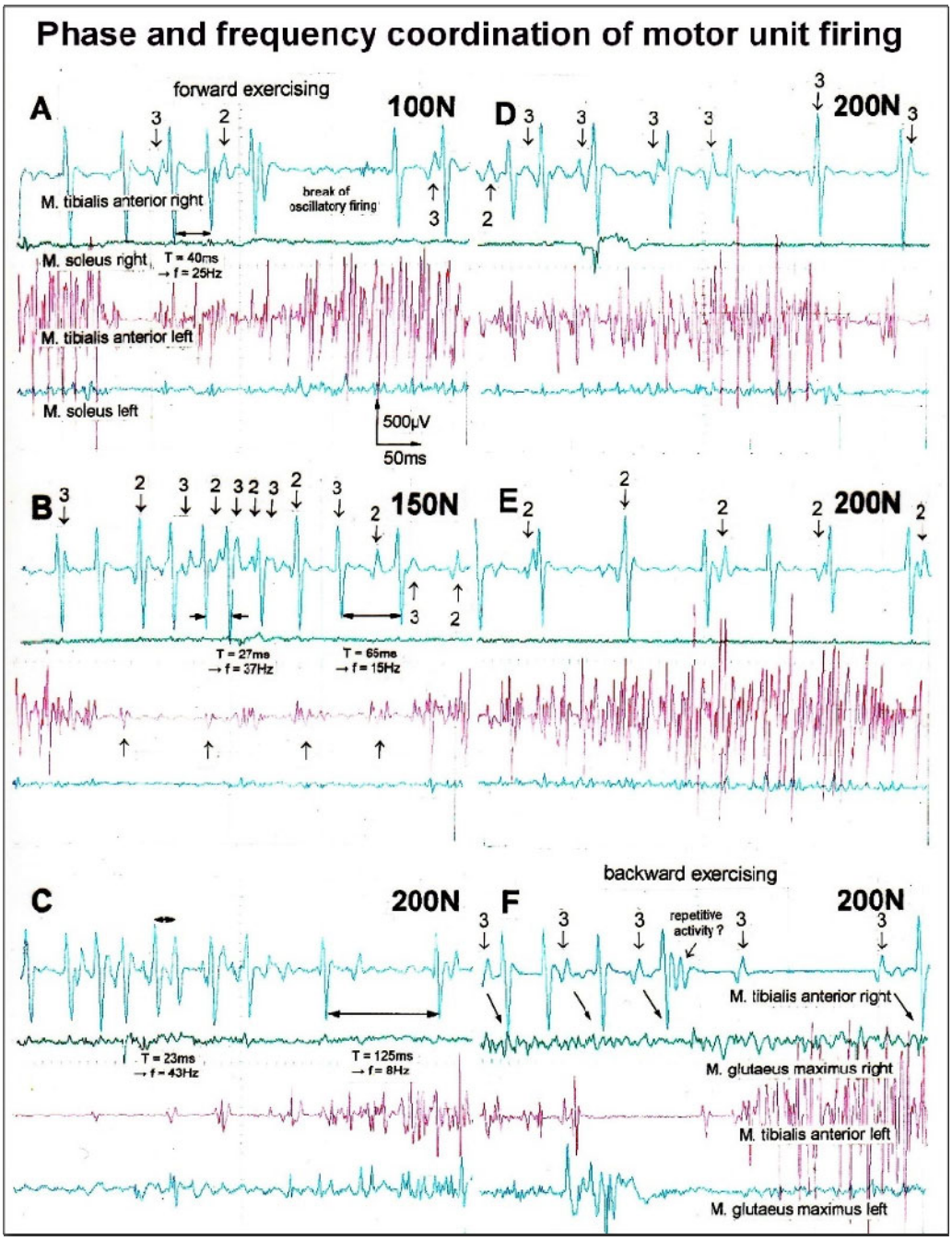

Figure 34. Phase and frequency coordination between oscillatory firing of 3 motor units (FF-type, motor units '2' and '3' are partly marked) during the generation of a motor program when exercising on the special coordination dynamics therapy device at loads increasing from 100 to 200N. Oscillation periods (T) and oscillation frequencies (f [Hz]) of oscillatory firing motor unit 1 (largest motor unit) are partly indicated. 'C, F' soleus electrodes shifted to gluteus muscles. In 'F', some coordination's between motor unit '3' and '1' are marked.

This partly impaired phase and frequency coordination at the single neuron level, the assembly level and the macroscopic level can be measured macroscopically when the patient is exercising on a special coordination dynamic therapy device **(Figures 9 and 34A)** on which arms and legs turn with a slightly different frequency (transmission 19 (arms): 18 (legs)). The phase coordination between arms and legs is imposed by the device. The loss of phase and frequency coordination between arm and leg movements becomes visible and measurable by the arrhythmicity of turning. During a turning cycle the coordination between arms and legs changes between pace and trot gait and according to the difficulty of the coordination the turning frequency increases and decreases. This frequency variation (df/dt; f = frequency) can be recorded, quantified and displayed on a computer screen **(Figure 35)**.

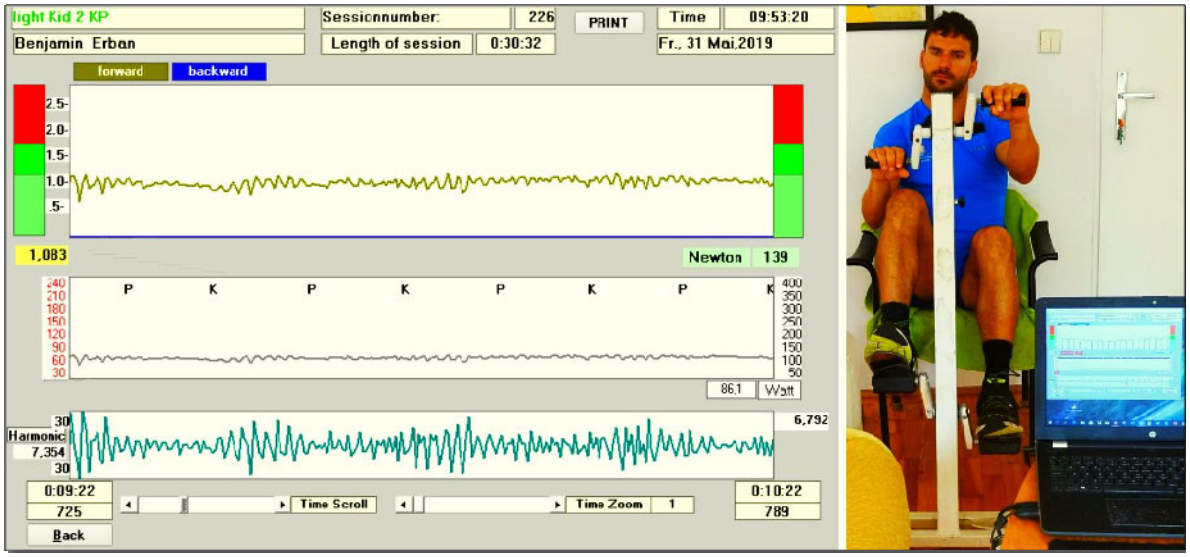

Figure 35. Coordination dynamics display. The brain-injured patient and disabled athlete Benjamin Erban is exercising on a special CDT device and the arrhythmicity of exercising (df/dt, lower trace) is displayed. At this moment, he is exercising at 139Newton. The mean value of arrhythmicity per min (coordination dynamics value) is 6.792. Note that between K (trot gate) and P (pace gait) the amplitude of arrhythmicity is higher, but not between P and K. Upper trace = frequency of exercising, middle trace = load in Watt. After 20 years of CDT, the severely brain-injured patient runs 100m in 14s and jumps 4m long. In Grosseto 2016 he won a bronze medal in running for disabled.

During the functional reorganization of the injured CNS of patients, the relative phase and frequency coordination of neuron firing has to be entrained as exactly as possible by the movement induced afferent impulse patterns from the receptors (learning through feedback information) to restore coordination in the range between 3 and 5 milliseconds **(Figure 25)**. The device has therefore to impose the exercising patient a coordination in the millisecond range for the different coordination's of arm and leg movements between pace gait and trot gait. The easy pace and trot gait coordination's, but not the difficult intermediate coordination's, can often be performed by the patient easily. Therefore, the continuous change from the easy to the difficult coordination's and backwards diagnoses the capability of the CNS to organize easy and difficult organizational states. If the movement state can be easily generated by the neuronal networks of the CNS, then the frequency variation of turning is small during the turning cycle (**Figure 35**, between P (pace gait) and K (trot gait)), and if the movement state is difficult to organize by the CNS, then the frequency variation is large (**Figure 35**, between K and P).

A healthy person can walk or crawl (automatisms) in trot or pace gait coordination, but not in a coordination in between. When exercising on the special CDT device, on the other hand, he is able to adapt to the intermediate difficult coordination's. A rat or dog is probably not able to adapt to the difficult coordination's, because of missing complexity of their neural networks. If one changes the nerve supply of flexor and extensor muscles, the rat cannot relearn [21], the monkey can after some time [22] and the human can re-learn nearly immediately [23].

The cerebral palsy girl Sophie learned walking **(Figure 36)**, balance and other motor functions through CDT [20]. But when training even more complicated coordination's between arm and leg movements, her higher mental functions improved strongly **(Figure 37)**, so that had not to be pushed so much anymore to train. She enjoyed it to train by herself with the family **(Figure 38)**.

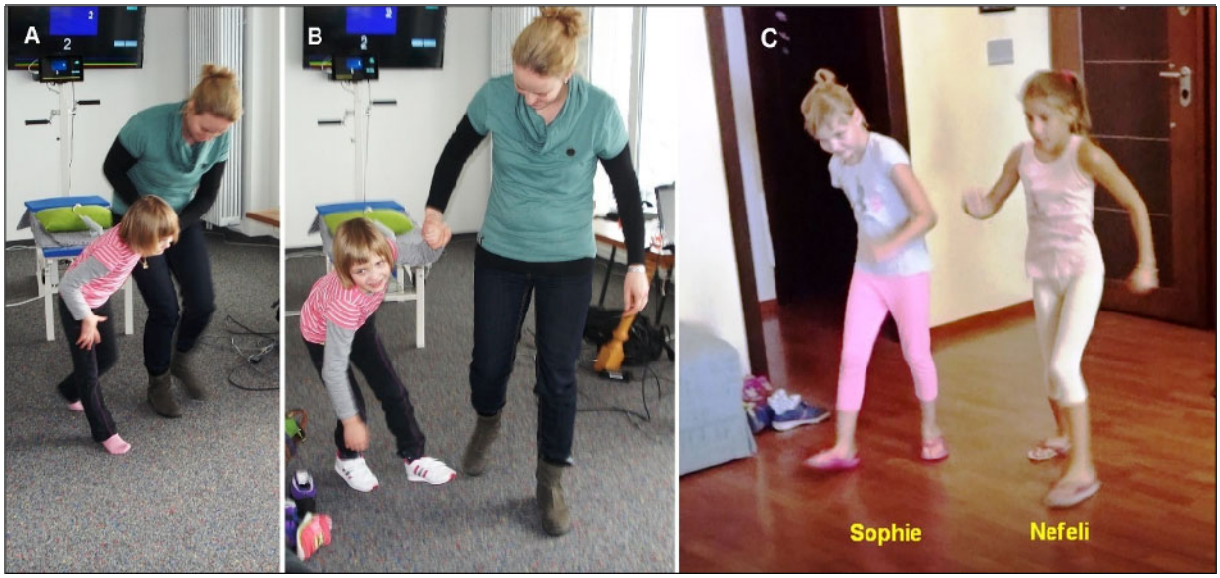

Figure 36. A, B. Sophie, the cerebral palsy girl with an atrophy of the cerebellum and pons, was unable to walk with her mother before CDT was started. She could not generate a walking pattern. Knees were overstretching (A) which blocked the walking pattern; she was immediately falling when trying to walk (B). C. Sophie (left) learned walking through CDT. When Sophie (cerebral palsy) and Nefeli (spinal cord injury) were training together (here walking), they motivated each other to fight more.

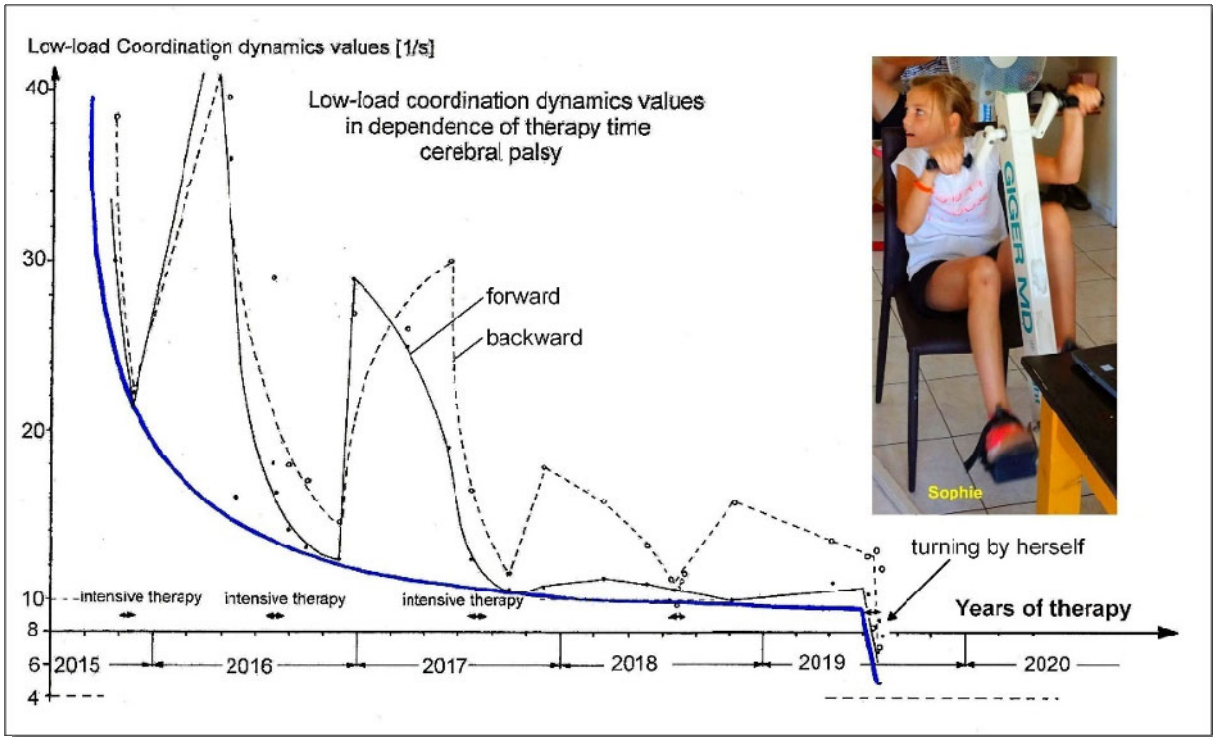

Figure 37. Improvement (lowering) of the low load coordination dynamics values with ongoing coordination dynamics therapy (CDT). During extensive therapy she improved strongly; with little or no therapy she got worse (higher values). The solid thick line connects the best values, which reached nearly a plateau of no further progress. When using a special CDT device with more complicated coordination's between arms and legs, the CDT values substantially improved (lowered) further. With this improvement of brain functioning, the cerebral palsy girl Sophie started to turn by herself.

It seems therefore that if it possible to train phase and frequency coordination in the deep complexity of CNS organization. Therefore, more repair is possible, especially with respect to the higher mental functions. To improve sufficiently phase and frequency coordination and CNS organization in the deep complexity of neural network organization, the patient has to train also at higher loads (1), at higher coordinated complexity (2) for longer times (3). Mental discipline is needed. Further, also easy coordination's have to be trained as walking or running for CNS stability. A balance between variability and stability is needed, because it can happen that CNS organization is drifting.

Figure 38. The cerebral palsy girl Sophie during training by herself with the mother and the grandparents. Sophie trains to improve her brain functioning and the others to improve their general health. The inset shows the MRI of Sophie with atrophy of cerebellum and pons.

I in the injured pathologically functioning CNS of patients, often coordination's other than pace and trot gait are the easy coordination's. A coordination coordinate is needed to judge the coordination dynamics. The pace and trot gait coordination's are used for the calibration, since both coordination's between arm and leg movements occur naturally during rhythmic coordinated (automatic) movements like creeping, crawling, walking and running.

The imposed coordination of arm, leg and trunk movements, upon exercising on the special coordination dynamics therapy and measuring device **(Figures 8 and 9)**, is in accordance with the coupling possibilities of premotor α_1 (8-20Hz), α_2 (5-9Hz) and α_3-oscillators (0.1-4Hz), even though the frequencies are only a relative coordination parameter, whereas the phase is an absolute coordination parameter.

When the hand levers are turned at between ≈ 0.4-1.5 Hz, the resulting frequency difference in turning between arms and legs is approx. 8.5 Hz (low α_1-oscillator frequency or high α_2-frequency) for low hand-turning frequency of 0.5Hz (low α_3-frequency). A slower turning of the hand levers would train directly more the premotor α_2-oscillators ($f < 8.5$Hz). Faster turning of the hand levers (higher α_3-frequency) would train directly the α_1-oscillators in the higher frequency range ($f > 8.5$Hz). Therefore, similar frequencies appear with respect to the frequency of turning on the device for measuring CNS organization and reorganization as have been measured for premotor spinal oscillators.

Improvement of the organization in the occasional and oscillatory firing mode

When turning the levers steadily with medium or high strength, the premotor spinal oscillators in the patient's CNS are entrained because premotor spinal oscillators self-organize themselves for high activation **(Figure 12D)**. The turning of the levers is therefore an oscillator (or assembly) formation therapy. The members of premotor oscillator assemblies (most likely the motoneuron and interneurons) are entrained to improve activation and inhibition by adjusting, for example, the efficacies of the corresponding activated synapses.

By turning the levers with little strength at approx. 0.4Hz (releasing the power (load)-setting knob), the motoneurons get only partly organized into premotor spinal oscillators. The motoneurons are firing mainly in the occasional firing mode and are trained for a better recruitment according to the size principle (rhythmicity of repeated recruitment ≈ 0.4Hz **(Figure 39)** [24]. Between the motoneuron firings in the occasional and oscillatory firing modes, a better coordination of both firing modes is entrained **(Figures 39 and 40)** [24].

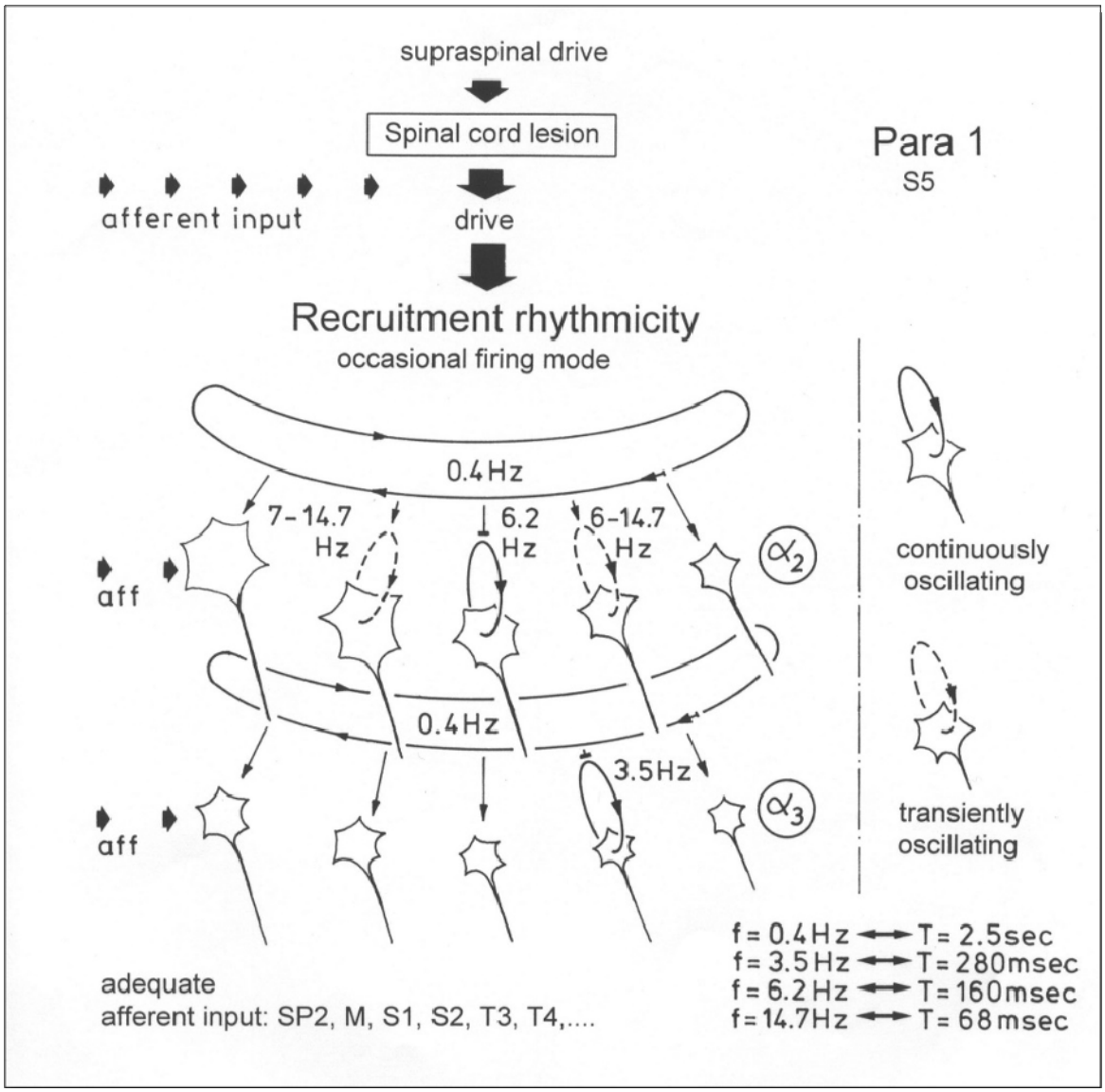

Figure 39. Recruitment rhythmicity of firing, drawn for α_2 and α_3-motoneuron axons, in an S5 nerve root in paraplegic 1. The changes in γ-motoneuron recruitment are not shown; neither the co-recruitment of γ_1 and α_2-motoneurons is indicated. The arrows pointing towards the motoneuron somas indicate recruitment; no arrow = no recruitment. SP2 = secondary muscle spindle afferents (affs), M = mucosal affs, P = pain affs, S1 = bladder stretch receptor affs, S2 = flow receptor affs, T3 = low threshold skin affs.

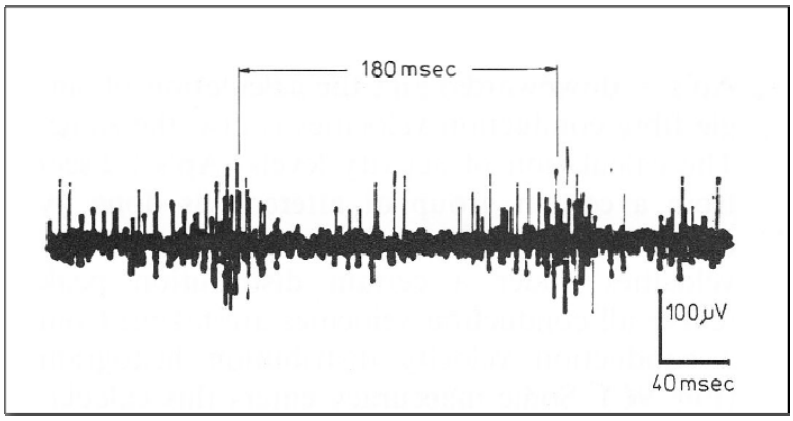

Figure 40. Overall efferent activity recorded from an S5 dorsal root 20 s after pulling the bladder and anal catheters. The rhythmic activity interval is marked by a 180ms distance. Brain-dead HT4.

OCCASIONALLY FIRING OF α AND γ-MOTONEURONS FOR LOW ACTIVATION - RECRUITMENT ACCORDING TO THE SIZE PRINCIPLE

Conduction velocities in dog and man

In man α and γ-motoneuron groups were identified by the group conduction velocities and partly by group nerve fiber diameters **(Figures 6 and 41)** and by the measured impulse patterns conducted along the fibers. Even though the conduction velocities were measured over small distances (10mm), the relative group conduction velocities were very reliable, because the conduction velocities of all nerve fiber groups were measured simultaneously and were calibrated by the calibration relation: secondary muscle spindle afferents conduct with the same velocity as the α_2-motoneurons, and the calibration relation is temperature independent, even though the conduction velocities themselves are strongly temperature dependent (**Figure 32** of [**7**]). Sufficient characterization of nerve fiber types is a principal problem when nerve fibers have to be safely identified for the understanding of neuronal network self-organization or the clarification of peripheral receptor properties of muscle spindles.

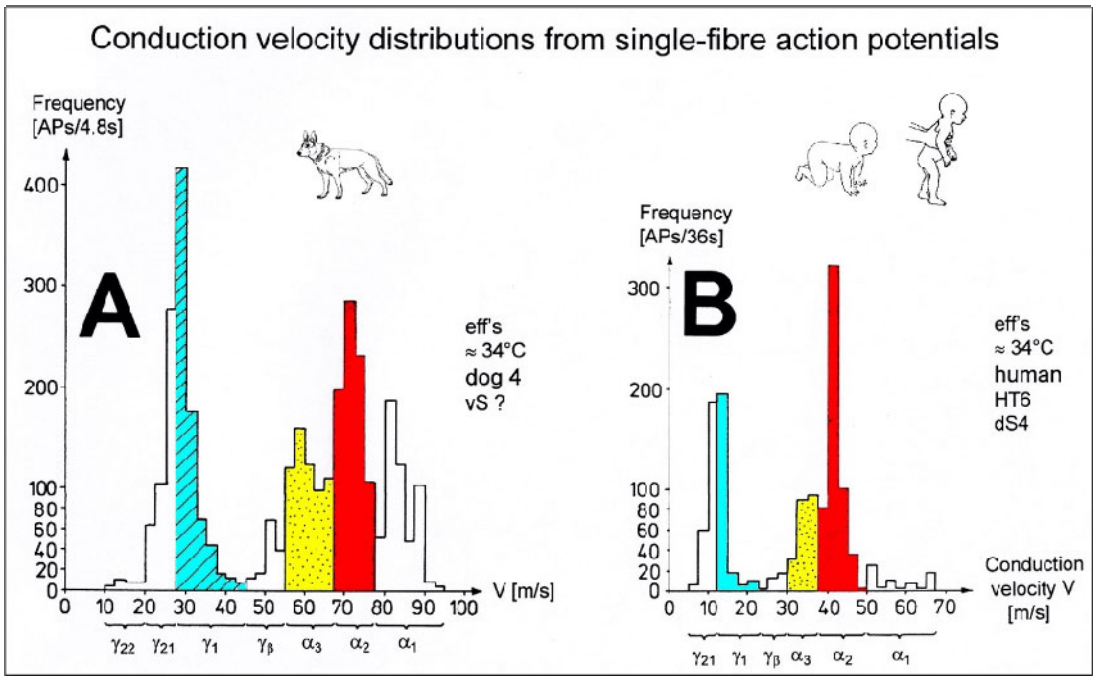

Figure 41. Distribution histograms of conduction velocity frequencies: efferent APs from a dog (A) and human (HT6; dS4) (B) lower sacral nerve roots. The distribution peaks are labelled according to the respective groups they represent. Motoneuron velocity ranges are indicated. In A, 24 sweeps of 0.2s, and in B, 30 sweeps (stimulated and non-stimulated) of 1.2s duration were used.

Since group conduction velocity distributions overlap, γ (and α) -motoneurons have to be identified additionally by their functions (by their natural impulse patterns).

In measurements in man, the groups of α and γ-motoneurons were identified by the speed and the dynamics to respond to natural stimulations such as touch, pinprick and catheter pulling, and by the conduction velocity [11]. The characteristics of the static (γ_2) and the dynamic (γ_1) γ-motoneurons are not the same as in animal research. In humans, the γ-motoneurons were therefore characterized by CNS properties, namely by the cell soma and in what neuronal networks the motoneuron cells are integrated, whereas in animal research, they were characterized by the periphery, namely how do primary muscle spindle afferents respond to repetitive 75 Hz stimulation (not always 75 Hz) of the static and dynamic γ-motoneurons in parallel with a ramp stretch [25]. To fulfil the needs of the human research and the clinical demands, we need a multiple group characterization of γ-motoneurons, which can be used in animal research and in the clinical setting. For α-motoneurons, this has partly been achieved. α_2-Motoneurons, for example, fire for continuous high activation at a frequency of about 6.7 Hz, have a group conduction velocity of 50 m/s, a group nerve fiber diameter of 10.2 μm and innervate FR-type muscle fibers, which are fast oxidative glycolytic fibers **(Figure 10)**. For dynamic and static γ-motoneurons, such a multiple characterization is not known in humans. In human measurements, three conduction velocity peaks of γ-motoneurons (γ_1, γ_{21}, γ_{22}) seem to exist. The γ_1-motoneurons respond faster to stimulation than the γ_2-motoneurons [11]. It has to be shown whether the human γ_1-motoneurons (identified centrally) actually correspond to the dynamic γ-motoneurons as identified in animal research (identified in the periphery) and whether the γ_2-motoneurons correspond to the static γ-motoneurons. The notion will be helpful that there is no tapering of nerve fibers. First electrophysiologic measurements from single human muscle spindles in the periphery indicate that the human muscle spindles may function similarly as do cat spindles, even though the human muscle spindles seem to be more complex [26], and human muscles may be quite different in different parts of the body.

Occasionally, transient oscillatory and continuous oscillatory firing mode

The method of single-nerve fiber action potential recording from whole nerve roots in humans was used to develop a precise classification scheme of nerve fiber groups in the PNS: the individual nerve fiber groups are identified by the group nerve fiber diameter and their group conduction velocity. Based on this classification scheme, receptor properties of skin, urinary bladder and anal canal afferents have been analyzed. The natural impulse patterns of motoneurons are characterized by the occasional firing mode, the transient oscillatory and the continuous oscillatory firing mode. The oscillatory firing has been displayed above. Now the recruitment of motoneurons in the occasional firing mode will be analyzed.

Comparison of conduction velocity distributions of humans and animals

To analyze recruitment of α and γ-motoneurons in the occasional firing mode in animals and humans, first a comparison between the velocity distributions of a human and a dog is given **(Figure 41)**. **Figure 41** shows such conduction velocity distribution histograms of a human (B) and a dog (A) measured with the same method, the same equipment and at similar temperatures. It can be seen that the velocity distribution of the dog is very similar in their peaks, apart from the higher group conduction velocity values. The dog α_2-motoneurons, for example, conducted at 70 m/s whereas the human ones at 40 m/s at 34°C. The difference between the human and the animal peripheral nervous system, however, may not just be that human nerve fibers conduct proportionally more slowly. Transmission frequencies of secondary muscle spindle afferents in man were measured to be as high as 5,000 Hz. It may be, therefore, that other human neuron membrane parameters differ from those of animals. The lower conduction velocity values in man may be the price for a higher transmission frequency. A higher transmission frequency may allow higher pattern variability and complexity.

Recruitment according to the size principle in each group of α and γ-motoneurons in dog and man with unspecific low-level stimulation - muscle tonus

Distribution changes of conduction velocities in each group of α_2, α_3 and γ-motoneurons were used for recruitment analysis. As was shown above, the α-motoneurons increase their firing rate upon the increase of their adequate afferent input from firing occasionally to firing oscillatory. It has been shown in humans for low activation that the α and γ-motoneurons are recruited with the increasing conduction velocity, i.e., according to the thickness of the axon, thus according to the motoneuron size. The slowly conducting fibers are recruited before the faster conducting ones in each motoneuron group [27,28]. In man, with no additional stimulation, the slowly and fast conducting α_2 and α_3-motoneurons are recruited repeatedly every 2s **(Figure 42A)**. In the dog (for identification of nerve fiber groups, see Figure 41A), with no additional stimulation, slowly (and fast) conducting γ_{21} and α_3-motoneurons showed repeated activation every 3 to 4s **(Figure 43)**.

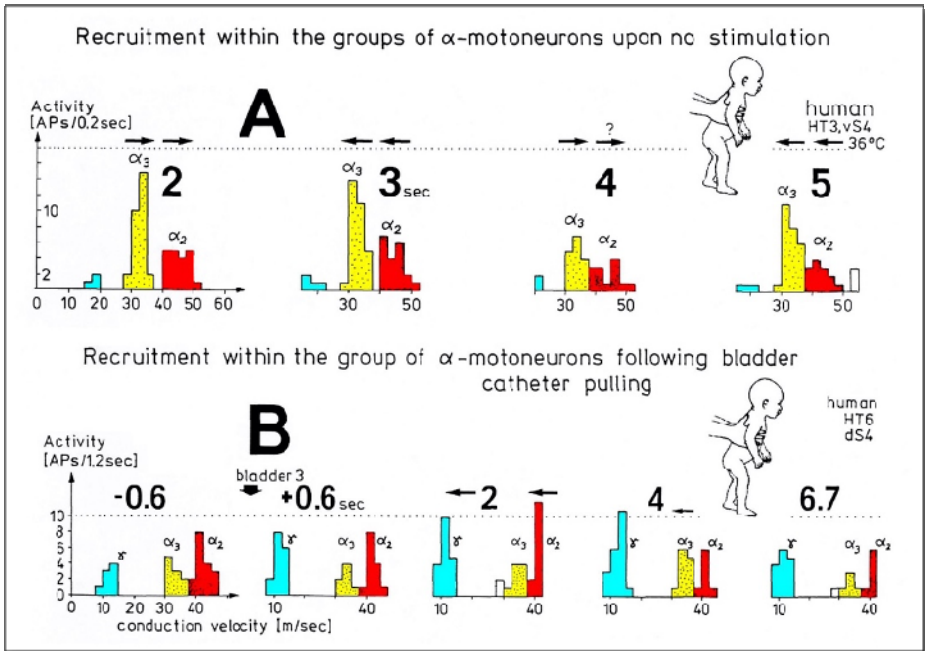

Figure 42. Frequency of the occurrence changes of single-fiber conduction velocities (recruitment changes) within the groups of α- and γ-motoneurons in man upon no stimulation (no catheter positioned, A) and following strong bladder catheter pulling (B). The velocity ranges in B are taken from **Figure 53**. Time in seconds following start of measurement or stimulation is indicated (e.g., 2: 2.0 to 2.2s). The arrow directions on top of the histograms indicate stages, at which motoneurons in a certain group with low or high velocities are preferentially activated, as can be calculated from the histograms. Note in B, the co-recruitment of γ_1 and α_2-motoneurons, and that α_2-motoneurons are recruited before α_3-motoneurons. HT3; vS4 (A) and HT6; dS4 (B).

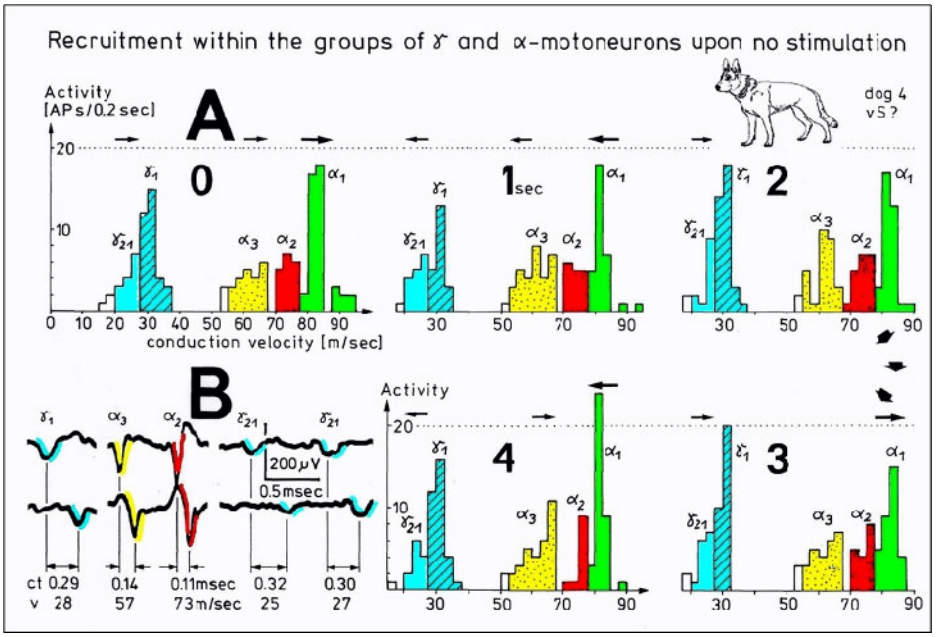

Figure 43. A. Frequency of occurrence changes of single-fiber conduction velocities within the groups of γ_1, α_3 and α_2-motoneurons (recruitment) in a dog sacral ventral root upon no stimulation. The group conduction velocity ranges are taken from **Figure 53**. Measurement times in seconds are indicated (e.g., one second: 1.0 to 1.2s). The arrow directions on top of the histograms indicate stages, at which motoneurons in a certain group with low or high velocities are preferentially activated, as can be calculated from the histograms. Columns for γ_1-motoneurons are crosshatched, those for α_3 are dotted, and those for α_2 are filled. Dog 4, bladder catheter positioned. B. A sweep piece from a recording from dog 4. Conduction times (ct) and conduction velocities (v) and α and γ-motoneurons are indicated.

A subgroup of α_1-motoneurons showed repeated recruitment every 2s **(Figure 43)**. In a slowly conducting rat subgroup of α_1-motoneurons, without specific stimulation, the motoneurons were recruited according to

the size principle every 2s. It seems, therefore, that in rats, dogs and man with unspecific low-level stimulation, α and γ-motoneurons are recruited repeatedly according to the size principle in each motoneuron group [27]. The period of repeated recruitment varies between 2 and 4s. The recruitment in the different groups may be synchronized or not. The recruitment within the different α and γ-motoneuron groups for low level activation is important to understand muscle tone (apart from mechanical muscle properties); however, it is difficult to measure the recruitment because of low activity, which makes the sampling intervals large to get sufficient events.

Recruitment of α and γ-motoneurons in dog and man following specific stimulation

Following bladder catheter pulling, the human slowly conducting γ_1 and α_2-motoneurons were recruited 2s after the pulling, the slowly conducting α_3-motoneurons 4s after the pulling **(Figure 42B)**. In the dog, following bladder catheter pulling, the slowly conducting γ_1 and α_2-motoneurons were recruited directly following the pulling, and the slowly conducting α_3-motoneurons were recruited 1s later **(Figure 44)**. In the rat, the slowly conducting α_1-motoneurons were recruited directly following pinpricking of the limb, the slowly conducting α_2-motoneurons 0.2s later, and the slowly conducting α_3-motoneurons 1s later. Therefore, following specific additional stimulation, the more dynamic motoneurons (α_1, α_2, γ_1) are recruited according to the size principle before the more static motoneurons (α_3, γ_2), depending on the function stimulated. Often, there was co-recruitment of α and γ-motoneuron groups.

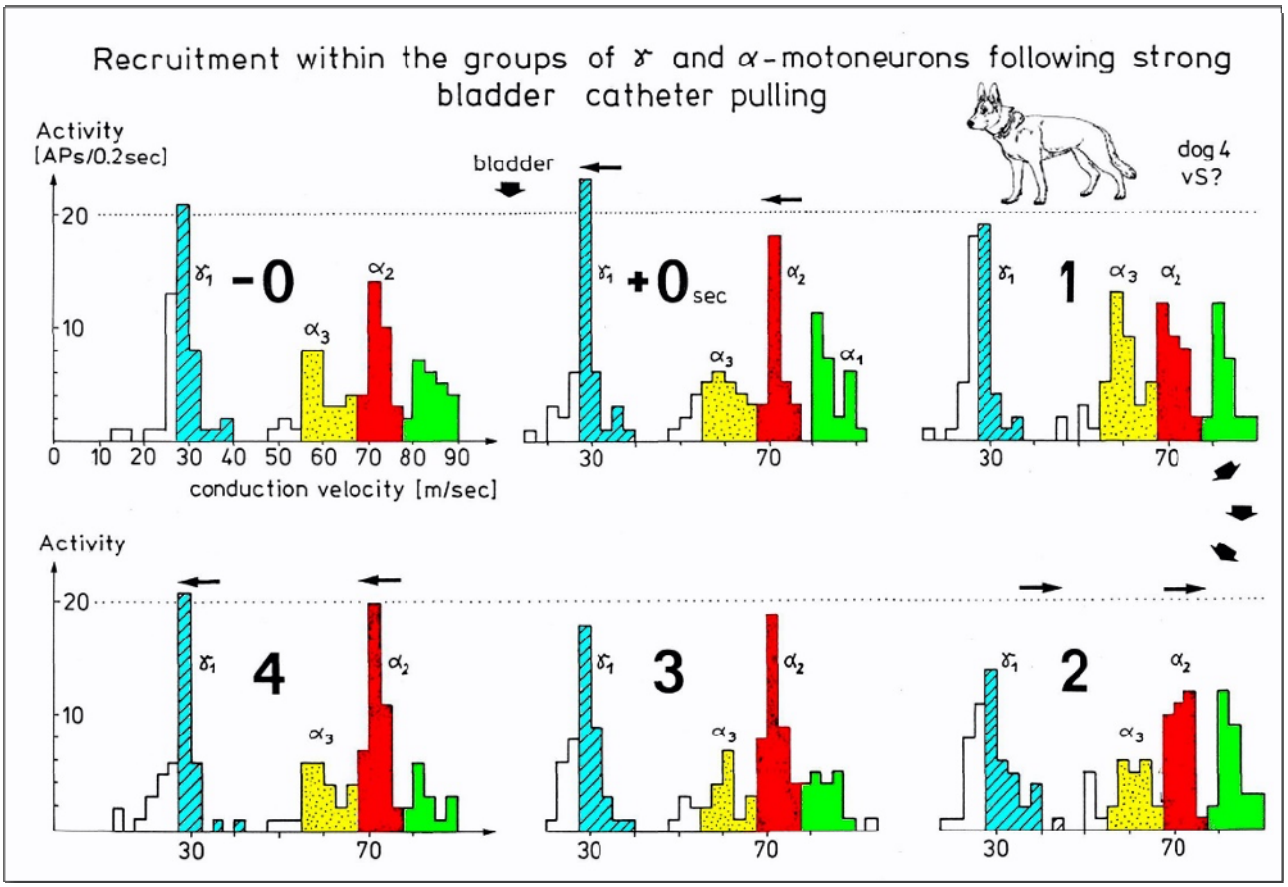

Figure 44. Recruitment of α and γ-motoneurons in a sacral ventral root of dog 4 following strong bladder catheter pulling. For further description, see legends to previous Figures. Note that α_2-motoneurons are recruited before α_3-motoneurons, and the co-recruitment of γ_1 and α_2-motoneurons.

Recruitment of motoneurons in the occasional firing mode following spinal cord injury - Pathologic recruitment

Upon no additional stimulation in a paraplegic patient, slow and fast conducting motoneurons were recruited repeatedly within the groups of α_2 and α_3-motoneurons every 2.5s in similarity to the rather physiologic case

(HT3, **Figure 42**). But the level of activation of the α and γ-motoneurons was higher in the paraplegic patient **(Figure 45)** than in the brain-dead human **(Figure 42)**, even though the S4 roots **(Figure 42)** are expected to contain more fibers than an S5 root **(Figure 45)**. The higher activation of the neuronal networks of the spinal cord below the injury is in accordance with the pathologic over-activation of muscles (spasticity) in para- and tetraplegic SCI patients.

Following anal catheter pulling, the slowly conducting α_3-motoneurons (S) were recruited directly following the stimulation, whereas the faster conducting α_2-motoneurons (FR) were recruited approx. 1 s later **(Figure 46)**. The faster recruitment of α_3-motoneurons (more static) in comparison to the α_2-motoneurons (more dynamic) differed from the recruitment observed during measurements in brain-dead humans and in rats and dogs and may be caused by the loss of interneurons in the spinal cord and is in accordance with the pathologic activation of muscles in paraplegia. Bladder catheter pulling does not activate so many α_3-motoneurons (the external urethral sphincter mainly is mainly innervated by α_2-motoneurons) and is therefore not suitable for comparing the recruitment speed between α_2 and α_3-motoneurons.

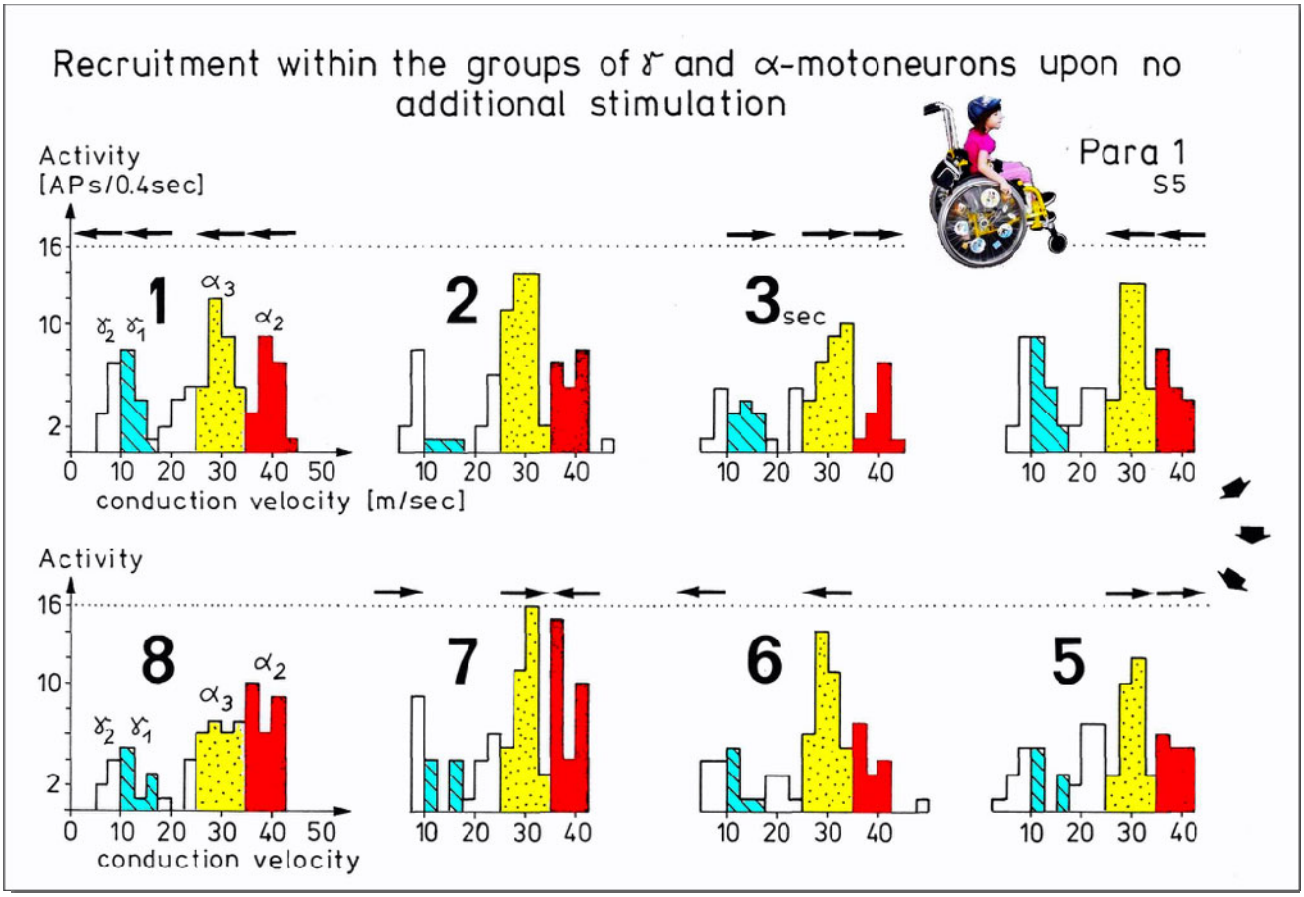

Figure 45. Frequency of occurrence changes of single-fiber conduction velocities in paraplegic 1 upon no stimulation, with the anal and bladder catheters positioned. The arrows on top of the histograms indicate stages at which α and γ-motoneurons in a certain group are preferentially activated with low or high conduction velocities. Note that there is mainly co-recruitment of γ_1, α_3 and α_2-motoneurons with rhythmicity.

Recruitment according to the size principle in each motoneuron group

In an easy understanding, Hennemann's recruitment according to the size principle can be understood as a special case of motoneuron recruitment (namely, recruitment among α_1-motoneurons only) of the above-mentioned more general recruitment principle. Upon recording with EMG surface electrodes, e.g., from the musculus tibialis anterior of a healthy human individual, it can be seen that with low muscle activation, the single motor unit APs have a small amplitude, whereas with higher activation motor units with larger AP amplitudes are recruited.

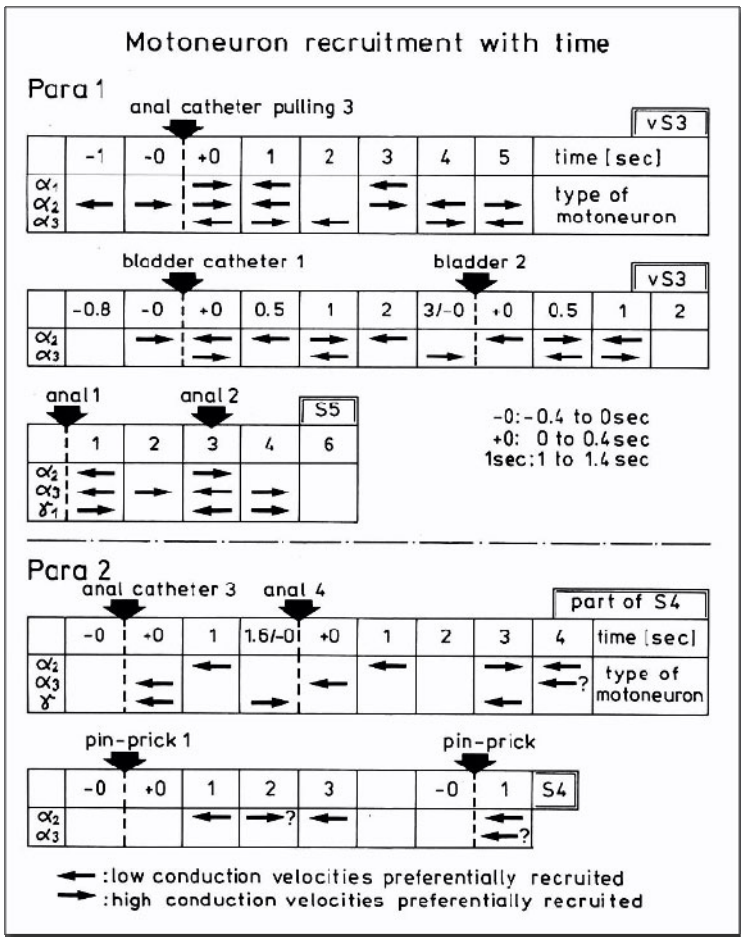

Figure 46. Summed recruitment changes in the occasional firing mode with ongoing time as measured in two paraplegics (1 and 2). The arrows direction indicates whether preferentially motoneurons with low or high axon conduction velocities are recruited (within the time interval of 0.4s) after a certain time. Para 1; Para 2.

Since FF type motor units have much larger AP amplitudes than FR and S type motor units, one mainly recognizes the recruitment of FF type motor units. Taking the recruitment of motoneuron groups according to the size principle in each motoneuron group into account, the recruitment of motoneurons in the occasional firing mode is quite complex. In the occasional firing mode in man (low activity mode, when premotor spinal oscillators are not organized), the different α and γ-motoneuron groups have been shown to be recruited according to the conduction velocity (and axon diameter) in each nerve fiber group approx. every 2.5 s. Directly following natural stimulation (touch, pinprick, anal and urinary bladder catheter pulling), the faster conducting nerve fibers (FF) are activated before slower conducting nerve fibers (S). But the activation order can change following spinal cord injury.

The recruitment of motoneuron axons according to the size principle in each motoneuron group seems to be in contradiction to the Hennemann's motor unit recruitment according to the size, disregarding the motoneuron group.

When recording single motor unit action potentials (MUAPs) electromyographically from human leg muscles, it is obvious that with the increasing volitional muscle activation, on the average, the activated motor unit potential amplitudes increase in size. Since we can assume that the larger motor unit potentials will on the average be innervated by the larger sized motoneurons, this motor unit recruitment seems to be in contradiction to the motoneuron axon recruitment while in accordance with the Hennemann's size principle. **Figure 27** of Chapter III of [7] shows that the motoneurons emerging from the intumescentia lumbosacralis are mostly of α_1-motoneuron type. Consequently, records from most leg muscles are mainly records from α_1-motor units. In a first approximation, there is, therefore, no contradiction to the above motor axon recruitment if there is mainly only one motoneuron type innervating the different muscles. Further, since there is indication that the motor unit

potential amplitudes decrease from the FF to the FR and S-type motor units, it is anyway more difficult to identify the FR and S-type motor unit potentials innervated by the α_2 and α_3-motoneurons. Potentials not fitting the size principle can be falsely excluded by claiming that the not-fitting small motor unit action potentials were probably generated too far from the recording electrodes to give a large potential (MUAP amplitude reduction due to volume conduction). Further, in the oscillatory firing mode, the very low amplitude α_3-motor units are difficult to identify, since close potentials start to fuse, because the duration of the interspike intervals of the impulse trains can be close to the range of those of the motor unit potentials (≈ 5 ms).

The problem of the type identification is less difficult when recording single-nerve fiber action potentials, because the single-nerve fiber action potential durations are approximately shorter by a factor of 10 than the motor unit action potentials **(Figure 23)**, and the action potential amplitudes may not decrease as much when changing from α_1 to α_3-motoneuron axons. For a comparison between single-nerve fiber action potentials and motor unit action potentials, see **Figure 9** of Chapter II. The recording from a population of nerve fibers therefore provides more precise knowledge concerning the recruitment of motoneurons and in turn on the regulatory mechanisms of neuronal networks. The main disadvantages of recording from nerve fibers include the invasive nature of the method and difficulties of getting an opportunity for recording. On the other hand, the electromyographic recording of motor unit action potentials with surface electrodes is simple to perform and presents practically no risks. It seems therefore worthwhile to try to improve the interpretation of motor unit action potentials recorded with surface electrodes.

Recruitment according to the size principle in each motoneuron group

In an easy understanding, Hennemann's recruitment according to the size principle can be understood as a special case of motoneuron recruitment (namely, recruitment among α_1-motoneurons only) of the above-mentioned more general recruitment principle. Upon recording with EMG surface electrodes, e.g., from the musculus tibialis anterior of a healthy human individual, it can be seen that with low muscle activation, the single motor unit APs have a small amplitude, whereas with higher activation motor units with larger AP amplitudes.

Parkinsonian tremor is generated by the synchronization of α_1- and α_2- premotor spinal oscillators because of impaired phase and frequency coordination due to missing inhibition

Impaired phase and frequency coordination among α-motoneurons measured with sEMG

With the single-nerve fiber action potential recording method it was shown that the phase and frequency coordination among neuron firing **(Figure 25)** became impaired following spinal cord injury **(Figures 28 and 29)**. It will be shown now with sEMG that pathologic motor programs occur and that the motor bursts are structured with tremor, clonus and rhythmic motor activity. It will be shown that in patients with Parkinson's disease or spinal cord injury some motoneurons fired spontaneously in an oscillatory manner. The more the CNS functioning was impaired, the more pathologic the motor programs became. In patients with Parkinson's disease oscillatory firing motoneurons synchronized their firing to give rise to tremor. Tremor and rhythmic firing of motor units occurred in motor burst of motor programs in some muscles. Some muscles were not activated at all or were continuously activated during the motor program. In patients who have suffered a spinal cord injury, muscles were not activated or activated continuously (spasticity) during the motor programs. Motor bursts were partly structured with clonus activity and the oscillatory firing of motoneurons was partly synchronized.

Uncontrolled synchronized firing of motor units in Parkinson's disease patients

It was shown above that oscillatory firing motoneurons and oscillatory firing motor units coordinated their firing so as not to fire in a synchronized manner **(Figure 24B)**; this may be achieved by some kind of lateral field inhibition. It will be shown below in a Parkinson's disease patient that if this kind of coordinated firing is impaired, some motor units start to fire in a synchronized manner.

In **Figure 47B**, we see mainly FR-type motor units (identified by low motor unit amplitude and FR-type frequency range (≈ 5Hz)) firing in a synchronized manner oscillatory in the right soleus muscle at a frequency of 4.55Hz. In the right tibialis anterior muscle, also FR-type motor units oscillated in a synchronized manner antagonistically to the motor units in the soleus muscle. On top of the low-amplitude FR-type motor unit activity, large amplitude FF-type motor unit activity can be seen, which was synchronized. The duration of FR and FF-type activity is marked in one activity burst in the right tibialis anterior muscle. Synchronized oscillatory firing of mainly FR-type motor units can further be seen in the soleus, the biceps brachii, and the triceps brachii muscles in **Figure 47D**. In **Figures 47C and 47D** further synchronized activity of FR and FF-type motor units can be seen in the right tibialis anterior muscle.

It can partly be seen from **Figure 47A** that this synchronized oscillatory firing of FR and FF-type motor unit's builds up and then ceases. In **Figure 47A**, the

tremor ceases. At first, more and more FF-type units stopped firing and then also the FR-type motor units stopped firing. However, when the tremor starts, first the FR-type units fire synchronously in an oscillatory manner to which then the FF-type units synchronize. The process first affects the smaller units with lower amplitudes and then the larger units with larger amplitudes. There is some variation in this rule because of the different distances of the motor units to the recording electrodes.

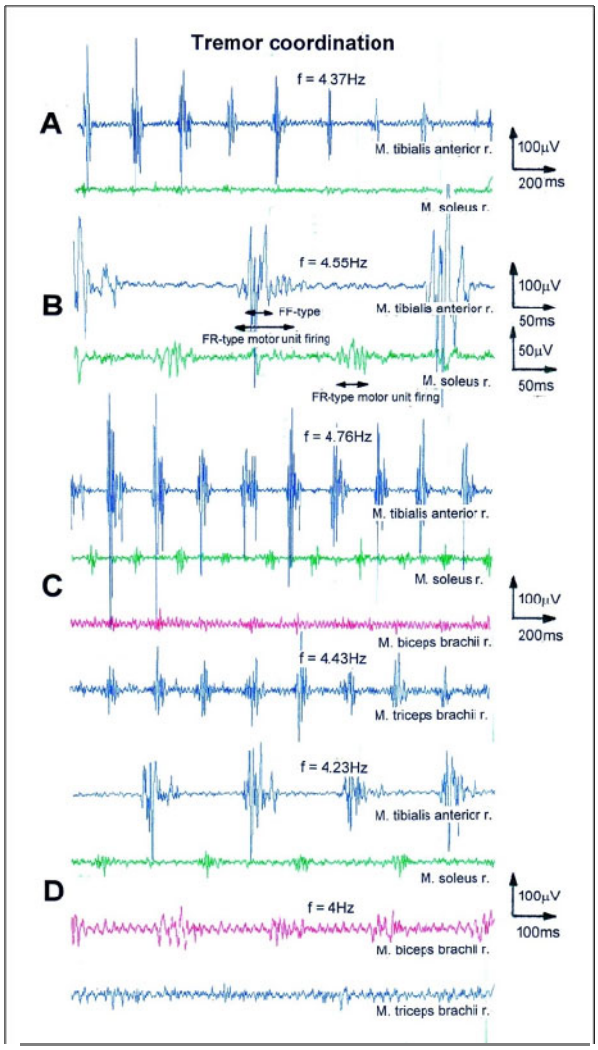

Figure 47. EMG recordings of tremor coordination and synchronization of FF and FR-type motor unit firing, giving rise to tremor in a patient with Parkinson's disease. A. Ceasing of tremor activity in the right tibialis anterior muscle; no tremor activity in the right soleus, right biceps brachii, and triceps brachii muscles. B. Antagonistic tremor activity in the right tibialis anterior and soleus muscles. The EMG activity in the soleus muscle stems mainly from FR-type motor units and those in the tibialis anterior muscle from FR (small-amplitude) and FF-type (large-amplitude) motor units. No clonus activity in the other two muscles. C. EMG tremor activity in the tibialis anterior, the soleus and the biceps brachii muscles. The clonus activity in the right soleus and the right tibialis anterior muscles shows antagonistic coordination. The activity in the biceps brachii muscle (f = 4.43Hz) was not in coordination with those of the tibialis anterior and soleus muscle (f = 4.76Hz). D. EMG tremor activity in the tibialis anterior, the soleus, the biceps brachii, and the triceps brachii muscles. There was antagonistic tremor coordination between the antagonistic tibialis anterior and soleus muscles and between the antagonistic biceps and the triceps brachii muscles.

As can be seen from **Figures 47B-47D**, the tremor in antagonistic muscles is mostly antagonistic, probably due to the antagonistic proprioceptive input. Some agonistic tremor coordination seems visible. The seemingly low-amplitude agonistic tremor coordination may also be due to crosstalk of sEMG activity; this means that, for example, some tibialis muscle activity was recorded in the soleus muscle. The coordination of the sEMG-displayed tremor between different muscles may depend on the agonistic and antagonistic afferent input.

Motor program bursts in patients with Parkinson's disease structured with tremor activity and motor unit oscillatory activity

The impaired coordination leading to spontaneous oscillatory firing and synchronized oscillatory firing of FR and FF-type motor units and tremor should also be seen during movements because also then coordinated organization of the CNS networks is needed.

In the motor program bursts shown in **Figure 48A**, rhythmic activity can be identified, which cannot be seen in the rather physiologic motor pattern. The highlighted rhythmic firing at 11.4 and 11.8Hz may indicate oscillatory firing of FF-type motor units innervated by α_1-motoneurons.

In another, more time-stretched motor program recording, such rhythmic firing can be seen more clearly **(Figure 48B)**. Rhythms of 5 and 4.2Hz were most likely induced by oscillatory firings of an α_2-motoneuron, and those of 9.5 and 11 Hz were most likely induced by oscillatory firings of an α_1-motoneuron.

Three important conclusions can be drawn from **Figure 48**. First, the term referring to the symptom 'resting tremor' is not correct. Tremor not only occurs during rest, but also during movement. The reduced intensity of tremor during movements may indicate entrainment of neuronal networks resulting in a reduction of tremor in the short-term memory. Second, FF and FR-type motor units, innervated by α_1 and α_2-motoneurons respectively oscillate with their 'Eigen-frequencies' for high activation during motor program burst. This was shown earlier in patients with spinal cord injury for muscles only innervated by a few motoneurons. Third, since synchronized oscillatory firing in tremor can also be seen in motor bursts during movements, two organizations, namely tremor and movement were organized in the neuronal networks at the same time.

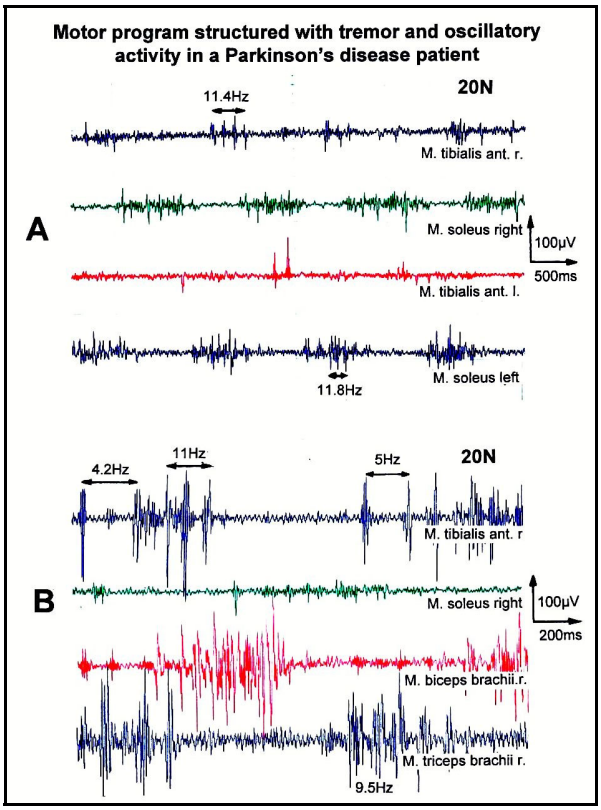

Figure 48. Surface EMG motor programs of a patient with Parkinson's disease during the exercise on the special coordination dynamics therapy device at the low load of 20N. The motor program muscle bursts are more or less structured by rhythmicity (no rhythmic structure occurs in normal motor bursts). In A, rhythmic activity at a frequency of 11.4 and 11.8Hz is suggested. In B, (faster sweep and partly different muscles) low-frequency rhythmicity of 4.2 and 5Hz (frequency range of α_2-motoneuron oscillatory firing) and higher frequency rhythmicity of 11 and 9.5Hz (frequency range of α_1-motoneuron oscillatory firing) are suggested to be seen.

Motor program bursts in patients who suffered a spinal cord injury, structured with clonus activation and rhythmic firing of FF-type motor units

In patients with Parkinson's disease (probably due to the lack of supraspinal inhibition) and in patients with an incomplete spinal cord injury (probably due to the damage of inhibitory tract fibers) it could be demonstrated that few (in spinal cord injury) and many (in Parkinson's disease) motoneurons started to fire spontaneously or nearly spontaneously oscillatory (**Figure 71** of [8]). In addition, in Parkinson's disease patients the oscillatory firing motoneurons partly synchronized their firing **(Figure 47)**, probably due to the missing of some kind of

lateral field inhibition. In patients with a spinal cord injury, there was very little or no synchronization in the oscillatory firing of motoneurons. Tremor therefore was not observed in spinal cord injury patients.

However, marked clonus, which is not functionally dissimilar from tremor, can often be observed in patients with spinal cord injury. Instead of tremor of the hands and feet marked at rest, the feet perform consecutive dorsal and plantar flexions. The reason for that rhythmic dorsal and plantar flexion is probably rhythmic activation of a very sensitive regulation loop between the feet and the spinal cord rather than synchronization of oscillatory firing motor units.

In **Figure 49B** a pathologic motor program of a patient with an incomplete thoracic spinal cord injury can be seen. The motor program is poor, because there is no motor program in the right tibialis anterior muscle and the motor bursts in the right and left gastrocnemius muscle are structured with rhythmicity, i.e., with clonus activity. A typical clonus recording when not exercising can be seen in **Figure 49A**.

The impaired coordination of motor unit firing can also be seen in the movement patterns in **Figure 49**. On a stretched time scale the clonus can clearly be seen in the right and left gastrocnemius muscles **(Figure 49C)**. In the left gastrocnemius muscle, the motor program burst is structured with three clonus bursts, which are in turn structured by rhythmic activity at 26 and 40Hz which probably originates from the oscillatory firing of FF-type motor units innervated by α_1-motoneurons.

Since tremor, clonus and rhythmic firing of FF-type and FR-type motor units can be seen in motor programs, they all go through the same final premotor network.

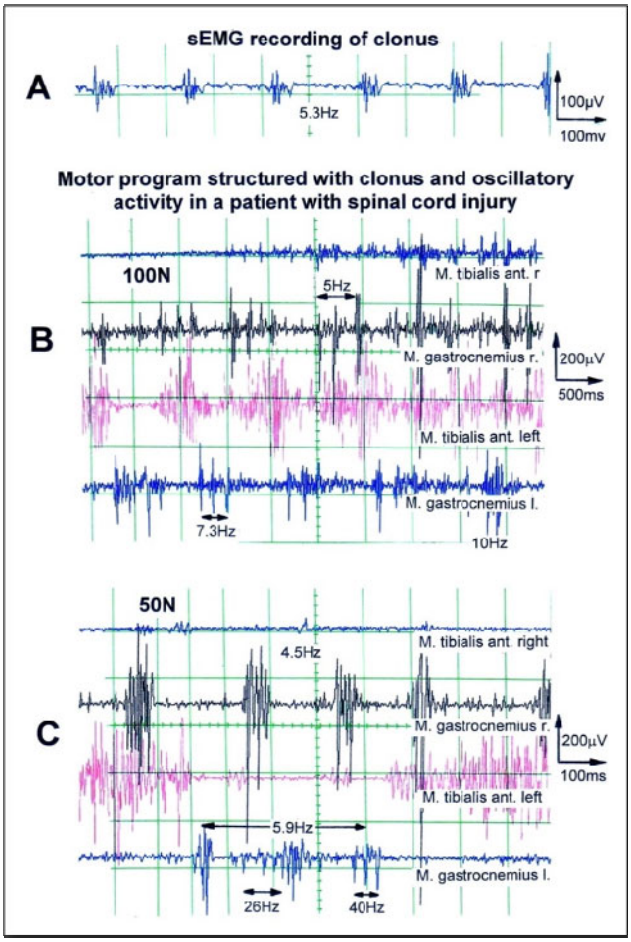

Figure 49. A. EMG recording of a clonus (f = 5.3Hz) in the right tibialis anterior muscle of a patient who suffered a complete spinal cord injury sub Th5/7; the patient was not exercising. B, C. Motor programs of a patient who suffered an incomplete spinal cord injury sub Th4 upon exercising on the special coordination dynamics therapy device at 50 and 100N (medium to high load). In B, motor program bursts are structured by rhythmicity; frequencies of 5 and 7.3Hz are suggested. No motor program in the right tibialis anterior muscle; some motor program structure in the right gastrocnemius muscle. In C (faster sweep), there is no motor program in the right tibialis anterior muscle. Mainly clonus activity at a frequency of 4.5Hz can be seen in the right gastrocnemius muscle. Two physiologic motor program bursts can be seen in the left tibialis anterior muscle (not structured by rhythmicity). In the left gastrocnemius muscle, a motor program burst can be seen which is structured by 5Hz rhythmicity (clonus frequency, see clonus in the right gastrocnemius muscle) and higher frequency rhythmicity (26 and 40Hz).

Oscillatory firing of motoneurons originates in the spinal cord

Rhythmic firing of FF and FR-type motor units was recorded with no or nearly no volitional activation in patients with Parkinson's disease and in patients who have suffered a spinal cord injury. These findings support earlier measurements with the single-nerve fiber action potential recording method of α-motoneurons firing oscillatory for high activation, also when disconnected from supra-spinal drive. Recordings from the isolated spinal cord in patients with complete spinal cord injury, taken from below the injury level, showed less regular rhythmic firing **(Figure 19)**. Recordings from the whole spinal cord connected with the lower part of the reticular formation in brain-dead humans showed more regular oscillatory firing **(Figures 19 and 30)**. In the presence of damage to the pre-existent descending pathways, activation of redundant pathways (and may be redundant neurons), reorganization in spared descending tracts and building of new pathways is required for functional repair in spinal cord injury.

Motor bursts structured with rhythmic activity

When patients exercised coordinated arm and leg movements on a special coordination dynamics therapy device **(Figures 8 and 9)**, rhythmic activity could be observed in the motor bursts for low load in Parkinson's disease patients **(Figure 48)** and for higher loads in patients who suffered a spinal cord injury **(Figure 49)**. First, this rhythmic activity during motor bursts supports the conclusion that during the motor burst, highly activated motor units fire in an oscillatory manner. Second, this partly synchronized and therefore uncoordinated uncontrolled rhythmic activity was still partly controlled by coordinated afferent input, as rhythmic firing was only present during the motor burst and not continuously. In very severe CNS malfunctioning, such firing can also occur between the motor bursts. The partial control of tremor activity was further indicated by the fact that in different muscles the tremor was mostly coordinated with respect to agonist and antagonistic muscles, depending on the rhythmic movements of arms, legs and fingers **(Figure 47B-47D)**.

The triggering mechanisms of Parkinsonian tremor and large-scale coordination

In **Figures 50A and 50B** two mechanisms of tremor induction are shown. The patient was positioned on a chair at the special coordination dynamics therapy device but was not exercising. In **Figure 50A** one FR-type motor unit in the gastrocnemius muscle (innervated by an α_2-motoneuron) started to oscillate (first triggering mechanism), i.e., fired rhythmically with an impulse train consisting of 3 motor unit potentials. Most likely, the gastrocnemius muscle was not moving. Then more FR-type motor units and maybe some S-type motor units started to fire synchronously **(Figure 50C)**. The gastrocnemius muscle may have moved a bit with a frequency of 4.1Hz. The triceps brachii muscle moved, because a movement artifact was recorded from it **(Figure 50C)**. With the start of FF-type motor unit firing, synchronized with the FR-type motor unit firing (**Figures 51A, 51B 50E and 50F**, tibialis anterior r.), the muscle moved rhythmically.

A second tremor or muscle movement triggering mechanism concerned FR-type (and may be S-type) motor units synchronizing their oscillatory firing. In the left part of **Figure 50B** the FR-type motor units oscillated but not in synchronization; no movement artifact at the electrodes of the triceps brachii muscle was recorded. When the FR-type motor units started to oscillate in a synchronized manner at a frequency of 4.2Hz (right part of **Figure 50B**), then a rhythmic movement artifact (f = 4.8Hz) was generated at the surface electrodes of the triceps brachii muscle. Since the triceps brachii muscle is sited in the arm and the gastrocnemius muscle in the leg, the oscillatory firing networks of the arm (network assemblies in the intumescentia cervicalis) and the leg (assemblies in the intumescentia lumbosacralis) did communicate with each other. There were therefore large-scale synchronization and coordination at least between the intumescentia cervicalis and lumbosacralis, which is a distance of approximately 300 mm.

The full muscle movement or tremor was generated when the FF-type motor units (innervated by α_1-motoneurons) synchronized their firing with the firing of the FR-type motor units **(Figures 50E and 50F)** (third triggering mechanism). With the synchronization of the FF-type motor units, the muscle movement or tremor frequency changed to match frequency coordination between the driving oscillatory firing of α_1 and α_2-motoneurons. In **Figure 50D**, the common frequency of the synchronized oscillatory firing α_2-motoneurons (and maybe α_3-motoneurons) was 3.3Hz. With the synchronization of the α_1-motoneurons, the common synchronized frequency increased to 3.6Hz **(Figure 50F)**. The α_1-motoneurons could have fired in an oscillatory manner at a frequency of 7.2Hz, so that a single FF-type motor unit potential could have fired in coordination with every second muscle activation burst of the tremor. If another α_1-motoneuron oscillated at 10.8Hz, the innervated FF-type motor unit potential could have fired in coordination with every third activity burst.

In conclusion, in this patient the Parkinsonian tremor started with the synchronized oscillatory firing of FR-type motor units (innervated by α_2-motoneurons). With the synchronized firing of FF-type motor units (innervated by α_1-motoneurons) the full muscle movement or tremor was generated.

The reason that the FF-type motor units synchronized their rhythmic firing and that the FF-type motor units synchronized their firing with those of the FR-type motor units and not vice versa is that α_2-oscillators have a high and α_1-oscillators a low stability.

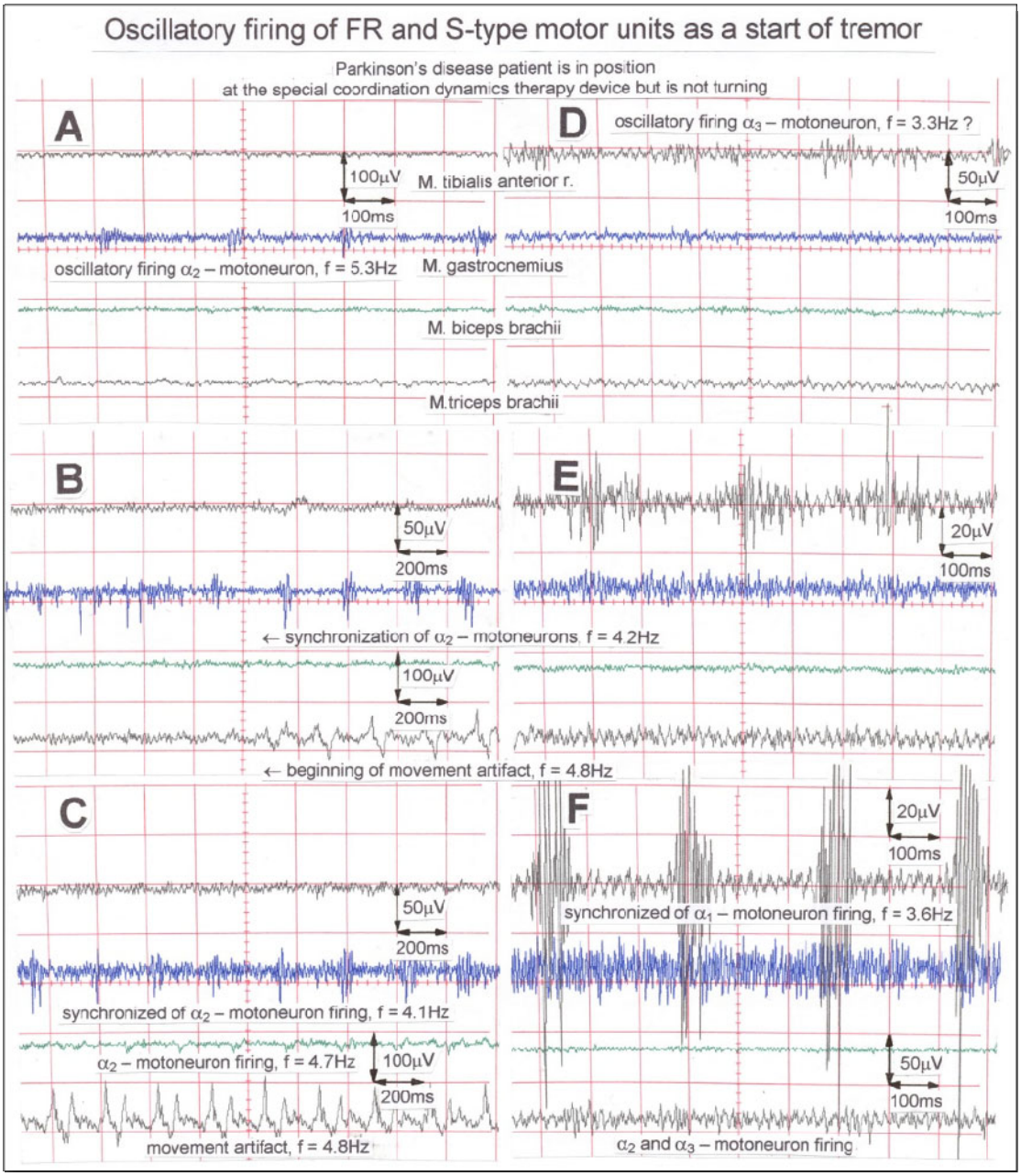

Figure 50. Oscillatory firing of α_2-motoneurons and the synchronization of oscillatory firing α_2 and α_1-motoneurons. Recordings were done with sEMG. A. Oscillatory firing of a single α_2-motoneuron motor unit (f = 5.3Hz; amplitude ≈ 35µV, triplet-firing) in M. gastrocnemius. B. Synchronization of mainly oscillatory firing α_2-motoneuron motor units (FR, f = 4.2Hz) in gastrocnemius muscle. With the synchronization of the oscillatory firing α_2-motoneurons a movement artifact was induced in the electrodes on M. triceps brachii. C. Synchronized oscillatory firing of α_2-motoneuron motor units, mixed with a few α_1-motoneuron motor units of small amplitude in the gastrocnemius muscle. In musculus biceps brachii an α_2-motoneuron motor unit fires at 4.7Hz not synchronized with the α_2-motoneuron firings in gastrocnemius muscle. Rhythmic movement artifact in triceps brachii muscle (f = 4.8Hz) indicating an arm tremor of 4.8Hz. D. Possible oscillatory firing of an α_3-motoneuron motor unit (f = 3.3Hz; amplitude ≈ 10µV; long impulse train) in tibialis anterior muscle; a few α_2-motoneuron motor unit potentials (larger amplitude) fire synchronized. E. Synchronized oscillatory firing of mainly α_2 and α_3-motoneurons (f ≈ 3.3Hz). F. Synchronized firing of α_1-motoneuron unit potentials (FF-type) of large amplitude (up to 200µV) with the oscillatory firing α_2 and α_3-motoneuron motor unit potentials (FR and S-type) in gastrocnemius muscle a few min later (resulting frequency = 3.6Hz). Rhythmic firing of α_2 and α_3-motor unit potentials in the triceps brachii muscle in some coordination to the rhythmic firing in tibialis muscle giving rise to substantial rhythmic movements of tibialis anterior muscle. D, E, and F are consecutive recordings. Recordings from a 70-year-old patient with Parkinson's disease for 6 years (U.H.); tremor on both sides.

Synchronization and de-synchronization of FF-type motor unit firing with oscillatory firing FR-type motor units

In **Figure 51**, the synchronization and de-synchronization of FF-type motor units (innervated by α_1-motoneurons) with FR-type motor units (innervated by α_2-motoneurons) is shown. In **Figure 51A**, FR and S-type motor units (small motor unit amplitude) fired rhythmically at a common frequency of 3.9Hz in the right tibialis anterior muscle. In **Figures 51B and 51C**, FF-type motor units (large unit amplitude) fired synchronized with the FR-type motor units; large FR-type motor unit potentials appeared on top of the small FR-type motor unit potentials. The common rhythmic frequency is now 3.4 and 3.3Hz. It can be seen that the large amplitude FF-type motor unit potentials slightly changed their synchronization phase with respect to the low amplitude FR-type motor unit potentials; sometimes the low amplitude FR-type motor unit potentials started earlier in the activity burst and sometimes they lasted longer than the large FF-type potentials in the burst **(Figures 51B and 51C)**. In **Figure 51D** additionally FR-type motor units started to fire rhythmically in the biceps brachii muscle at a frequency of 4.5Hz. In **Figure 51F** FF-type motor unit potentials no longer fired in the tibialis anterior muscle, only FR-type potentials were recorded. The rhythmically firing FR-type motor unit potentials in the biceps brachii muscle increased their firing frequency to 5.5Hz. In this patient the tibialis anterior muscle was only moving up and down when the FF-type motor units fired in addition.

In **Figure 51E**, the rhythmically firing motor units are displayed on a time-stretched scale. It can be seen that the FF-type motor units had a motor unit action potential duration of approximately 8ms (amplitude ≈ 150μV) and the FR-type motor unit potentials had a duration of 17ms (amplitude ≈ 15μV). The single nerve-fiber action potentials have a much shorter duration (approximately 0.3ms).

Contribution of FF and FR-type motor unit firing to the generation of tremor

There is evidence to suggest that the tremor in Parkinson's disease patients starts with synchronized oscillatory firing of FR-type motor units, innervated by α_2-motoneurons **(Figures 50 and 51)**, to which then FF-type motor units (innervated by α_1-motoneurons) synchronize, because the tremor frequencies are in the range of the Eigen-frequencies of oscillatory firing α_2-motoneurons (≈ 5Hz) and the α_2-premoter spinal oscillators have a higher stability. Premotor spinal oscillators probably consist of a neuronal network, with the motoneuron being a part of it. α_2-Motoneuron oscillators are less dependent on afferent input, and are therefore more stable. Moreover, the Eigen-frequencies of the muscle-limb mechanics, for example of the arm and hand are also within the range of 5Hz. It then depends on quantitative effects, i.e., which oscillator type contributes to what extent to the rhythmic movement, at which frequencies the arms, hands and fingers shake. Since the contributions of rhythmically firing FF and FR-type motor units changed as did the strength of activation, the tremor frequency varied during the measurements. Since FF-type motor units develop more power, substantial tremor movement was only observed if substantial numbers of rhythmically firing FF-type motor units contributed. After the start of tremor with the synchronization of FR-type motor units, first the small FF-type (and further FR-type) motor units started to fire synchronously, followed by larger FF-type motor units with, on average, larger potential amplitudes. This may indicate recruitment according to the size principle among FF-type motor units. When the tremor ceased, the large FF-type motor units stopped firing first followed by the smaller FF-type ones and then also the small-amplitude FR-type motor units **(Figure 47A)**.

Only a little information was obtained concerning the contribution of S-type motor units, innervated by α_3-motoneurons, since their motor unit action potentials seem to be very small to be detected safely by sEMG so far. They even seemed to synchronize their firing with the FR-type motor units. α_3-Motoneuron oscillators fire in the range of 1Hz **(Figure 10)**. Higher-quality recordings are needed to identify S-type motor unit firing safely also by sEMG.

So far, we only have been considering coordination of oscillatory firing motor units. It was observed with the single-nerve fiber action potential recording method that occasionally firing motoneurons had the tendency to coordinate their firing with oscillatory firing motoneurons **(Figure 40)**. The problem arises how to measure coordination among occasionally firing neurons or motor units since they are difficult to identify in the natural impulse traffic of many neurons or motor units. The only feature to identify occasionally firing neurons or motor units is the waveform. The advantage of oscillatory firing neurons is that they can be additionally identified by the rhythmic firing pattern.

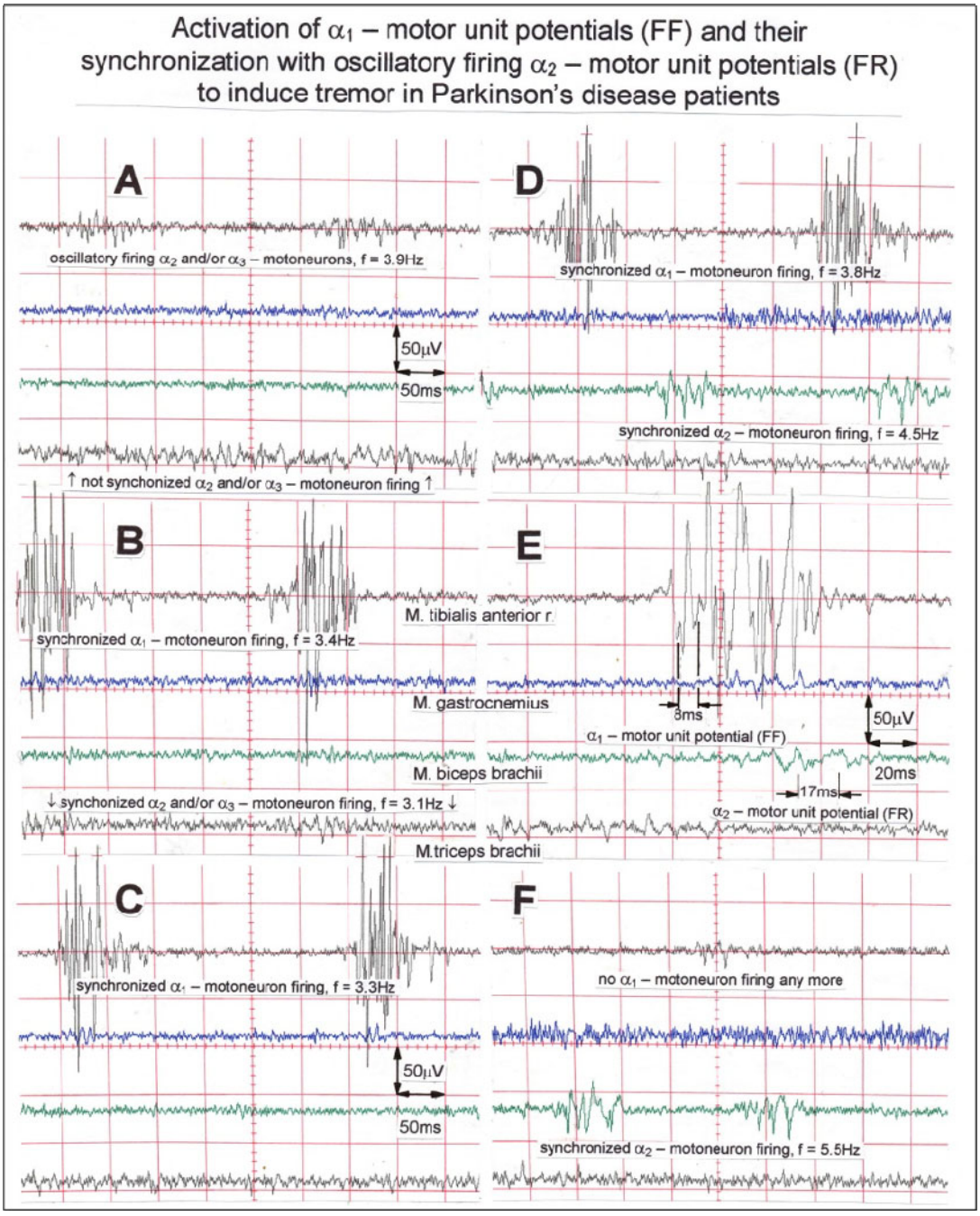

Figure 51. Time course of transient tremor induced by the activation of α_1-motor unit potentials (FF-type) and their synchronization with oscillatory firing α_2 and α_3-motoneuron motor unit potentials (FR and S-type). A. Synchronized oscillatory firing of α_2 and α_3-motor unit potentials in tibialis anterior muscle (f = 3.9Hz). No synchronized firing of α_2 and α_3-motor unit potentials in triceps brachii muscle. No movement of tibialis anterior muscle. B. α_1-motor unit potentials are activated and synchronized with the α_2 and α_3-motor unit potentials (f = 3.4Hz). Tibialis anterior muscle moves visibly. α_2 and α_3-motor unit potentials in biceps brachii muscle fire partly synchronized with the motor unit potentials in tibialis anterior muscle. α_2 and α_3-motor unit potentials can be seen before and after the α_1-motor unit potentials in the activity burst. C. Similar firing as in 'B', but nearly no motor unit firing in triceps brachii muscle. D. Rhythmic firing of motor units giving rise to up and down movement (f = 3.8Hz) of tibialis anterior muscle. Synchronized α_2 and α_3-motor unit firing in biceps brachii muscle (f = 4.5Hz), not coordinated with the rhythmic firing in tibialis anterior muscle. α_2 and α_3-motor unit potentials are activated in gastrocnemius muscle. E. Time-stretched motor unit action potentials: duration of α_1-motor unit potential = 8ms (amplitude ≈ 150µV), α_2-motor unit potential = 17ms (amplitude ≈ 15µV). F. Cessation of rhythmic firing of α_1-motor unit potentials in tibialis anterior muscle; no visible contraction of tibialis anterior muscle anymore; some α_2-motor unit firing still occurring. Synchronized α_2-oscillatory firing still in biceps brachii muscle. Recordings from a 70-year-old patient with Parkinson's disease for 6 years (U.H.); tremor on both sides; measurements were performed on the more affected right side. During the measurements the hands and feet of the patient were in the position for exercising on the special coordination dynamics therapy device.

Lack of inhibition as one reason for tremor

It was shown using the single nerve-fiber action potential recording method that α_1 and α_2-motoneurons fire oscillatory, that they can synchronize their firing following repetitive stimulation, and that these oscillatory firing motoneurons can build up an external loop to the periphery in the way that γ-motoneurons and muscle spindle afferents get included in the rhythmic coordinated firing **(Figure 33)**. But the synchronization of oscillatory firing is only transient, and in non-Parkinson patients the building up of an external loop to the periphery could only be observed upon strong repetitive reflex stimulation. It is therefore concluded that patients with Parkinson's disease lack inhibition, so that motoneurons can start to fire in an oscillatory manner upon virtually no stimulation (spontaneously); and, secondly, they lack mutual inhibition between oscillatory firing motoneurons, so that oscillatory firing motoneurons can synchronize their firing to give rise to rhythmic muscle contractions and movements resulting in tremor.

It is likely that the rhythmic firing during tremor starts with α_2-motoneurons because their firing is more stable and their firing frequency range is similar to the Eigen-frequencies of the muscle-limb mechanics. By building up an external loop to the periphery **(Figure 33)** by the synchronously firing α_2-motoneurons, primary muscle spindles are probably also activated, which in turn stimulate α_1-motoneurons to fire. Inhibiting input to the premotor network will probably first inhibit less stable oscillatory firing α_1-motoneurons followed by the more stable oscillatory firing α_2-motoneurons.

There is indication that in patients with Parkinson's disease and in patients who suffered a spinal cord injury, the inhibition necessary to prevent spontaneous oscillatory firing of motoneurons is missing or impaired. A second type of inhibition is missing in Parkinson's disease patients to avoid synchronization among motoneuron firing.

REPAIR OF PHASE AND FREQUENCY COORDINATION IN PATIENTS WITH PARKINSON'S DISEASE THROUGH EXERCISING ON THE SPECIAL CDT DEVICE

Improvement of phase and frequency coordination as a CNS repair strategy

By use of sEMG in Parkinsonian patients it will be shown how highly coordinated arm and leg movements, imposed by a special coordination dynamics therapy device **(Figures 8 and 9)**, can improve the coordinated firing of neurons and motor programs in Parkinson's disease patients. The coordination dynamics therapy (CDT) uses the same principle for the re-learning of movements, vegetative and higher mental functions as the CNS uses for its own organization improvement, namely the enhancement of the accuracy of phase and frequency coordination among neuron firings. When exercising on the special coordination dynamics therapy device, the neurons, activated for generating the specific motor program, communicate via phase and frequency coordination with the neurons which simultaneously generate the physiologic and pathologic network organization, including tremor, and entrains them by building up coordinated functional connections. To put it simply, the physiologic network organization 'catches' the pathophysiologic network organization and entrains it [29]. Entrainment in Parkinson possibly reduces the efficiency and amount of excitation and increases that of inhibition by changing weights of synapses and building of new connections. The building of new inhibitory nerve cells can probably only be achieved through an intensive program of CDT of at least one year in duration.

Reduction of tremor muscle activity in the short-term memory after exercising on the special coordination dynamics therapy device

When the patient was positioned on the special coordination dynamics therapy device, but not exercising on it, rhythmic muscle activity was recorded from the right tibialis anterior muscle. The rhythmic activity occurred at a frequency of 3.4Hz and the amplitude was ≈ 200μV **(Figure 52A)**. No activity was recorded from the gastrocnemius, biceps brachii and triceps brachii muscles. When the patient exercised on the device, muscle motor programs were recorded from all of the four above mentioned muscles **(Figure 52B)**. Motor program activity and tremor muscle activity was recorded from the tibialis anterior muscle **(Figure 52B)**. The frequency of the motor program activity during exercise was f = 0.9Hz and the frequency of rhythmic tremor activity was now 1.7Hz. The tremor activity reduced from 3.4Hz **(Figure 52A)** to 1.7Hz **(Figure 52B)** and coordinated its firing with those of the motor program. The tremor amplitude reduced from 200μV to 100μV and the duration of the tremor activity bursts became shorter.

In conclusion, the tremor muscle activity coordinated its firing with the movement-induced motor program and reduced in general during exercise on the special CDT device. The tremor activity was therefore brought under the control of the movement activity and was influenced by it to reduce.

In another recording set from the same patient **(Figure 52D)** it seemed as if the tremor reduction was more pronounced for higher (20N) than for lower load exercise (10N). This is to be expected since exercising at higher load will activate the CNS more integrative, so that the influence of the physiologic CNS organization upon the pathologic organization will be larger. With ongoing exercising on the device, tremor reduction could nicely be seen from the reduction of tremor arm movements. At the

beginning of exercising, the arm tremor amplitude was large and afterwards reduced. The patient had tremor of arms, legs and face on both sides of the body. Visible tremor reduction need not mean however that the rhythmic tremor muscle activity had reduced, since the tremor amplitude could have been influenced by movement kinetics. It was therefore important to show through sEMG that the muscle activity leading to tremor really had reduced.

The reduction of tremor muscle activity means that less upstream motoneurons synchronized their firing in the short-term memory. The coordinated firings of neurons had improved in the short-term memory. With repeated training on the special CDT device, the improved phase and frequency coordination will be established in the long-term memory.

In another measurement **(Figure 53E)**, the tremor muscle activity reduced in the recorded sweep piece; tremor reduced from 5Hz to 1.8Hz.

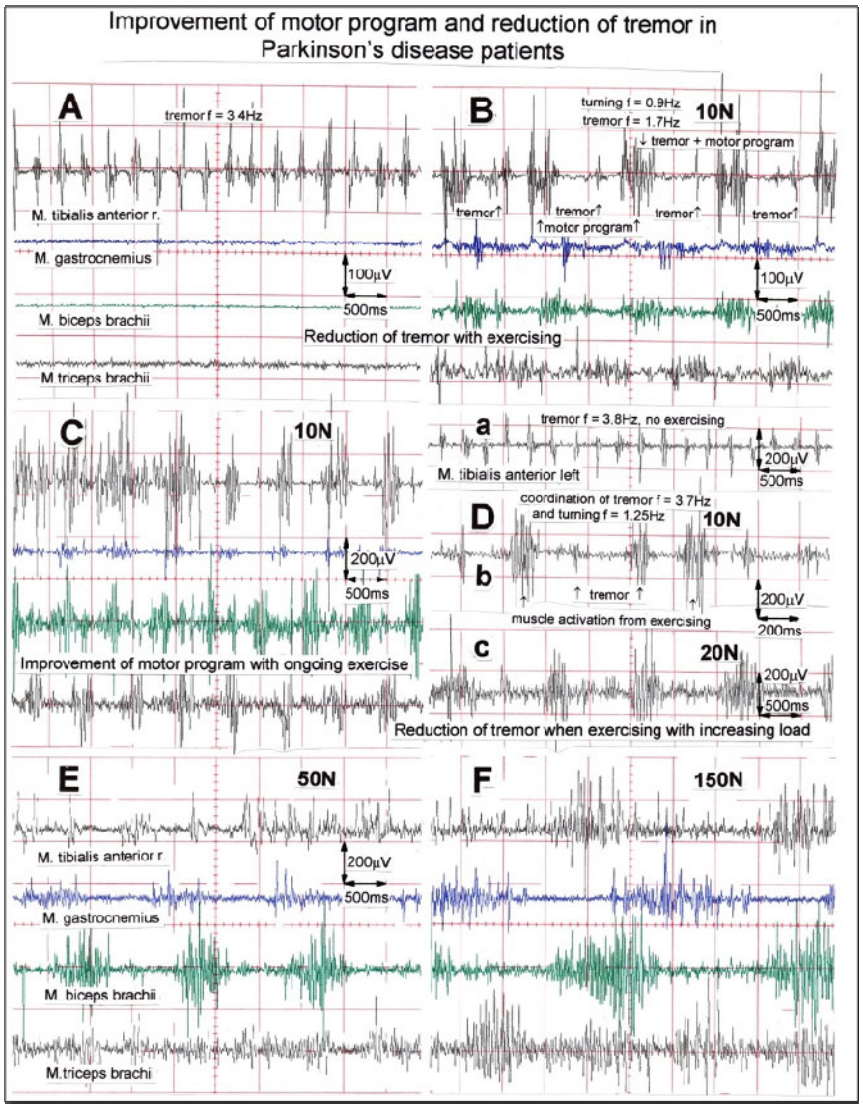

Figure 52. Improvement of the motor program and reduction of tremor in 3 Parkinson's disease patients upon exercising on the special coordination dynamics therapy device. A. Patient is in position at the special coordination dynamics therapy device, but not exercising. Non-voluntary rhythmic muscle activation with f = 3.4Hz is recorded from the tibialis anterior muscle of the right side. B. When exercising on the device at 10N, a motor program appears in all muscles recorded from. The tremor activation in the tibialis anterior muscle reduced in amount and frequency (to 1.7Hz), and the tremor muscle activation synchronized with the motor program. C. Improvement of motor program in the tibialis anterior muscle with ongoing exercising. D. Reduction of tremor in the tibialis anterior muscle with increasing load when exercising on the special coordination dynamics recording and therapy device: a. no exercising, tremor muscle activation full present. b. Tremor reduced in amount and frequency (from 3.8 to 1.25Hz) when exercising at 10N. c. No strong tremor muscle activation visible at 20N. E, F. Improvement of the motor program in the tibialis anterior and triceps brachii muscles upon exercising on the special coordination dynamics therapy device at increasing load from 50 to 150N. A, B, D, a 70-year-old female Parkinson's disease patient (U.H.), C, a 76-year-old female Parkinson's disease patient (I.K.), and E,F, from a 70-year-old male Parkinson's disease patient (V.H.).

Improvement of the motor program

In two patients with Parkinson's disease the motor program improved after a few min of exercising on the device **(Figure 52)**. Figure 52C shows that the motor program improved in the tibialis anterior muscle during that sweep piece when exercising at a load of 10N. From **Figures 52E and 52F** it becomes evident that the motor program improved substantially in the tibialis anterior muscle when increasing the load from 50N to 150N. Therefore, the motor program improved with ongoing exercise and increasing load, provided that the patients could manage the load.

Tremor changes in different muscles

Figures 53A-53D shows that the tremor muscle activity changed in different muscles depending on the position, concentration and other influences. The patient was positioned on the special coordination dynamics therapy device but was not exercising on it. Rhythmic tremor activity can be seen in the tibialis anterior, the gastrocnemius, the biceps brachii and the triceps brachii muscles. The biceps and triceps brachii muscles fired in synchronization with a frequency of 4.6Hz **(Figure 53A)**. The tremor muscle activity in the tibialis anterior and gastrocnemius muscles was coordinated in an antagonistic way (f = 4.5Hz), and the activity of the tibialis anterior muscle was synchronized with those of the biceps and triceps brachii muscles. Sometime later, there was nearly no tremor activity in the gastrocnemius muscle and the tremor activity in the biceps brachii and triceps brachii muscles were less rhythmic **(Figure 53B)**. Still at a later point there was no tremor activity in the tibialis anterior muscle, but more activity in the gastrocnemius muscle **(Figure 53C)**. The rhythmic activity in the biceps and triceps brachii muscles increased again. In **Figure 53D** similar tremor activity can be seen as in **Figure 53A**. The tremor frequencies were slightly different. The higher muscle activity amplitudes were mainly due to a different amplitude calibration. Little tremor movements were observed in this patient in comparison to the patient shown in **Figure 52.**

In conclusion, it was shown that spontaneous EMG activity was changing in frequency and amplitude with time. Probably, the amplitude change of the rhythmic muscle activity was mainly due to the extent of the contribution from FF-type motor units since FF-type motor unit action potential amplitudes are much higher than those of FR and S-type motor units. The change in the frequency of the muscle tremor activity was due to contributions from all the three muscle fiber types, probably especially from the FR-type motor units since α_2-motor units have the steadiest oscillatory pattern.

But changes in tremor frequency may also come from degenerative changes of the ensemble networks generating the oscillatory firing. Premotor spinal oscillators could be shown to partly lose their rhythmic properties as a consequence of CNS injury **(Figure 19)**.

Integrative organization mechanism to reduce Parkinsonian tremor

It is evident from **Figure 52AB** that during exercise on the special CDT device the tremor muscle activity **(Figure 52A)** became coordinated with the motor program **(Figure 52)**. The tremor frequency in the tibialis anterior muscle reduced from 3.4Hz to 1.7Hz at a turning frequency of 0.9Hz, and tremor activity bursts reduced in size and duration **(Figure 52B)**, indicating that less motor unit firings contributed to the tremor activity, which means that Parkinsonian tremor had been reduced in the short-term memory.

The question arises as to how the physiologic motor program can reduce pathologic motoneuron activation, leading to tremor. During the exercise on the special CDT device, CNS neurons organized themselves by relative phase and frequency coordination in cooperation with the movement induced re-afferent input and descending volitional input patterns. The uncontrolled synchronized oscillatory firing of motoneurons and their upstream driving interneurons, giving rise to tremor, were influenced by the physiologic network organization, since the activated neuronal networks for the coordinated arm and leg movements and the tremor activity overlapped. It is likely that some interneurons and motoneurons will have even contributed to both network organizations. The neurons which are directly responsible for the coordinated arm and leg movements and the tremor activity will be directly entrained because they serve both functions at the same time. Other neurons are only entrained by the functional projections they receive.

It has been shown that different activations can cross in neuronal networks via synfire chains [30]. Neurons can therefore serve at a certain moment several functions (organizational states), if the coordinated firing is sufficiently precise with respect to time and space. In reverse logic, if coordinated firing of neurons is substantially impaired, it is difficult for the neuronal networks to organize several functional states at the same time. Injured or pathologically functioning neuronal networks may be able to generate only one network state at a time or there may be a mixture of states taking place or sudden changes from one network state to another one take place. A mixture of movement states, sudden changes between different movement states or patients are only being able to do one thing at a time, for example walking or speaking, can be observed in brain-injured patients.

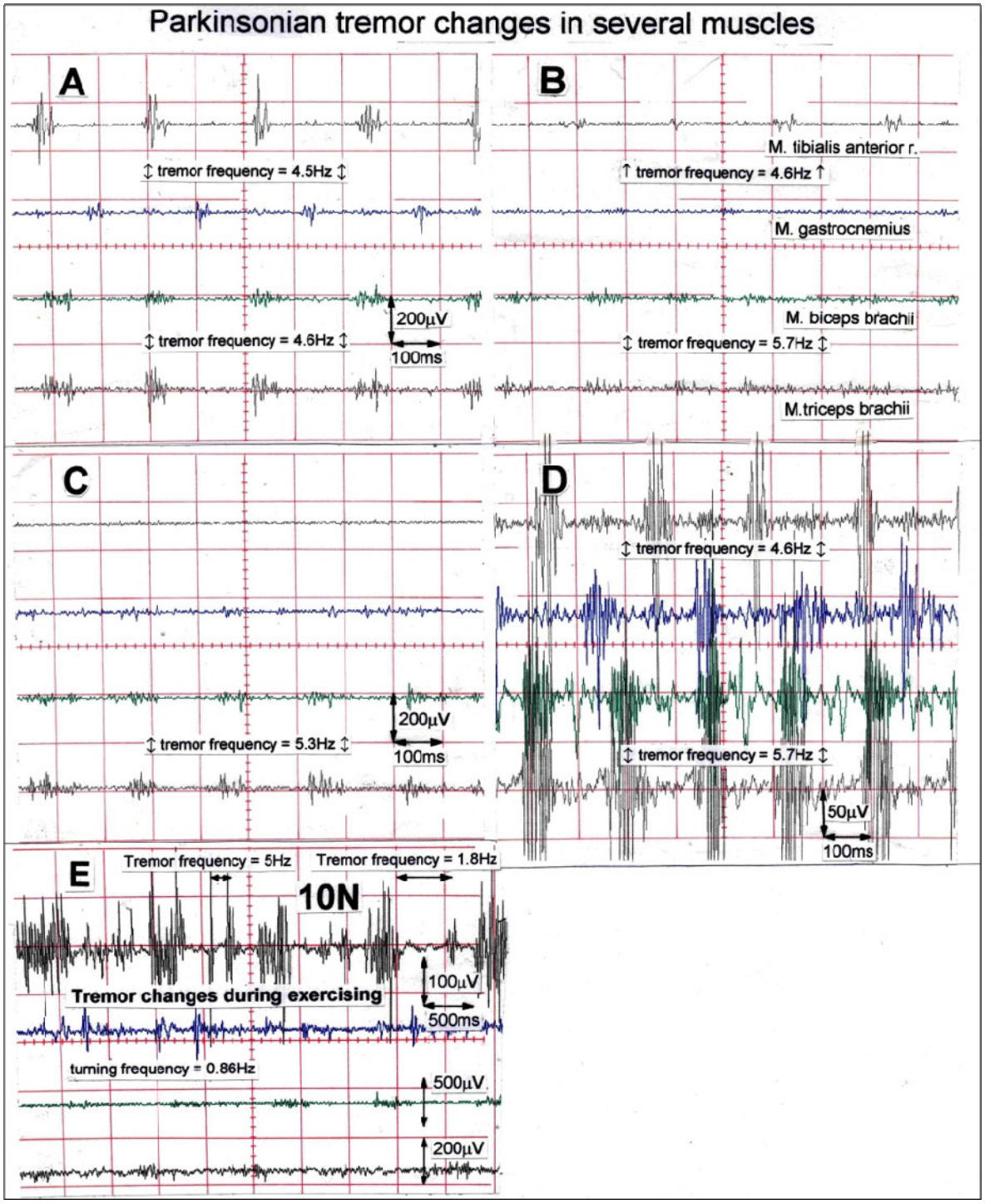

Figure 53. Tremor muscle activation changes in tibialis anterior, gastrocnemius, biceps brachii and triceps brachii muscles in a 65-year-old Parkinson's disease patient (K.V.) positioned at the special coordination dynamics therapy device but not exercising. A. Coordinated antagonistic tremor muscle activation in tibialis anterior and gastrocnemius muscle, frequency = 4.5Hz. Synchronized muscle activation in the biceps and triceps brachii muscles (f = 4.6Hz) synchronized with the tibialis anterior muscle. B. No tremor muscle activation in the gastrocnemius muscle. C. No tremor muscle activation in the tibialis anterior muscle, and activation in the gastrocnemius muscle is approximately synchronized with that in the biceps and triceps brachii muscles, unlike in 'A' and 'D'. D. Tremor muscle activation as in 'A', but different amplitude calibration. E. Tremor changes during exercising (f = 0.86Hz) at a load of 10N. In the upper trace the tremor changes from 5Hz to 1.8Hz during the exercise. In the lower traces only motor program activity can be seen at that amplification. Note that the time calibration in A through D is 100ms, and that in E is 500ms; the tremor activity has a frequency of approximately 5Hz and the motor program, due to exercising, of 1Hz; with a calibration difference of a factor of 5, tremor activity and motor program show some similarity.

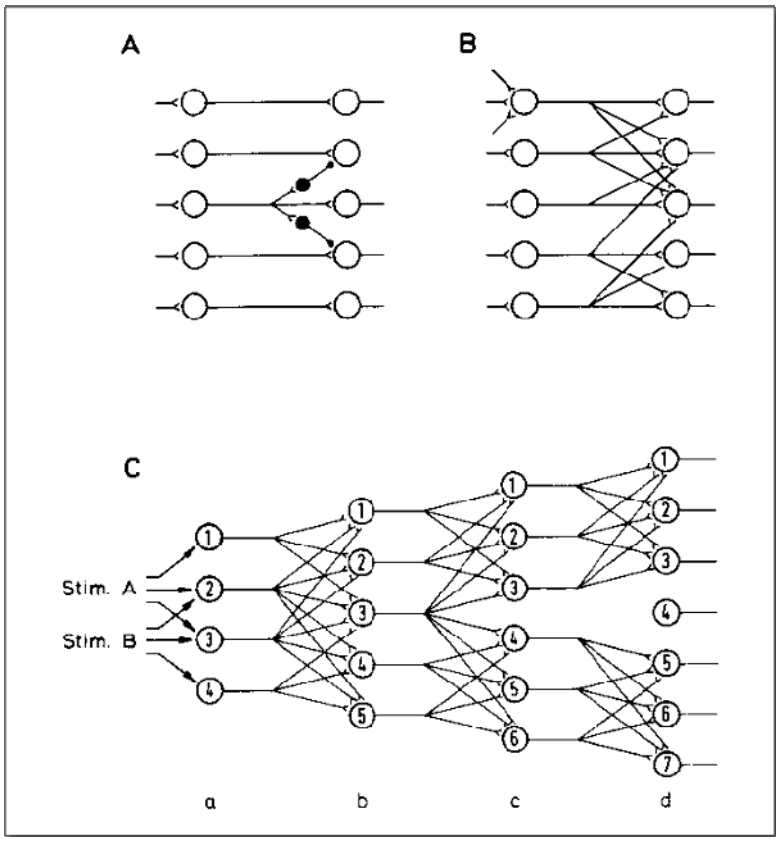

Figure 54. Different types of neural chains. A. Dedicated lines established by one-to-one connections with superimposed lateral inhibition. B. "Synfire chain" with different numbers of synaptic connections from pre- to postsynaptic neurons. C. Separation of stimuli affecting overlapping sets of neurons. (from [30]).

Neural network repair In Parkinson's disease patients through CDT

Low-intensity CDT in a group of patients

The four basic clinical features of Parkinson's disease are tremor (5-6 Hz), bradykinesia, rigidity (resistance to motion) and deficit in postural reflexes. It is believed that Parkinson's disease occurs because of a striatal dopamine deficiency. This view is supported by the effectiveness of dopamine (L-dopa) therapy.

A second treatment strategy (besides dopamine therapy) to improve CNS functioning of patients with Parkinson's disease is the 'behavioral plasticity', namely to repair the neural networks by movement-based learning. The developed coordination dynamics therapy (CDT) includes structural changes in the brain and spinal cord at the cellular, molecular and systems level, with the convergence of these mechanisms. Since the neural networks are repaired by learning this method is healthy and can be combined with the drug therapy to reduce the drug dosage.

It has been shown that the combination of drug and movement-based learning therapy enables the patient to live longer with a better quality of life [31]. Eight patients (mean age 69, a single one shown in **Figure 55**) in whom Parkinson's disease had set on 5 to 10 years earlier underwent low intensity CDT with an average of 4 h per week for 2.5 months. The ongoing pharmaco-therapy and conventional fitness training for 1 to 2 h per week were not changed. With the CDT the functioning of the CNS of the Parkinson's disease patients improved by 35%, as quantified by coordination dynamics measurements. Following 3 months of no CDT, but further ongoing pharmaco-therapy and fitness training the CNS functioning worsened again by 21% **(Figure 56)**. It is concluded that pharmaco-therapy and conventional fitness training alone could not prevent the worsening of the CNS functioning in progressing Parkinson's disease, but additional CDT may can.

A combined drug and learning therapy was more successful than each therapy administered in isolation. Combined therapies may be important in severe cases of the disease.

Figure 55. 65-year-old Parkinsonian patient (K.V.) during exercising on the special coordination dynamics therapy device. The author records the coordination dynamics (arrhythmicity of turning) and electric muscle activity (sEMG: tremor and movement pattern). In this case, sEMG recordings were taken from leg muscles of both sides (tibialis anterior and triceps surae muscles). The recordings were pre-amplified (1000x), displayed on an oscilloscope and printed out.

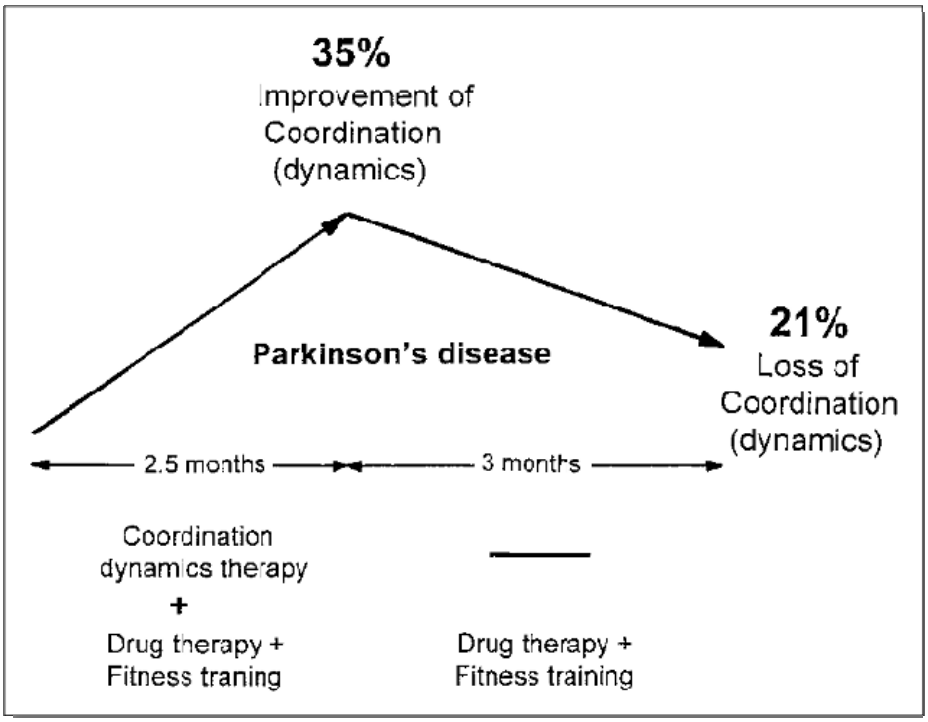

Figure 56. Improvement of coordination dynamics values with CDT and loss of good coordination dynamics values after the termination of coordination dynamics therapy. Group study in 8 patients, 4 h CDT per week.

No further progress of the Parkinson's disease via intensive CDT - a case report

Above it was shown that low intensity CDT could reduce the progressing of Parkinson's disease. The question is now, can an intensive CDT stop the disease? The important answer is that an intensive CDT can stop the progressing of the Parkinson's disease. A patient underwent intensive CDT, his symptoms improved and he could keep the achieved level for three years.

At an age of 68, Parkinson's disease was diagnosed in a male patient and drug-therapy and CDT started. When after three years of CDT the physiotherapist, administering CDT, died, the patient contacted the Author, who continued CDT with him. The therapy per week consisted of exercising 7 h on the special CDT device, 5 h movement and fitness training and drug-therapy. The medication included low level of L-dopa (750mg Madopar per day) and drugs to dilute the blood, decrease the blood pressure and improve prostate function. β-blocker were also administered.

An intensive movement therapy, especially CDT, probably keeps the prostate in a good condition, because movement therapy inhibits breast cancer growth [32] and probably also the growth of other cancers including prostate cancer. Further, CDT reduces the blood pressure **(Figure 59)**, improves CNS functioning in Parkinson's disease patients [31] and improves urinary bladder functions [33]. Very frequent desire to void is mostly not the consequence of prostate cancer or hyperplasia, but the consequence of degeneration or aging of the nervous system and of a very arteriosclerotic artery of Adamkiewics which supplies the lumbar micturition center and becomes very sclerotic in aging [34]. But since the patient obtained the medication for a few years, it will not be easy to reduce the drug concentrations because his body got used or addicted to them.

Figure 57 shows the coordination dynamics of the now 72-year-old patient with Parkinson's disease who trained approximately 12 h per week in the last year. His coordination dynamics values did not get worse (higher) in spite of his getting older **(Figures 57A and 57B)**.

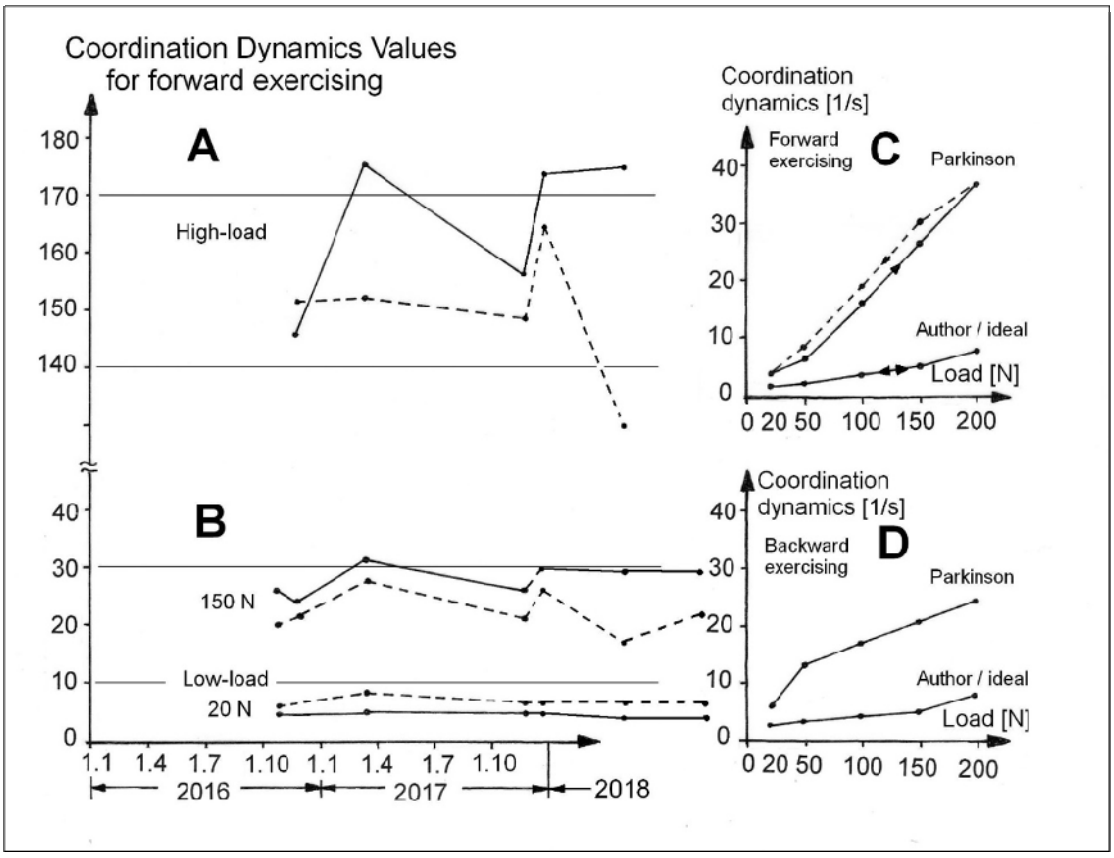

Figure 57. A, B. High-load and Low-load coordination dynamics values with ongoing therapy of a patient with Parkinson's disease. Solid line, forward exercising; dashed line, backward exercising. Note, the high and low load CD values did not get worse (higher) with ongoing time. C, D. Coordination dynamics values for increasing (solid line) and decreasing (dashed line) load (N = Load in Newton) for the patient in comparison to the values of the healthy Author. In D the values for increasing and decreasing load are the same.

The coordination dynamics (CD) values for 20N and 150N did not get worse with therapy from 2016 to 2018 **(Figure 57B)**. Also, the High-load coordination dynamics values did not get worse **(Figure 57A)**. Even though the CD values are far away from the ideal ones for exercising in the forward **(Figure 57C)** and backward direction **(Figure 57D)** for increasing and decreasing load, they are very good in comparison to normal persons [35, 36]. As can be seen from **Figures 57C and 57D**, the patient was fit, because when decreasing the load again during the high-load test, the CD values were not higher (worse), to indicate an exhaustion. Only in **Figure 57C** the CD values were a bit higher (dashed line).

There are mainly two possibilities that the coordination dynamics did not get worse with ongoing years. The disease was cured, which is quite unlikely, or the nervous system could continuously repair the damage caused by the progressing disease. Since the resting tremor did not disappear, the disease was not cured. But it could be that the progress was stopped. For a repair of the tremor, the patient did not train sufficiently intensive per day on the special CDT device and also the therapy time of three years would be too short to repair the tremor. Likely is that the therapy was mainly repairing the ongoing injury caused by the disease but had only little effect on the tremor, which did not get worse. In the group of patients, it was shown that only the exercising on the special CDT device could improve CNS functioning as measured by the CD values **(Figure 56)**.

Further, it is believed that repair shows similarity to development. During development children turn transiently very fast on the special CDT device. Even in the Author, transient fast exercising can be recognized to a lower extent **(Figure 58C)**, when he tries to repair his CNS following chemo and radiation therapy following cancer removal [32]. Such fast exercising could not be observed at all in the patient with Parkinson' disease **(Figure 58A)**. It seems therefore that the patient could only compensate for the continuously occurring damage with the 12 h therapy per week. An even higher CDT intensity may have achieved more repair, including the reduction of tremor. When the Author administered to himself more than 20 CDT per week, he had the impression that the general health improved. High intensity CDT may be a fountain of youth.

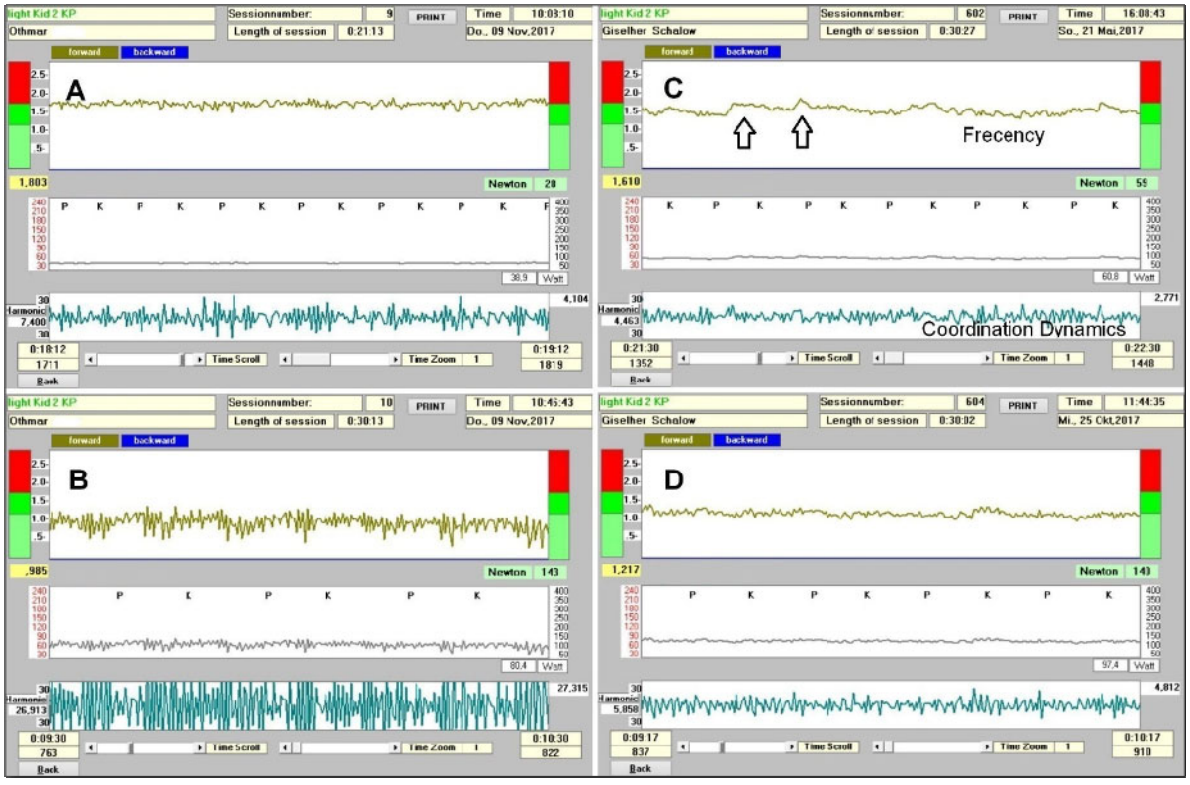

Figure 58. Coordination dynamics of a 72-year-old patient with Parkinson's disease (A, B) in comparison to those ones of the Author which are nearly ideal. Note, in the recordings of the Author transient fast exercising, marked with arrows, can be seen (C), but not in the recordings of the patient (A). Note further that the Author could exercise much more smoothly (D) than the patient (B) for higher loads (140N).

Blood pressure lowering in a patient with Parkinson's disease and hypertension

The above patient with Parkinson's disease obtained angiotensin receptor blocker, thiazide-diuretic and β-Blocker for antihypertension therapy and drugs to dilute the blood and improve prostate function. If coordination dynamics therapy (CDT) could reduce the arterial blood pressure, then the medication could be reduced. CDT was started at the time when the Parkinson disease was diagnosed, four years ago. The antihypertensive drug therapy was started already six years ago, that means before Parkinson's disease was diagnosed and treated.

Figure 59 shows that during exercising on the special CDT device the blood pressure lowered when turning 1000 and 2000 times. In the patient with Parkinson's disease and antihypertensive drug therapy the arterial blood pressure lowered less strong than in the normal case (Author, comparable age). Interesting is that the pulse rate in the patient was lower than that in the normal case, which is probably due to the administered β-Blockers. Anyhow, the blood pressures lowered also in the patient in spite of the plenty of drugs being administered.

It is shown in this 72-year-old patient with Parkinson's disease, that CDT could successfully treat the Parkinson disease not to get worse **(Figure 57)** and reduce the hypertension **(Figure 59)**. Therefore, CDT was able to treat several diseases at the same time (here 2) in a healthy way. In aging often several diseases have to be treated at the same time. Improving the cardio-vascular performance to reduce the blood pressure and avoid heart attack and stroke is of importance for the general health. For critical cases of hypertension, it would be good to know the time cause of resting blood pressure lowering through CDT to optimize the healthy movement-based learning therapy. In the next section it will be shown that the blood pressure lowering lasts for 5 to 8 h and that repeated exercising on the special CDT device can lower the blood pressure over 24 h.

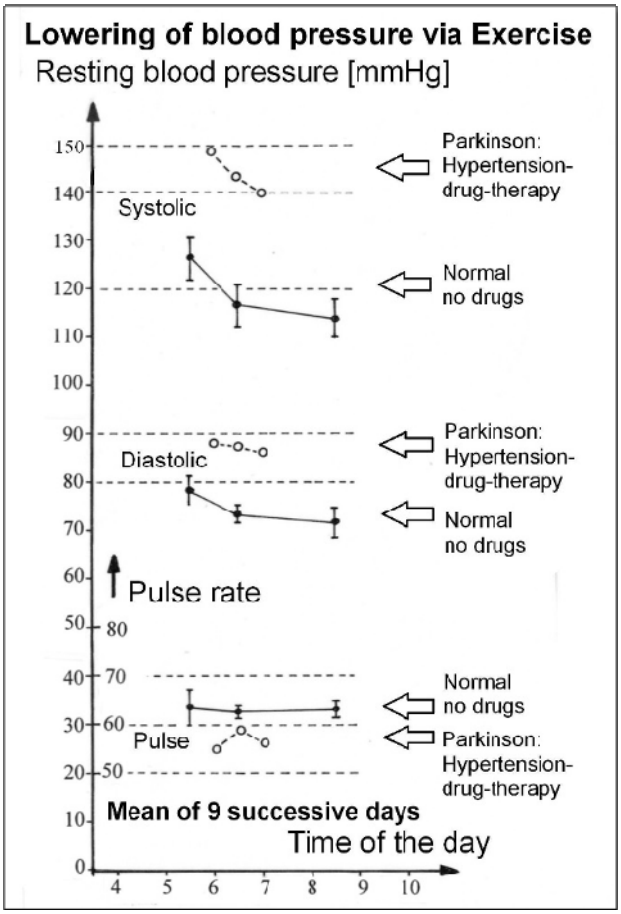

Figure 59. Lowering of the blood pressure of a patient with Parkinson's disease and hypertension during the day in the morning. The resting blood pressure (open circles) was measured before exercising and after 1000 and 2000 turns. For comparison normal blood pressure lowering (solid line) of the Author is shown, who takes no drugs. Note that the lowering in the normal case is stronger. The values are means of 9 or 10 successive days. For the normal case (Author) standard deviations are indicated.

Time course of resting blood pressure lowering in an aging healthy person achieved when exercising on the special CDT device

Figure 60 shows the time course of resting blood pressure lowering of a rather healthy aging person when exercising at low and transiently high load on the special CDT device. The Author was used for that experiment because his blood pressure was normal but close to the upper limit and he was performing CDT for 10 to 15 h per week in similarity to the patient with the Parkinson's disease.

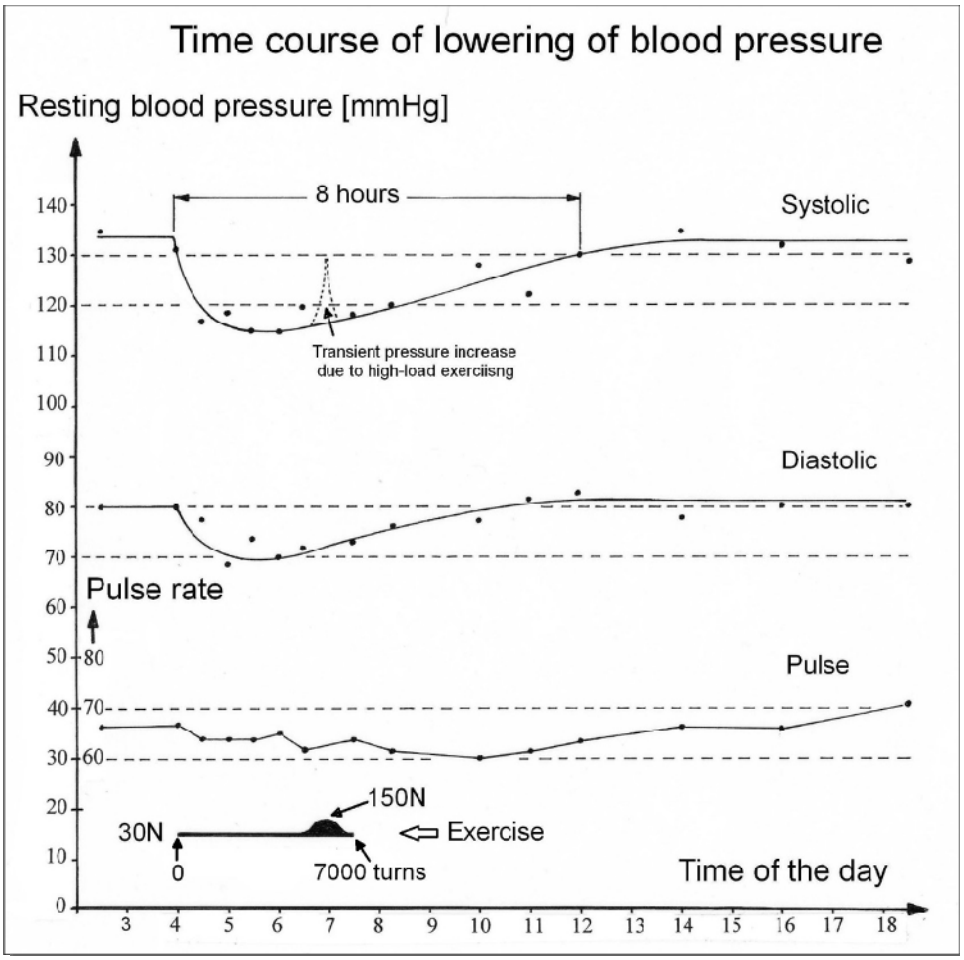

Figure 60. Time course of the lowering of the arterial blood pressure (Author) when exercising at 30N (and transiently up to 150N). Note, measured transient pressure increase due to high-load exercising (dashed line) is indicated.

As can be seen from **Figure 60**, a rather healthy fit person over 70 (Author) probably has a transient resting blood pressure lowering for approximately 8 h. This healthy lowering of the blood pressure can also be used for patients with hypertension. When exercising every 6 h for 60min (2000 to 3000 turns), including transiently against higher loads, he can probably lower his resting systolic blood pressure by 10 to 20mmHg. If he has no adverse heart problems, he does not need to exercise at night. But if he has, maybe he should also train once at night. Most elderly get up at night. It would be no problem for them to exercise also at night. An exercise session before going to sleep most likely increases the length and deepness of the sleep.

One could argue that this repeated exercising is a big effort to just reduce the systolic blood pressure by 10 to 20 mmHg. Such lowering of the systolic blood pressure could be easily achieved by medication. But one should not forget that simultaneously the functions of urinary bladder (continence) and kidneys are improved, the sexual function improved, the cardiovascular performance trained, cancer grows inhibited (including breast and prostate cancer [32]) and the nervous system (including the vegetative nervous system) repaired or in its functioning improved. The lowering of the blood pressure by exercise would be only one part of the improvement of health. The lowering is something like a part of the general improvement of body functions. When the general health has been improved, the number of exercise

sessions could be reduced to two, one in the morning and one before going to sleep. The exercising before going to bed may reduce the probability of adverse health problems in the night. With nearly 8 h health improvement following exercising, the health is partly supported at night.

Repeated lowering of the blood pressure in an aging healthy person to reduce the blood pressure during 32 h

To lower the blood pressure rather continuously, the exercising on the special CDT device has to be performed repeatedly. Such repeated lowering is shown in **Figure 61**. With every exercising the blood pressure went down, but not to the same amount as in **Figure 61A**. After exercising for approximately 1 h in the morning after a long good sleep, the systolic pressure reduced by 21mmHg (A). After stopping the exercise, the pressure slowly increased. When exercising again, the pressure lowered again, but not so much, only by 9mmHg (B). Exercising for a longer time would not have helped, because the lowering had reached its maximum under that condition. Further exercising would not reduce the pressure further. The special condition was, that the Author had a heavy meal before and probably blood was needed for digestion, which increased the blood pressure.

Following another exercise in the early evening, the systolic blood pressure could be lowered again by 15mmHg (from 135 to 120mmHg; **Figure 61C**). From feeling it seemed that the heavy meal was mainly digested at that time. Next morning at 4.30 after a good sleep, the systolic blood pressure was still low and could be lowered from 120mmHg to 109mmHg. With no eating, the blood pressure lowering lasted for 7.5 h **(Figure 61D)**.

In conclusion, the systolic blood pressure could be lowered in an aging person successively by exercising several times for one or two h. The lowering lasted up to 8 h depending on the situation.

Time course of blood pressure lowering in a patient with Parkinson's disease achieved when exercising on the special CDT device

To get more information about the blood pressure lowering in the patient with Parkinson's disease and hypertension of above, it is tried to analyze the time course of lowering as was done in the healthy case **(Figures 60 and 61)**. The situation is more complicated because of the many drugs being administered to the patient.

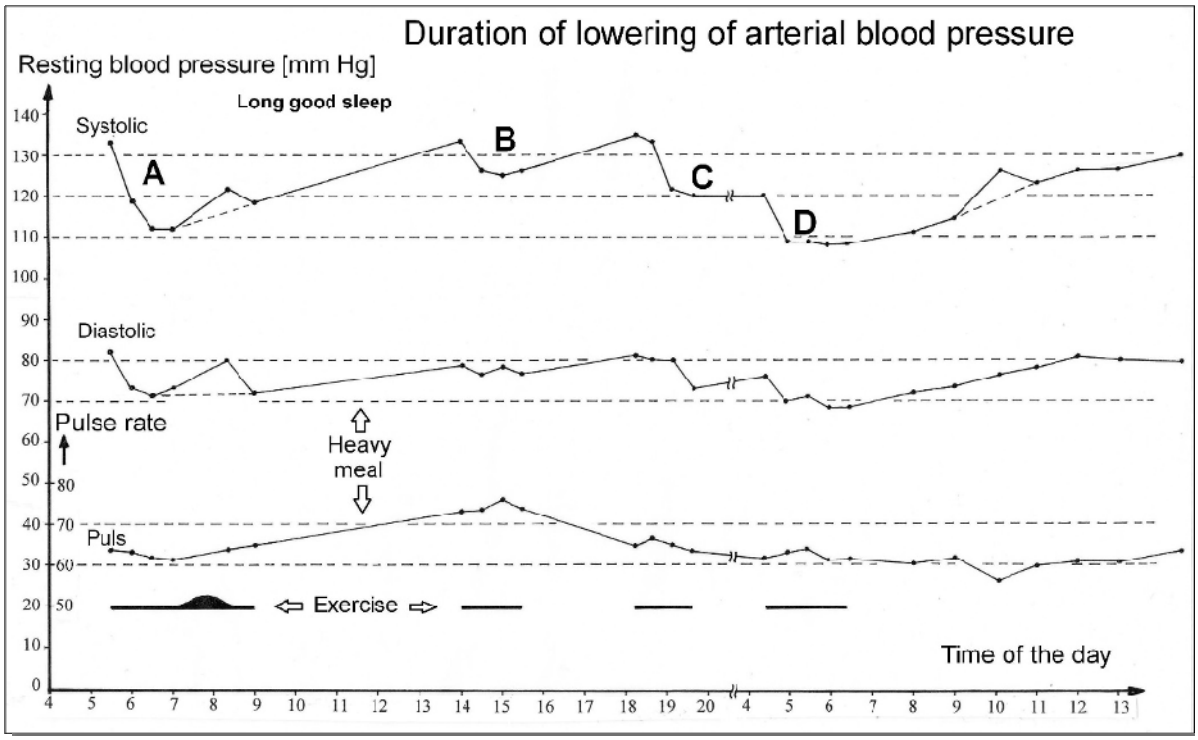

Figure 61. Repeated lowering of the resting blood pressure (A, B, C, D) achieved by exercising on a special CDT device for two days following long good sleep (Author). The pressures were measured before exercising and then mostly every 1000 turns; once up to 7000. Each pressure was at least the mean of three values. Exercise durations are indicated by bars.

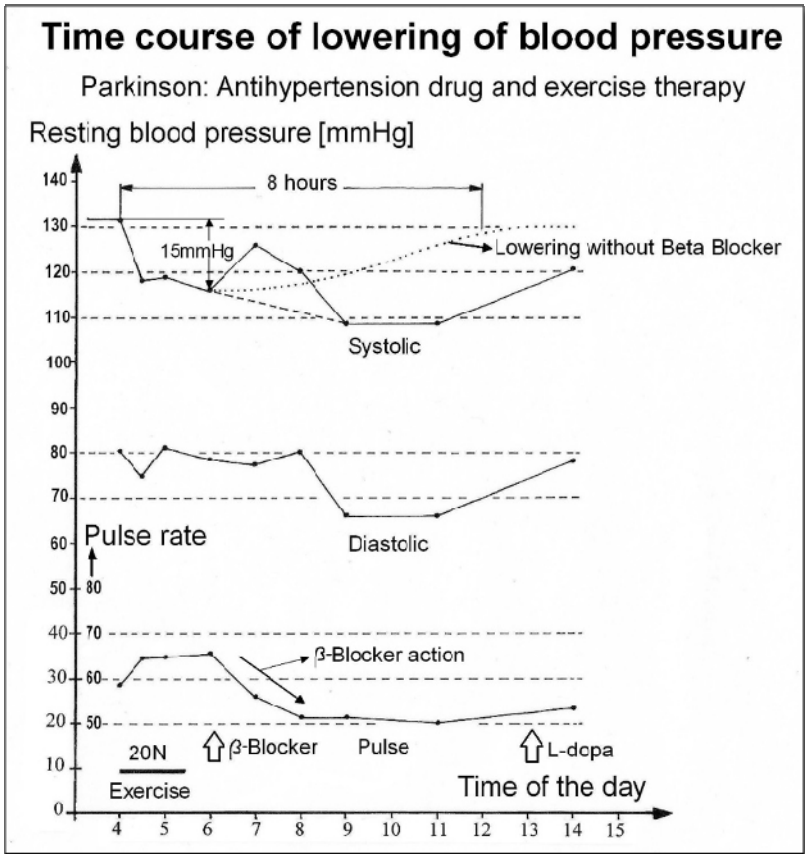

Figure 62. Lowering of blood pressure and pulse rate via exercising on the special CDT device, indicated by a black bar, in a 72-year-old patient with Parkinson's disease for 4 years and hypertension. Arrows indicate β-Blocker and L-dopa administration. The probable lowering of the systolic pressure without beta blocker is indicated by a dotted line. The other antihypertensive drugs angiotensin receptor blocker and thiazide-diuretic were administered later on in the late afternoon.

Figure 62 shows the time course of the blood pressure lowering in the patient with Parkinson's disease. It seems that between 4 and 6 o'clock in the morning the systolic blood pressure was lowered by 15mmHg achieved by the exercising on the special CDT device. The following increase and decrease were probably due to the administered β-Blockers. It seems therefore that the blood pressure can also be lowered in this patient as in the healthy case **(Figure 60)**. The coordination dynamics therapy (CDT) can therefore also lower the blood pressure in a patient with hypertension and Parkinson's disease, but in a healthy way if the patient exercises several times per day **(Figure 61)**.

The low-load and high-load tests **(Figures 58A and 58B)** did not increase the blood pressure. The family doctor said to the patient, that his health condition is very good and his resting tremor did not increase [29].

By including in **Figure 62** the shape of the systolic blood pressure lowering of the healthy case **(Figure 60)**, it can be seen how the β-Blocker probably lowered the systolic pressure further after an initial increase. The extreme lowering of the pulse rate probably indicates the time course of the action of the Beta Blocker. The extreme lowering of the pulse rate in conjunction with the drug-induced blood pressure lowering may not be healthy, because there may be a lack of blood supply in the microcirculation. Not all capillaries may get sufficient blood with the possible consequence of lack of oxygen and fibrosis in the future and in conjunction with arteriosclerosis heart and brain are in danger. The Author suggested the patient to try out how the blood pressure values will be without the β-Blockers. The patient refused to stop the β-Blockers because he had the feeling that the β-Blockers reduced the tremor. It may well be that his body suffered withdrawal symptoms when stopping transiently the β-Blockers.

DISCUSSION

There is no alternative to CDT for general health care

By improving/repairing phase and frequency coordination among neuron firing and that other parts of the CNS can take functions over through CDT (plasticity), the functioning of the human brain can substantially be

improved. Since the CNS is involved in nearly all body functions, the general health will improve. In the case report of the patient with Parkinson's disease, the progress of the disease was stopped **(Figure 57)** and simultaneously the blood pressure lowered **(Figure 59)**.

Hippocrates' ancient wisdom that "natural forces within us are the true healers of disease" would mean that the body can repair most functions by itself. We just have to 'tell' the body what it has to do. Mainly through movement-based learning, the CNS recognizes where the deficits/damages are and repairs them. But why we have to use the special CDT device then to push the nervous system to repair the phase and frequency coordination. If the true healers are in the body, why cannot the nervous system repair the phase and frequency coordination by itself, if it is of fundamental importance for a healthy CNS functioning?

Indeed, the body can repair/improve the organization of the CNS in a natural way without a wheel turning device. Wheels are very important for transportation in cars, lorries and trains. But one can also transport goods by carrying them, but less efficient. The same holds for the improvement of phase and frequency coordination. The nervous system can learn/repair phase and frequency coordination in a natural way, but the repair is much less efficient and not always possible.

Coordination between arm, leg and trunk movements, and among neuron firings, can be improved when walking on uneven ground **(Figure 63)**. First, the patient can start to walk on a rather even ground in a nice and healthy surrounding **(Figure 63A)**. Later on, he can enhance the difficulty of the coordination task. More difficult coordination's are trained, when the patient has also to jump from stone to stone or from root to root **(Figure 63B)**. Even more difficult coordination's are trained when the patient is moving through a miracle looking like forest, where a lot of coordination's between arms, legs and trunk are needed to manage the path **(Figure 63C)**. When having a rest in the miracle forest, the patient may even have the impression that there are elves fairies who help to manage with the difficult coordination training **(Figure 63C)**.

Figure 63. Natural surroundings to train easy (A), more difficult (B) and very difficult coordination's (C) between arms, legs and trunk. Koli-National-Parc, Finland.

But how many patients are able to manage such natural coordination training to improve phase and frequency coordination and plasticity so that other brain parts take function over? The patient with Parkinson's disease of **Figure 55** may be able to hike on a path shown in **Figure 63A**. He would probably refuse to walk on the more complicated ground **(Figure 63B)**. When partly a bit of climbing is needed as in **Figure 63C**, the patient would become overloaded. Falling and breaking bones would be at risk. Rather young women with breast cancer, on the other hand, could manage these natural coordination training to inhibit cancer grows [32], but not elderly with probably overweight, missing fitness and balance problems. Such natural training of coordination and repair is also limited to good weather and having access to such healthy beautiful surrounding. Patients should be already happy if they can sometimes have a special CDT device in a healthy surrounding and be able to train there **(Figure 64)**. The routine of training 6 times a week without risks and independence of weather conditions is at home under supervision or in an up-to-date rehabilitation center, if existing. Elderly with overweight and balance problems and not fit can safely train at home on special CDT device in the sitting **(Figure 38)** or lying position **(Figure 9)**.

Figure 64. Repair of phase and frequency coordination when exercising on a special CDT device in the sitting position in a nice and healthy surrounding. Koli-National-Parc, Finland.

Additionally, the involutional training, when exercising on a special CDT device with an exactness of '4ms phase and frequency coordination' **(Figure 25)**, is much more efficient than the natural volitional coordination training.

A top brain repair training would be to exercise on a special CDT device as in **Figure 64** for two h, hiking afterwards in the forest like in **Figure 63** for two to three h, eating good food, including berries from the forest (approximately 10 real cranberries **(Figure 65)** contain already all necessary vitamins), having a sleep for one h, training again on CDT device for one h, because of necessary repeated exercising to keep a good level CNS organization **(Figure 61)**, do some intelligent brain work to activate specifically the higher mental functions, and train again for one h on the CDT device before going to sleep **(Figure 61)** to keep the CNS in a good organizational state through 24 h per day. With such an intensive CDT, many CNS diseases could successfully be attacked. When including fast walking and jogging to train the easy pace and trot gait coordination's, a good balance of CNS neural network organization can be achieved between variability (CDT device, difficult coordination's) and stability (walking and running, easy coordination's) of phase and frequency coordination.

Figure 65. Real cranberries (German: Moosbeeren; Vaccinium oxycoccus) grow in the shown swamp. Approximately 10 berries contain already all necessary vitamins for one day. Prehistoric men were probably eating them because you can keep them for a year in cold water (these berries contain natural preservative) and the prehistoric men could also take them from the soft ground in the spring when the ice melted away. Blueberries (antioxidant) and Preisselbeeren (Vaccinium vitis-idaea) were growing in the forest in the background. National-Parc, Finland.

1. Optimal training for cancer patients

Such optimal repair training would be suitable for patients operated for brain tumors. With family support, the whole repertoire of routine and natural movement-based learning therapy could be administered to repair the brain from the removal of the cancer and to inhibit further cancer growth. The success of brain repair and cancer grows inhibition depends on the efficacy of therapy to repair the brain and the efficiency of cancer growth inhibition and the aggressivity of the tumor. So far it seems that an astrocytoma cannot be stopped but may an anaplastic Oligodendroglioma [55]. If these aggressive tumors cannot be stopped, at least the cancer patient will live longer with a better quality of life, if the movement-based learning and repair method is administered in a beautiful surrounding which affects the psyche positively. Much more qualified research in movement-based-learning is needed to identify how epigenetic mechanisms can efficiently be modified for a repair of the human CNS **(Figure 66)** and for the killing cancer cells to replace operation, radiation and chemotherapy. A first step would be to get rid of the radiation and chemotherapy. The Author survived a 'squamous cell carcinoma (epithelioma) (a malign tumor) in the maxilla [32]. In spite of intensive CDT with 10 to 15 h per week for 10 years, he could not get fully rid of the side effects of chemo and radiation therapy! Not many such cancer patients are 10-year-survivors to report about the side effects of chemo and radiation therapy on the long term.

If movement-based learning can suppress genes by modifying the epigenome, it may also be able to activate genes with an anti-carcinogenic effect.

2. Brain tumor treatment through CDT

Qualified movement-based-learning (CDT) seems to be a suitable healthy treatment for brain tumors, because the brain can be repaired after the (partial) removal of the tumor and further growth of the tumor and metastasis are probably inhibited [55]. Even if the recurrence of the tumor cannot be stopped, the patient will live longer with a better quality of life.

Based on case reports and animal research there is indication that CDT can inhibit the growth of different kinds of cancer, especially breast cancer [32,40]. One mechanism of inhibition seems to be that immune cells are built by exercise to destroy the cancer cells. When exercising on a special CDT device, the performance of the cardiovascular and lymphatic system is improved so that the immune cells have a better access to the cancer cells. In the exercise-dependent control of tumor growth the Natural Killer (NK) cells seem to have a predominant role [41]. The NK cells represent a critical component of the innate immune defense even though they may have

some form of immunological memory. They recognize transformed cells independently of antibodies, while T cells are cytotoxic effector cells of the adaptive immune response. Both immune cell types are known to be regulated by exercise. During exercise, circulating lymphocytes increase in number and frequency. Of these lymphocytes, NK cells are the most responsive cells to the exercise-dependent mobilization. Thus, the importance of NK cells in the training-dependent control of tumor growth follows is their superior responsiveness to exercise. The specific movements, performed during CDT, are more efficient in cancer growth inhibition than general exercises, because the microcirculation of blood and lymph vessels is especially enhanced by learning transfer from movements to functions of the autonomic nervous system. The improved functioning of the autonomic nervous system includes the improvement of the peristalses and the repair of the lymph vessels. The depolarization of the smooth muscle membranes in the lymph vessel walls may contribute with their electric fields to the NK cell activating milieu in the lymph nodes and the tumor microenvironment. When exercising on the special CDT device, specific coordinated integrative movements are trained with little or moderate load; in this way a substantial number of exercises can be trained without overloading the body. CDT may provide relief from the emotional stress of cancer even before treatment (surgery, chemo and radiation therapy), especially when knowing that exercise inhibits cancer growth. The inhibition of cancer growth achieved by CDT works not only on the mobilization of NK and T cells and the better access of the immune cells to cancer cells, but also on the epigenetics to improve health in general. It is likely that the by CDT improved nervous system functioning in the short and long-term memory is contributing substantially to the cancer-inhibiting potential. Important questions remain. Can vigorous-intensity CDT stop disease recurrence or even protect against cancer occurrence? Can with the application of CDT the dosage of chemo and radiation therapy substantially be reduced? Till to what cancer stage is cure possible?

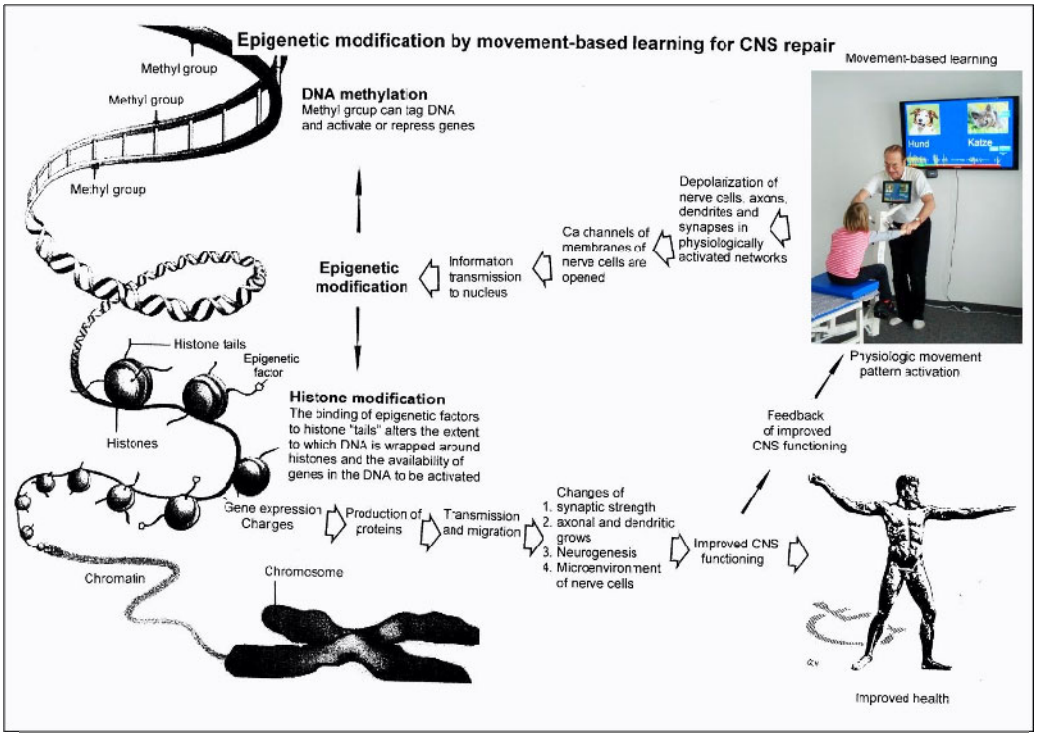

Figure 66. Epigenetic regulation for repair by movement-based learning. CDT-induced stimulation of the pathways that regulate neural network repair is a proven therapeutic and preventive tool. Epigenetic mechanisms, stimulated by physiologic network activation, are likely key players within signaling networks, as DNA methylation, chromatin remodeling and small non-coding RNAs superfamily are required for the fine-tuning and coordination of gene expression during neural network repair by learning. Since the nervous system is involved in nearly all body functions, CDT will improve health.

3. Regulation of epigenetic modification for repair by movement-based learning

To generate repair in the nervous system, it is likely that permanent changes in gene expression patterns are achieved through permanent changes in chromatin remodeling without changes in DNA sequence. The concept of chromatin remodeling addresses a key challenge of how stable changes in gene expression are induced [37] in neural networks to produce long-lasting changes in repair. DNA methylation is one of the many

epigenetic modifications that can alter gene expression. Dynamic and reversible DNA methylation may be essential for learning and memory formation and could transmit repair influences onto adult neurogenesis.

If the epigenetic definition that the events are the structural adaptation of chromosomal regions so as to register, signal or perpetuate altered activity states [38], that means the nature of epigenetics is responsiveness, then epigenetic regulation for repair should be stimulated by physiologic neural network activation. Un-physiologic neural network activation like electro stimulation (which is nearly always un-physiologic apart from the heart pace maker) stimulates chromosomal changes in a negative direction with respect to health. "The DNA methylation system and the Polycomb/Trithorax systems seem to respond to previous switches in gene activity" [38].

Understanding the complex epigenetic regulation of neural activity and adult neurogenesis is integral to designing therapeutic approaches to restore neurogenesis and cognitive functions. It will also give a tremendous insight into understanding how certain environmental or pathological influences, such as stress, physical activity, depression and epilepsy regulate adult neurogenesis [39]. **Figure 66** shows steps of epigenetic regulation induced by specific physical activity, namely movement-based learning.

Research in movement-based learning has to identify how epigenetic mechanisms can be efficiently modified by the performance of specific, corresponding movements or learning processes to improve development ("correction en route", which is particularly salient to the treatment of cerebral palsy) and the repair of the human CNS and to avoid pathologic CNS changes like epilepsy and cancer. The complexity of the epigenetic regulation (Figure 66) is tremendous. Already the neural network learning for repair is complex and needs human repair-neurophysiology **(Figure 67)** including new measuring methods.

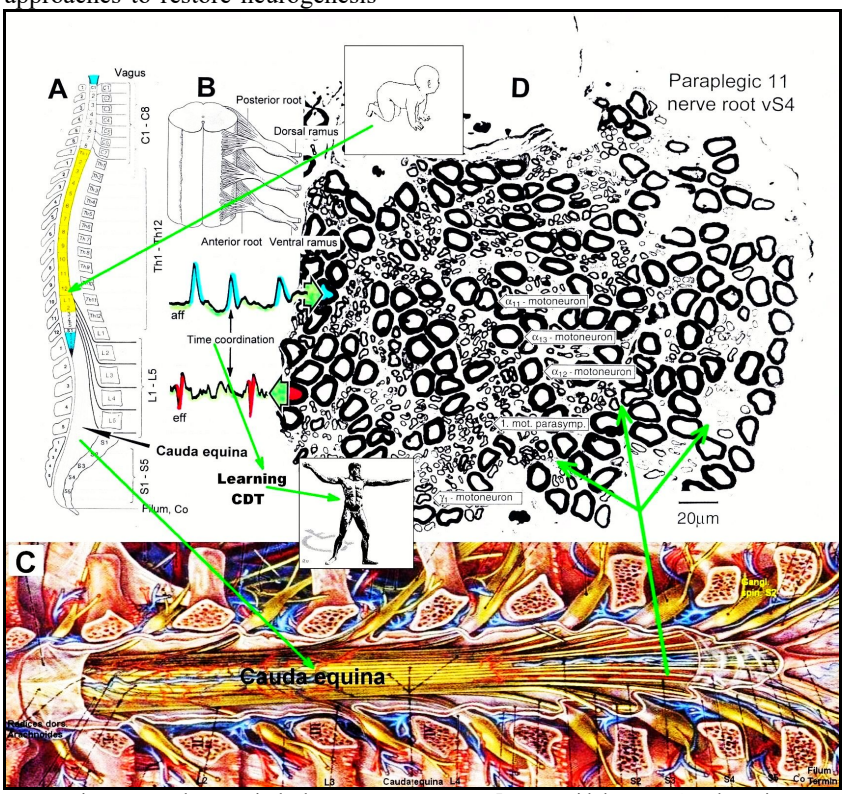

Figure 67. Principle of human neuroscience research to repair the human nervous system. It starts with humans. A. schematic anatomy of the spinal canal with the spinal cord, nerve roots (B) and cauda equina nerve roots due to the Ascensus of the spinal cord. C. Painting of the spinal canal with the cauda equina nerve roots. The caudal sacral nerve roots are much thinner than pictured. D. A real cross-section of the ventral sacral root S4. Single-nerve fiber action potentials, conducted into (aff) and out of the CNS (eff) for communication of the CNS with the outside world, are inserted. Out of the difference of the impulse patterns under physiologic and pathologic conditions a movement-based learning therapy was developed (CDT) with which patients can get their CNS repaired and leave the wheelchair behind **(Figures 1-3)**.

The improvement of phase and frequency coordination through CDT substantially contributes to the repair in cerebrum and cerebellum injury, spinal cord injury (SCI), cerebral palsy, stroke, myelomeningocele, aging and cancer. Even sportsmen benefit from an improved phase and frequency among neuron firing, because the coordination of arms, legs and trunk improve, to play better tennis or football and perform better other sports. Since CDT improves the functioning of every CNS, and the CNS is involved in nearly all body functions, the

regulations of body functions improve, especially the cardio-vascular performance, to live longer with a better quality of life through 10 to 15 h CDT per week.

4. Repair in different nervous system diseases

The importance to improve phase and frequency coordination of neural network organization in connection with the plasticity of the CNS and that cancer growth can be inhibited through CDT (movement-based learning) is supported by the clinical success. It has been shown that coordination dynamics therapy (CDT) can improve or repair central nervous system (CNS) functioning after stroke [42], traumatic brain injury [43,44], spinal cord injury [3,18,45-48], cerebellar injury [49], cerebral palsy [50], hypoxic brain injury [51], in Parkinson's disease [31], spina bifida (myelomeningocele) [52] and scoliosis [53]. Speech had been induced and improved in a patient with severe cerebral palsy [7]. A permanent coma patient could be brought out-of-coma and relearned to speak [54] and cancer grows could be inhibited through CDT [32]. Cardio-vascular performance could be improved (Figures 59-62). There is indication therefore that the general health can be improved via CDT to live longer with a better quality of life.

5. Out-of-date Human Repair-Neurophysiology of the universities worldwide by 30 years and the consequences for patients with CNS injuries

Even though already approximately 20 years ago there were books and publications available on coordination dynamics therapy **(Figure 68)**, the universities world-wide are not taking any afford to catch up with the available knowledge on 'Human Repair-Neurophysiology'. Probably several million people die per year because coordination dynamics therapy is not used.

Figure 68. Theoretical and clinical publications on coordination dynamics therapy published approximately 20 years ago.

Even recent open access publications on the improvement of health, including COVID-19 infection and cancer treatment [54-57], are ignored by the medical faculties of universities. Medical students learn, with respect to CNS repair, out-of-date treatments. An even for the Author shocking case will be reported shortly here, to show what the consequences are, if universities teach out-of-date knowledge.

The 5.5 years old Nefeli (see above) got cancer. The cancer was removed. By medical malpractice (mistake in hemostasis and missing care after the operation), she suffered an incomplete spinal cord injury (SCI). At an age of 9, through 4 years of Coordination Dynamics Therapy (CDT), she re-learned walking **(Figures 69A-69C)**, running, jumping and became continent again [3].

Figure 69. Bar foot walking of the patient Nefeli with a spinal cord injury before the second operation (A-C). Three months after the operation she could not walk freely anymore (D).

At an age of 14 an orthopedic surgeon made Nefeli and her parents believe that through an operation of the legs, her walking performance can substantially be improved. Against the strong advice of the Author 'to avoid an operation', because such operations in SCI reduce the plasticity, necessary for repair, the parents decided for an operation of the legs, with the consequence that the patient could not walk anymore 3.5 months following the operation **(Figure 69D)**, including 8 weeks of intensive CDT administered by the Author. Instead of getting better she got much worse with the operation. Even though the surgeon applied a standard operation, he did not know what he was doing. He tried to repair the CNS through an operation which is impossible. Further, the surgeon did not at all understood the response of the CNS to the operational injury and advised false physiotherapy.

When the Author saw Nefeli the first time, 6 weeks after the operation, she was in bed and could not move the legs **(Figure 70)**. The legs were in an extreme flexed position. No leg movement was possible. When it became later possible with tricks to extend the legs a bit **(Figure 71A)**, they went immediately into the flexed position when touched **(Figure 71B)**, independently where the leg was touched. When trying to put her onto the feet, the feet flexed **(Figure 71C)**, so that a standing was impossible. The patient had extreme flexor spasticity, rigor and cramps.

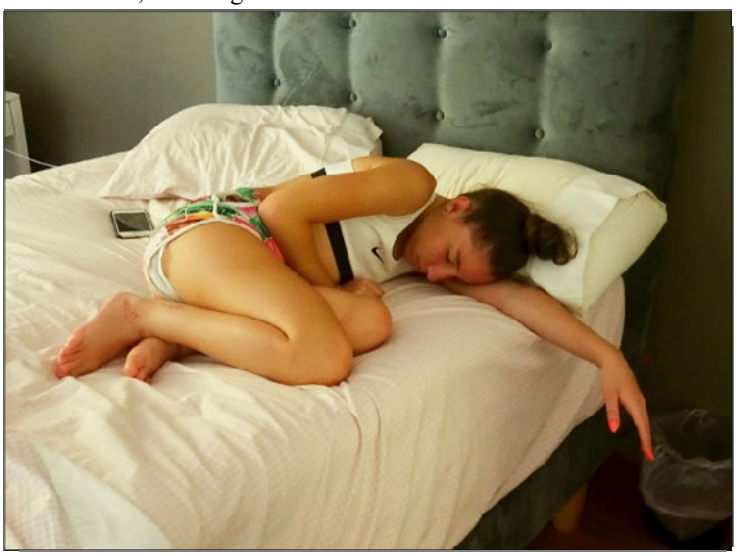

Figure 70. Six weeks after the operation the spinal cord injury (SCI) patient cannot move the legs at all, because of extreme flexor spasticity, which developed one to two weeks after the operation when the legs were in plastic up to the knees for 4 weeks.

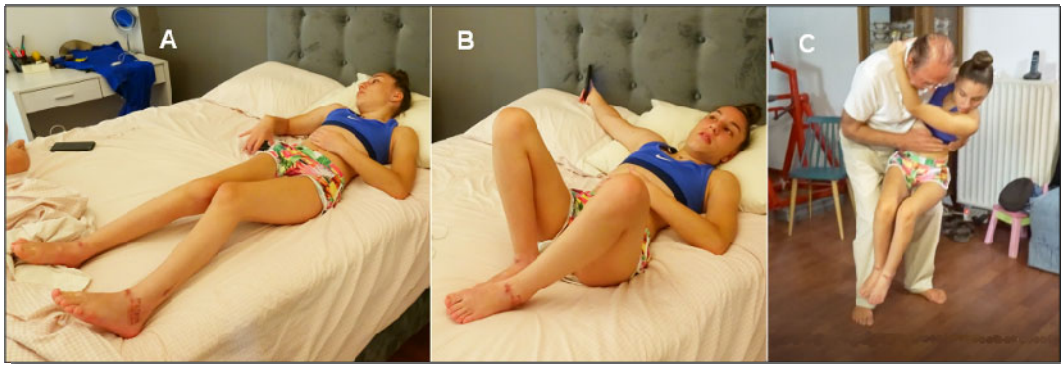

Figure 71. When it became possible by some tricks to get the legs somehow stretched (A) and one touched the legs, they went immediately into flexor spasticity position (B). When the Author tried to put the SCI patient onto the legs for standing, the legs flexed immediately (C).

The patient Nefeli reported that one week after the operation, when both legs till to the knees were in plastic, slowly she could not flex the leg anymore. A flexor spasticity built up, caused by the operation. The order from the surgeon, to use the legs, were useless because she could not move them anymore. The parents did not understand why Nefeli could not move the legs anymore and why they were always in an extreme flexed position. She had to be carried to the WC. Lucky that the continence was only disturbed transiently (mild transient spastic external bladder sphincter).

When the Author, 6 weeks after the operation, started to train Nefeli, he was able with the help of the special CDT device to reduce slowly the spasticity and made a training of movements possible. Without the special CDT, no other movement was possible at that time. But the 6 weeks immobilization did atrophy the not spastic muscles and made free walking impossible because of missing power and spasticity.

Nefeli was the wrong patient for such an operation. The fine balance of CNS functioning and the regeneration achieved through the 4 years of CDT was destroyed by the operation. The operation induced different input from the leg receptors (including pain) to the spinal cord and had changed CNS functioning. Because of the spinal cord injury (lost connections), the brain had not sufficient possibilities (connections) to correct for the changes in the periphery. The connections for corrections were missing. In patients with an intact spinal cord, a healthy human brain (not animal brain) can in min to h correct for changes in the periphery [21-23]. It seems that the surgeon had not learned that in his study.

Five months after the operation, Nefeli became able to walk a bit with orthoses again. But with the operation, she lost approximately 2 years of CDT. Before the operation she could walk, run and jump **(Figures 72A and 72B)** and after the operation she just managed to walk a bit with orthosis and shoes **(Figure 72C)**. Before the operation she could walk up to 1000m and after the operation she managed 10m. Before the operation, Nefeli could walk bar foot long distances **Figures 69A-69C**). Five months after the operation she still needed support for free walking **(Figure 73)**. Without support she managed 3 to 5 steps.

Figure 72. Spinal cord injury patient Nefeli can, through 4 years of coordination dynamics therapy, walk bare foot (and with shoes) and jump a bit before a foot operation (A, B) and can, after the foot operation, only walk a bit with shoes and orthosis (C), but not bare foot. The by the surgeon promised much better walking performance did not take place, the patient only lost leg functions as predicted by the Author.

Figure 73. Five months after the 'miracle operation' the SCI patient needed still support for free walking. Without support she just managed 3 to 5 steps.

In a following article [58], it will be analyzed in detail that the orthopedic operated without sufficient knowledge of the human nervous system, necessary especially in SCI. The operation-induced extreme flexor spasticity blocked the standing and the upright forward movements and could only slowly be reduced in spite of optimal CDT, administered by the Author.

REFERENCES

1. Schalow G (2005) Phase and frequency coordination between neuron firing as an integrative mechanism of human CNS self-organization. Electromyogr Clin Neurophysiol 45: 369-383.
2. Schalow G (2010) Scientific basis for learning transfer from movements to urinary bladder functions for bladder repair in patients with spinal cord injury. Electromyogr Clin Neurophysiol 50: 339-395.
3. Schalow G (2019) Regeneration of the human spinal cord via coordination dynamics therapy. Peertechz Publications. eBook. pp: 97.
4. Schalow G, Lang G (1987) Recording of Single Unit Potentials in Human Spinal Nerve Roots: A New Diagnostic Tool. Acta Neurochir 86: 25-29.
5. Schalow G (2006) Surface EMG- and coordination dynamics measurements-assisted cerebellar diagnosis in a patient with cerebellar injury. Electromyogr Clin Neurophysiol 46: 371-384.
6. Wattig B, Schalow G, Heydenreich F, Warzok R, Cervos-Navarro J (1992) Nucleotides enhance nerve fiber regeneration after peripheral nerve crush damage - Electrophysiologic and morphometric investigation. Arzneimittel-forschung 42(9): 1075-1078.
7. Schalow G (2013) Human Neurophysiology: Development and Repair of the Human Central Nervous System. Nova Science Publishers, Inc, Hauppauge NY, USA. pp: 734.
8. Schalow G (2015) Repair of the Human Brain and Spinal Cord. Nova Science Publishers, Inc, Hauppauge NY, USA. pp: 525.
9. Schalow G (2015) Neural network learning in human. Nova Science Publishers, Inc, Hauppauge NY, USA. pp: 324.
10. Schalow G (1991) Oscillatory firing of single human sphincteric α2 and α3-motoneurons reflexly activated for the continence of urinary bladder and rectum. Restoration of bladder function in paraplegia. Electromyogr Clin Neurophysiol 31: 323-355.
11. Schalow G (1993) Action potential patterns of intrafusal γ and parasympathetic motoneurons, secondary muscle spindle afferents and an oscillatory firing α2-motoneuron, and the phase relations among them in humans. Electromyogr Clin Neurophysiol 33: 477-503.
12. Schalow G, Zäch GA (1996) Mono and polysynaptic drive of oscillatory firing α1 (FF) and α2-motoneurons (FR) in a patient with spinal cord lesion. Gen Physiol Biophys 15: 57-74.
13. Schalow G, Bersch U, Zäch GA, Warzock R (1996) Classification, oscillatory and alternating oscillatory firing of α1 (FF) and α2-motoneurons (FR) in patients with spinal cord lesion. Gen Physiol Biophys 15: 5-56.
14. Schalow G (1993) Spinal oscillators in man under normal and pathologic conditions. Electromyogr Clin Neurophysiol 33: 409-426.
15. Schalow G (2009) The classification and identification of human somatic and parasympathetic nerve fibers including urinary bladder afferents is preserved following spinal cord injury. Electromyogr Clin Neurophysiol 49: 263-286.
16. Hess WR (1981) Biological order and human society. In: Akert, K. (Ed.), Biological Order and Brain Organization - Selected Works of W.R. Hess, Springer-Verlag, Berlin. pp: 3-15.
17. Schalow G, Zäch GA (1996) Reflex stimulation of continuously oscillatory firing α and γ-motoneurons in patients with spinal cord lesion. Gen Physiol Biophys 15: 75-93.

18. Schalow G (2009) Partial cure achieved in a patient with near-complete cervical spinal cord injury (95% injury) after 3 years of coordination dynamics therapy. Electromyogr Clin Neurophysiol 49: 199-221.

19. Schöner G, Zanone PG, Kelso JA (1992) Learning as change of coordination dynamics: Theory and experiment. J Mot Behav 24: 29-48.

20. Schalow G (2019) Brain repair and general health improvement through human neurophysiology and repair physiology (Review of Coordination Dynamics Therapy (CDT)). Clin Med Rep 2(2): 1-68.

21. Sperry RW (1945) The problem of central nervous system reorganization and muscle transposition. Quart Rev Biol 20: 311-369.

22. Sperry RW (1947) Effect of crossing nerves to antagonistic limb muscles in the monkey. Arch Neurol Psychiat (Chicago) 58: 452-473.

23. Weiss P, Brown PF (1941) Electromyographic study on coordination of leg movements in poliomyelitis patients with transposed tendons. Proc Soc Exper Biol Med 48: 384-387.

24. Schalow G, Zäch GA (2000) Reorganization of the Human CNS, Neurophysiologic measurements on the coordination dynamics of the lesioned human brain and spinal cord. Theory for modern neurorehabilitation (31 case reports). Gen Physiol Biophys 19: 1-244.

25. Boyd IA (1980) The isolated muscle spindle. Trends in Neurosciences 3: 258-265.

26. Gladden MH (1985) Efferent control of human muscle spindles. In: Boyd, I.A. and Gladden, M.H. (Eds.), The Muscle Spindle, Stockton Press, New York. pp: 243-254.

27. Schalow G (1992) Recruitment within the groups of γ1, α2 and α3-motoneurons in dogs and humans following bladder and anal catheter pulling. Gen Physiol Biophys 11: 101-121.

28. Bawa B, Binder MD, Ruenzel P, Henneman E (1984) Recruitment of motoneurons in stretch reflexes is highly correlated with their axonal conduction velocity. J Neurophysiol 52: 410-420.

29. Schalow G, Pääsuke M, Jaigma P (2005) Integrative re-organization mechanism for reducing tremor in Parkinson's disease patients. Electromyogr Clin Neurophysiol 45: 407-415.

30. Windhorst U (1988) How Brain-Like is the Spinal Cord? Springer Verlag, Berlin.

31. Schalow G, Pääsuke M, Ereline J, Gapeyeva H (2004) Improvement in Parkinson's disease patients achieved by coordination dynamics therapy. Electromyogr Clin Neurophysiol 44: 67-73.

32. Schalow G (2017) Breast cancer growth inhibition via Coordination Dynamics Therapy. In: "Horizons in Cancer Research. Editor: Hiroto S. Watanabe. Nova Science Publishers, Inc, Hauppauge NY, USA. Vol 68, pp: 125-151.

33. Schalow G (2010) Cure of urinary bladder functions in severe (95%) motoric complete cervical spinal cord injury in human. Electromyogr Clin Neurophysiol 50: 155-179.

34. Schalow G (1990) Feeder arteries, longitudinal arterial trunks and arterial anastomoses of the lower human spinal cord. Zentralbl Neurochir 51: 181-184.

35. Schalow G, Pääsuke M (2003) Low-load coordination dynamics in athletes, physiotherapists, gymnasts, musicians and patients with spinal cord injury, after stroke, traumatic brain lesion and with cerebral palsy. Electromyogr Clin Neurophysiol 43: 195-201.

36. Schalow G, Pääsuke M, Kolts I (2003) High-load coordination dynamics in athletes, physiotherapists, gymnasts, musicians and patients with CNS injury. Electromyogr Clin Neurophysiol 43: 353-365.

37. Colvis CM, Pollok JD, Goodman RH, Impey S, Dunn J, et al. (2005) Epigenetic mechanisms and gene networks in the nervous system. J. Neurscience 25(45): 10379-10379.

38. Bird A (2007) Perceptions of epigenetics. Nature 447: 396-398.

39. Covic M, Karaca E, Lie DC (2010) Epigenetic regulation of neurogenesis in the adult hippocampus. Heredity 105: 122-134.

40. Brown JC, Winters-Stone K, Schmitz KH (2012) Cancer, physical activity, and exercise. Compr Physiol 2: 2775-2809.

41. Christensen JF, Jones LW, Andersen JL, Daugaard G, Rorth M, et al. (2014) Muscle dysfunction in cancer patients. Ann Oncol 25: 947-958.

42. Schalow G (2002) Stroke recovery induced by coordination dynamic therapy and quantified by the coordination dynamic recording method. Electromyogr Clin Neurophysiol 42: 85-104.

43. Schalow G (2002) Improvement after traumatic brain injury achieved by coordination dynamic therapy. Electromyogr Clin Neurophysiol 42: 195-203.

44. Schalow G, Jaigma P (2006) Improvement in severe traumatic brain injury induced by coordination dynamics therapy in comparison to physiologic CNS development. Electromyogr Clin Neurophysiol 46: 195-209.

45. Schalow G (2002) Recovery from spinal cord injury achieved by 3 months of coordination dynamic therapy. Electromyogr Clin Neurophysiol 42: 367-376.

46. Schalow G (2003) Partial cure of spinal cord injury achieved by 6 to 13 months of coordination dynamic therapy. Electromyogr Clin Neurophysiol 43: 281-292.

47. Schalow G, Jaigma P, Belle VK (2009) Near-total functional recovery achieved in partial spinal cord injury (50% injury) after 3 years of coordination dynamics therapy. Electromyogr Clin Neurophysiol 49: 67-91.

48. Schalow G (2010) Cure of urinary bladder functions in severe (95%) motoric complete cervical spinal cord injury in human. Electromyogr Clin Neurophysiol 50: 155-179.

49. Schalow G (2006) Cerebellar injury improvement achieved by coordination dynamics therapy. Electromyogr Clin Neurophysiol 46: 433-439.

50. Schalow G, Jaigma P (2005) Cerebral palsy improvement achieved by coordination dynamics therapy. Electromyogr Clin Neurophysiol 45: 433-445.

51. Schalow G (2006) Hypoxic brain injury improvement induced by coordination dynamics therapy in comparison to CNS development. Electromyogr Clin Neurophysiol 46: 171-183.

52. Schalow G, Nyffeler T (2001) Coordination dynamics therapy: Myelomeningocele (spina bifida). Physical Therapy.

53. Schalow G, Nyffeler T (2000) Coordinate dynamics therapy: Scoliosis. Physiotherapy.

54. Schalow G (2019) Permanent coma patient re-learned to speak via Coordination Dynamics Therapy. Arch Clin Med Case Rep 3(2): 33-50.

55. Schalow G (2020) Anaplastic oligodendroglioma WHO III brain cancer-patient recovered following operation, radiation and chemotherapy through Coordination Dynamics Therapy, which is also a Covid-19 treatment without ventilator. Int J Med Clin Imaging 5(2): 165-210.

56. Schalow G (2020) From brain repair to Covid-19 treatment via Coordination Dynamics Therapy. (Video film contains therapy movements of patient's recent publications). Available online at: https://www.scitcentral.com/article/62/1656/From-Brain-Repair-to-COVID-19-Treatment-via-Coordination-Dynamics-Therapy-(CDT) Video conference on: August 19, 2020. (Download from www.coordination-dynamics-therapy.com).

57. Schalow G (2020) Classification and Identification of Human Peripheral Nerve Fibers by Conduction Velocity, Nerve Fiber Diameter and Natural Firing Patterns with Consequences for CNS Repair and Covid-19 Infection Treatment. Int J Med Clin Imaging 5(3): 231-314.

58. Schalow G (2021) CNS Repair in a Girl with a Spinal Cord Injury. Adv. Pub. Health Com. Trop. Med. 121: 201-226.